PHYSICAL MODELLING AND ADVANCED SIMULATIONS OF LIQUID VAPOR TWO-PHASE FLOWS WITH NEPTUNE_CFD CODE

STÉPHANE MIMOUNI ET AL.

JUNE 2025

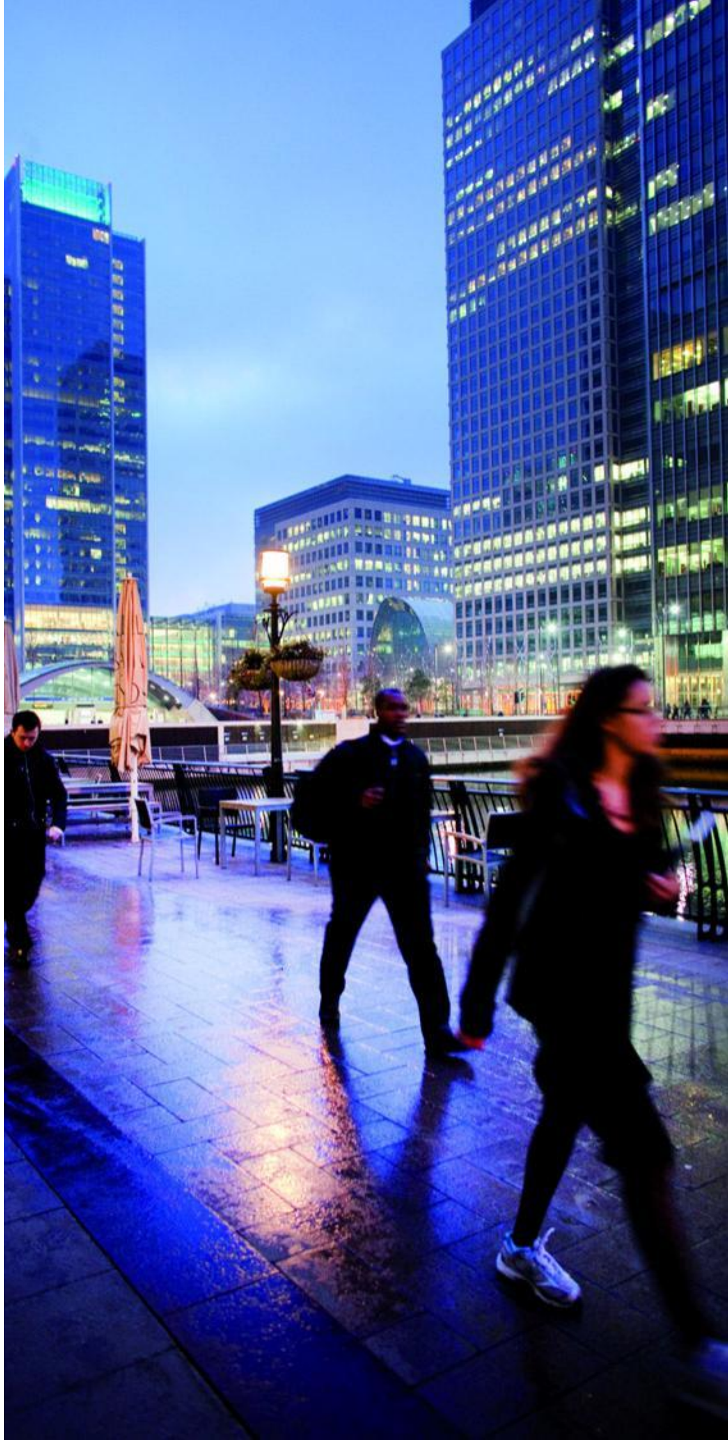

OUTLINE

0% → 100%

Void fraction

1. **CFD MODELLING OF DISPERSED TWO-PHASE FLOW FOR NUCLEAR POWER PLANT (6-EQUATION MODEL, EULER-EULER, NEPTUNE_CFD (EDF,CEA,IRSN,FRAMATOME))**

   RECENT ADVANCES IN NUCLEATE BOILING MODELLING

2. **MULTIFIELD CFD CALCULATIONS OF INDUSTRIAL GEOMETRIES : LARGE INTERFACES**

   FLOW PATTERN MAP : METERO, MAXI2 EXPERIMENTS

   TURBULENCE

   PHASE CHANGE

   CAPILLARY AND WETTABILITY EFFECTS

3. **TWO-PHASE FLOW IN CRACKS OR LEAKY RODS**

4. **CFD MODELLING OF DISPERSED TWO-PHASE FLOW FOR NUCLEAR POWER PLANT (6-EQUATION MODEL, EULER-EULER, NEPTUNE_CFD (EDF,CEA,IRSN,FRAMATOME))**

   MODELLING OF SPRAYS

1. CFD modelling of dispersed two-phase flow for nuclear power plant

RECENT ADVANCES IN NUCLEATE BOILING MODELLING AND APPLICATION TO DNB FOR UNIFORM AND NONUNIFORM HEAT FLUX

IMFT, CEA, IRSN, FRAMATOME
European projects : HZDR, GRS, PSI, KTH, UCL, JSI, VTT, UJV, KFKI, …

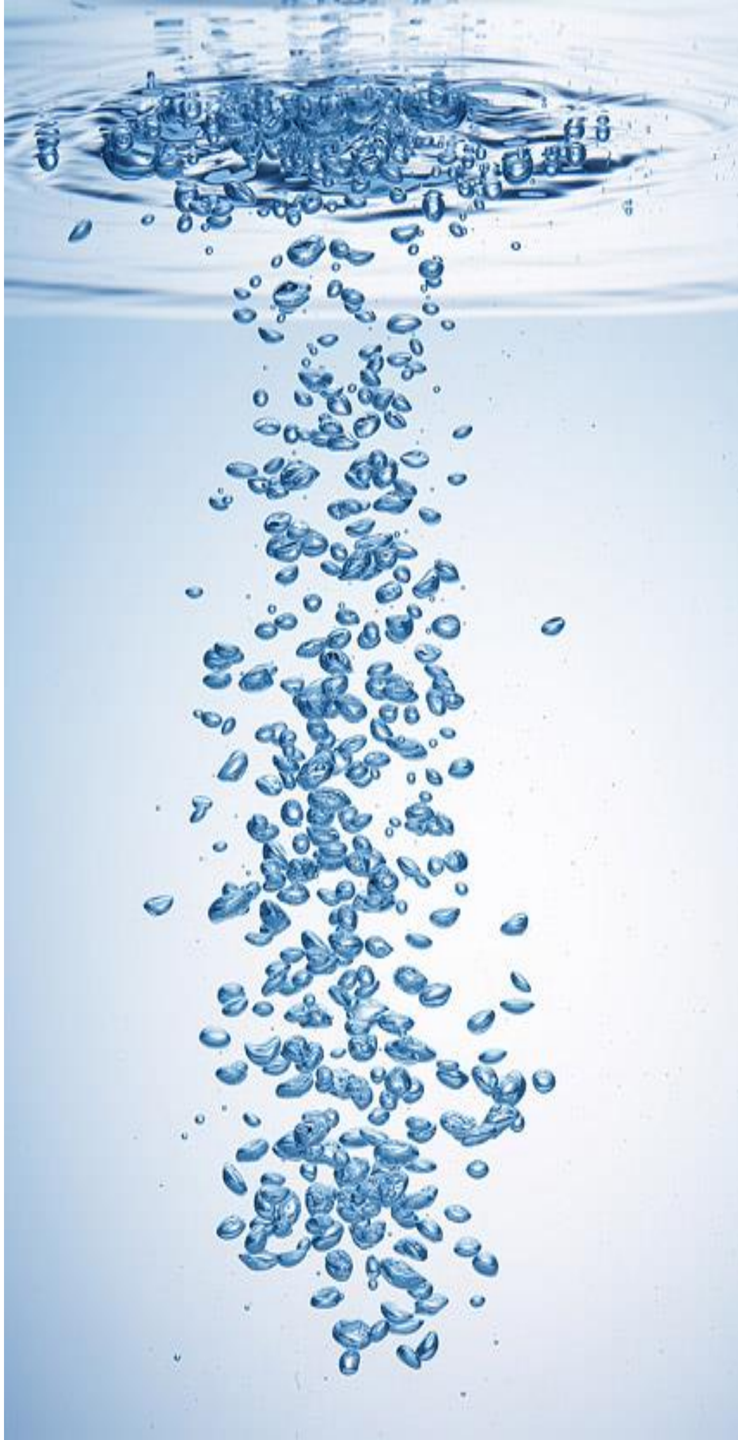

DNB : INDUSTRIAL CONTEXT

- In nucleate boiling, heat flux increases and reaches a maximum value with increasing wall temperature.
- → severe damage or meltdown of the surface.

A vapour film isolates the fuel from the water: the fuel heats up sharply and suddenly

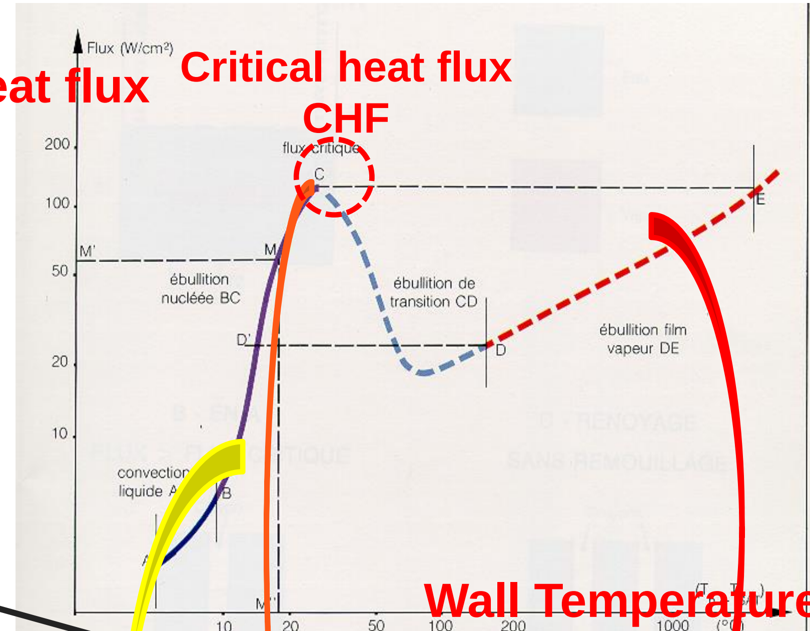

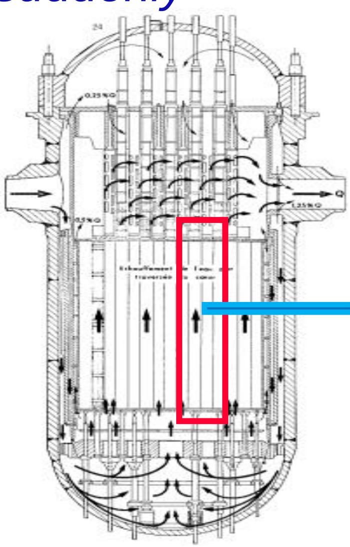

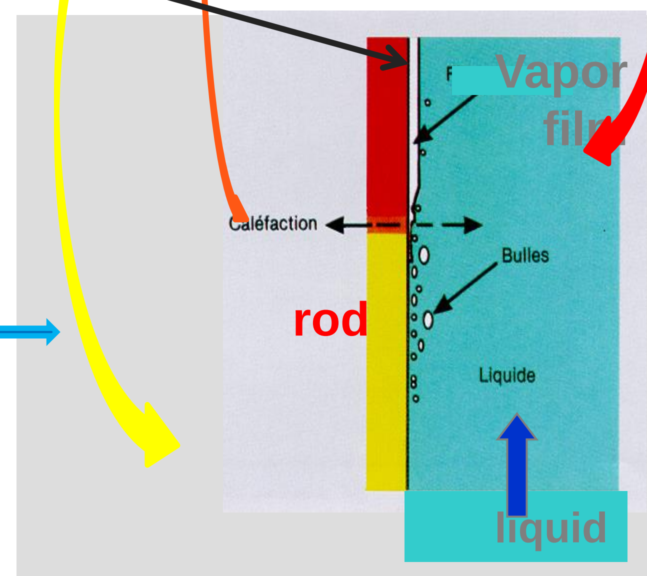

THE NEPTUNE_CFD SOLVER AND PHYSICAL MODELLING : BALANCE EQUATIONS : CFD 3D

The interfacial transfer terms of mass, momentum and heat.

Two mass balance equations:

$$\frac{\partial \alpha_k \rho_k}{\partial t} + \nabla.\left(\alpha_k \rho_k \underline{V}_k\right) = \Gamma_k$$

Two momentum balance equations:

Reynolds stress tensor

$$\frac{\partial \alpha_k \rho_k \underline{V}_k}{\partial t} + \nabla.\left(\alpha_k \rho_k \underline{V}_k \underline{V}_k\right) = -\alpha_k \nabla p + \underline{M}_k + \alpha_k \rho_k \underline{g} + \nabla.\left[\alpha_k \left(\underline{\underline{\Sigma}}_k + \underline{\underline{R}}_k\right)\right],$$

Two total enthalpy balance equations:

$$\frac{\partial}{\partial t}\left[\alpha_k \rho_k \left(h_k + \frac{V_k^2}{2}\right)\right] + \nabla.\left(\alpha_k \rho_k \left(h_k + \frac{V_k^2}{2}\right)\underline{V}_k\right) = \alpha_k \frac{\partial p}{\partial t} + \alpha_k \rho_k \underline{g}.\underline{V}_k$$

Wall transfer model for nucleate boiling

$$+\Gamma_k \left(h_{ki} + \frac{V_k^2}{2}\right) + \Pi'_k A_i + q'''_{wk} - \nabla.\left[\alpha_k \left(\underline{q}_k + \underline{q}_k^T\right)\right]$$

turbulent heat flux

$$\Gamma_l = -\Gamma_v = \frac{\Pi'_l + \Pi'_v}{h_{vi} - h_{li}} A_i$$

energy jump condition → mass transfer term

eDF

FORCES EXERTED ON BUBBLES

$$\underline{M}_g^{D} = -\underline{M}_l^{D} = -\frac{1}{8} A_i \rho_l C_D \left| \underline{V}_g - \underline{V}_l \right| \left(\underline{V}_g - \underline{V}_l \right) = -\alpha_g \rho_l F_D \left(\underline{V}_g - \underline{V}_l \right)$$

Drag force

drag coefficient for bubbles has been empirically modelled by Ishii (1990):

$$C_D = \frac{2}{3} d \sqrt{\frac{g\left|\rho_g - \rho_l\right|}{\sigma}} \left(\frac{1 + 17.67 \left(f(\alpha) \right)^{6/7}}{18.67 f(\alpha)} \right) \quad with \quad f(\alpha) = (1-\alpha)^{1.5} \quad for\ distorted\ bubbles$$

$$C_D = \frac{8}{3} (1-\alpha)^2 \quad for\ churn - turbulent\ regime$$

$$\underline{M}_g^{AM} = -\underline{M}_l^{AM} = -C_A^{\lg} \frac{1+2\alpha_g}{1-\alpha_g} \alpha_g \rho_l \left[\left(\frac{\partial \underline{V}_g}{\partial t} + \underline{V}_g . \underline{\underline{\nabla}} \underline{V}_g \right) - \left(\frac{\partial \underline{V}_l}{\partial t} + \underline{V}_l . \underline{\underline{\nabla}} \underline{V}_l \right) \right]$$

Added mass force

added mass coefficient which is equal to ½ for a spherical bubble and the factor (1+2α)/(1-α) takes into account the effect of the bubbles concentration

$$\underline{M}_g^{L} = -\underline{M}_l^{L} = -C_L \alpha_v \rho_l \left(\underline{V}_g - \underline{V}_l \right) \wedge \left(\underline{\nabla} \wedge \underline{V}_l \right)$$

Lift force

empirically modelled by Tomiyama = f(EoH)

$$Eo_H = \frac{g(\rho_g - \rho_l) d_H^2}{\sigma} \qquad d_H = \mathrm{D_b} \sqrt[3]{1 + 0.163 Eo^{0.757}}$$

where d_H is the maximum horizontal dimension of the deformed bubble, which is calculated using an empirical correlation given by Wellek

$$\underline{M}_g^{TD} = -\underline{M}_l^{TD} = -F^{TD} \rho_l \; k_l \nabla \alpha_g \ ,$$

Turbulent dispersion force

~~Lavieville (2016)~~

Stephane.Mimouni@edf.fr

WALL TRANSFER MODEL FOR NUCLEATE BOILING

In a first simplified approach, and following the analysis of Kurul (Kurul, 1990), the heat flux at the wall is split into three terms:

a single phase flow convective heat flux q_c at the fraction of the wall area unaffected by the presence of bubbles,

$$q_c = A_c h_{\log}\left(T_w - T_l\right)$$

a quenching heat flux q_q where bubbles departure brings cold water in contact with the wall periodically,

$$q_q = A_b t_q f \frac{2\lambda_l\left(T_w - T_l\right)}{\sqrt{\pi a_l t_q}}$$

a vaporisation heat flux q_e needed to generate the vapour phase.

$$q_e = f \frac{\pi d_d^{\,3}}{6} \rho_v \ell n$$

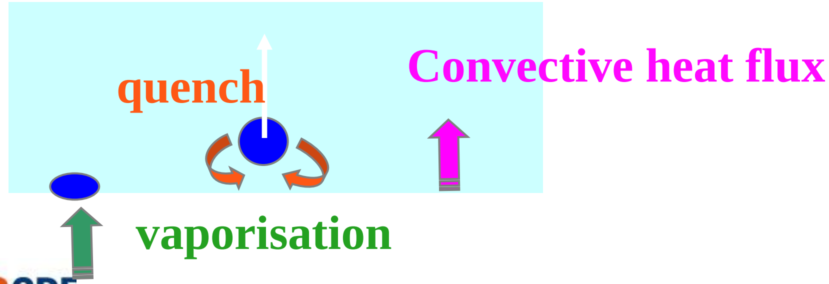

A_b : wall fraction occupied by bubble nucleation
bubble detachment frequency
bubble detachment diameter
active nucleation sites density

→ Empirical correlations

MODELLING OF THE LIQUID TURBULENCE ?
→LIQUID TEMPERATURE AND VOID FRACTION

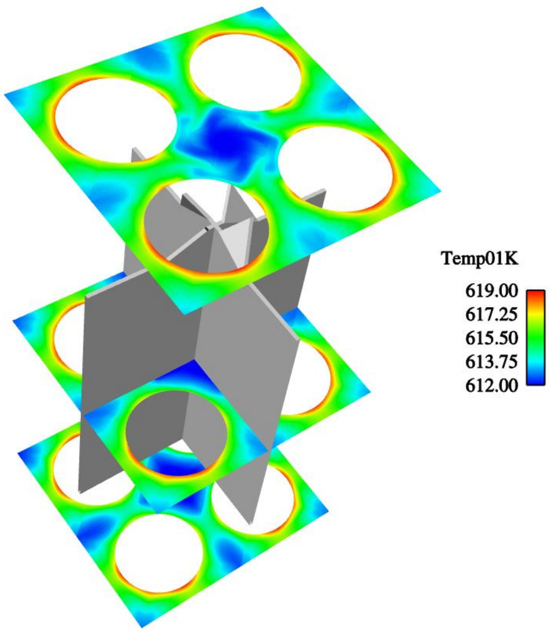

liquid temperature ($K-\varepsilon$).

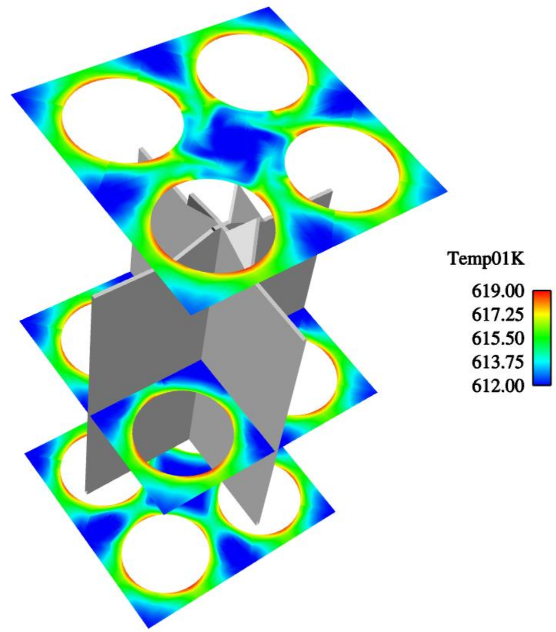

liquid temperature ($R_{ij}-\varepsilon$)

TOWARDS DNB MECHANISMS :
WALL FUNCTION FOR BOILING FLOWS

At subcooled flow boiling, the liquid velocity profile in the boundary layer is significantly disturbed by the bubble formation and detachment mechanisms on the heated wall. In the literature an over-prediction of liquid and gas velocity distributions in the boiling boundary region has been reported.

Roy et al (2002) : ASU experiment

$$u^+ = 1.8(\pm 0.25)\ln(y^+) + 5.9(\pm 1.0)$$

$$T^+ = 1.95(\pm 0.15)\ln(y^+) + 6.2(\pm 1.2)$$

Ramstorfer et al. (2005) :

$$u^+ = \frac{1}{\kappa}\ln(y^+) + B - \Delta u^+$$

$$\Delta u^+ = \begin{cases} 0; & k_r^+ \leq 11.3 \\ \frac{1}{\kappa}\ln(1 + C_{kr} k_r^+); & k_r^+ > 11.3 \end{cases}$$

offset of u+ due to the wall roughness

Mimouni et al (2010) :

$$k_r^+ = \frac{\rho_l k_r u_w}{\mu_l}$$

$$k_r = \alpha_v D$$

S. Mimouni et al., A second order turbulence model based on a Reynolds stress approach for two-phase boiling flow. Part 1: Application to the ASU-annular channel case, Nuclear Engineering and Design, Volume 240, Issue 9, September 2010, Pages 2233-2243

DNB MODELING

S. Mimouni, “Computational multi-fluid dynamics predictions of critical heat flux in boiling flow”
Nuclear Engineering and Design, *Volume 299*, *1 April 2016*, *Pages 28-36*

- Sensitivity to the mesh refinement

- Control of the oversaturation : If the liquid temperature in the nearest cell at the wall tends to the saturation temperature :

$$total\ heat\ \ flux = q_e + q_C + q_Q \rightarrow q_e$$

- Generalization of the Kurul-Podowski model : $q_v = h_{vap}\left(T_{wall} - T_v\right)$ heat flux, q_v, is the diffusive heat flux used to preheat the vapor phase :

$$q_{wall} = g_{\alpha,A}\left(q_c + q_q + q_e\right) + \left(1 - g_{\alpha,A}\right)q_v \quad \left[W/m^2\right]$$

Nucleate boiling regime Vapor film

$$g_{\alpha,A} = f_\alpha \qquad \rightarrow \qquad g_{\alpha,A} = f_\alpha \cdot f_A$$

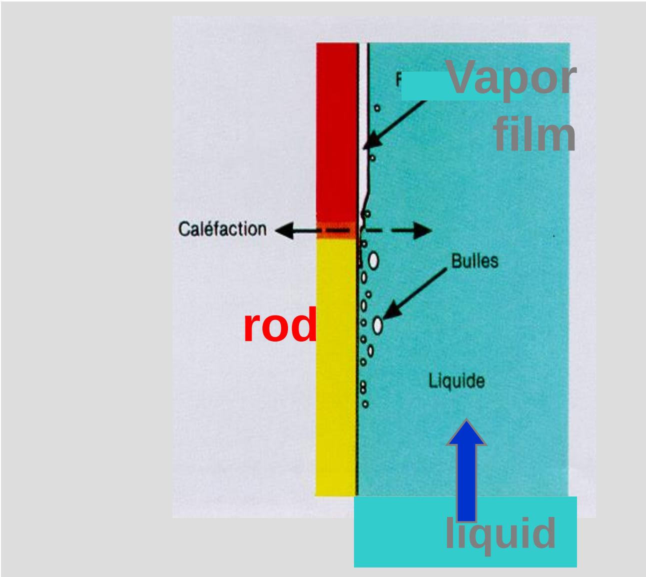

if $T_l(y^+)$ reaches the saturation temperature :

α_{crit}=0.5 and A_{crit}=0.5

otherwise α_{crit}=0.2 and A_{crit}=0.2

CALCULATIONS OF DNB TESTS IN A TUBE

Russian Academy of Sciences produced a series of standard tables of CHF as function of the bulk mean water condition and for various pressures and mass velocities for fixed tube diameter of 8 mm (Groeneveld, 1996). Heated length = 1m.

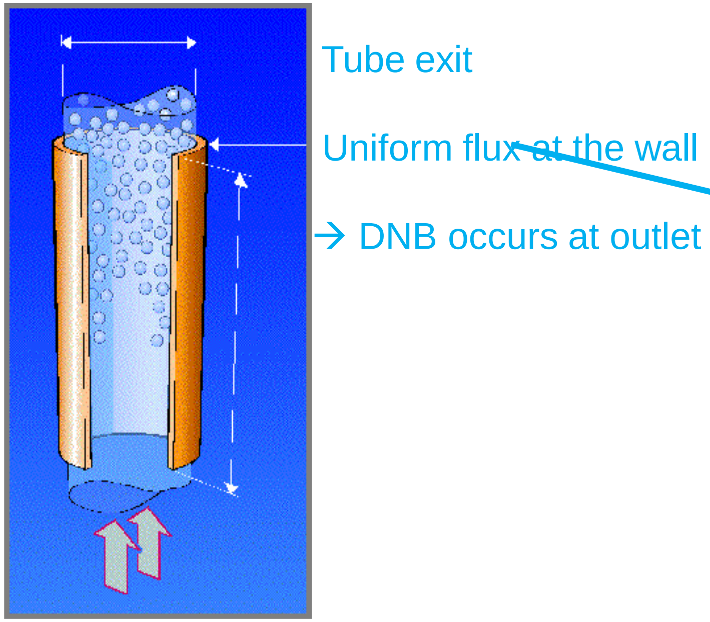

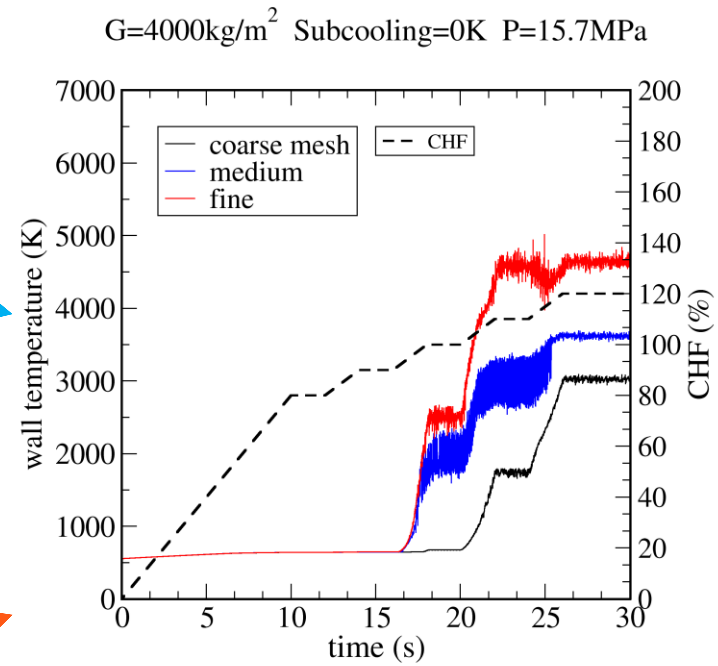

Calculation is started with wall heat flux equal to 70%CHF. Wall heat flux is after increased of 5% progressively. After this stage, wall heat flux reaches a plateau in order to stabilize the boiling flow. This procedure is repeated. In the calculations, CHF is detected when the wall temperature increases sharply.

Because of the sudden rise in temperature , results are weakly sensitive to the wall temperature chosen for CHF detection. (sudden drop of the vaporization heat flux).

1500 VALIDATION CASES

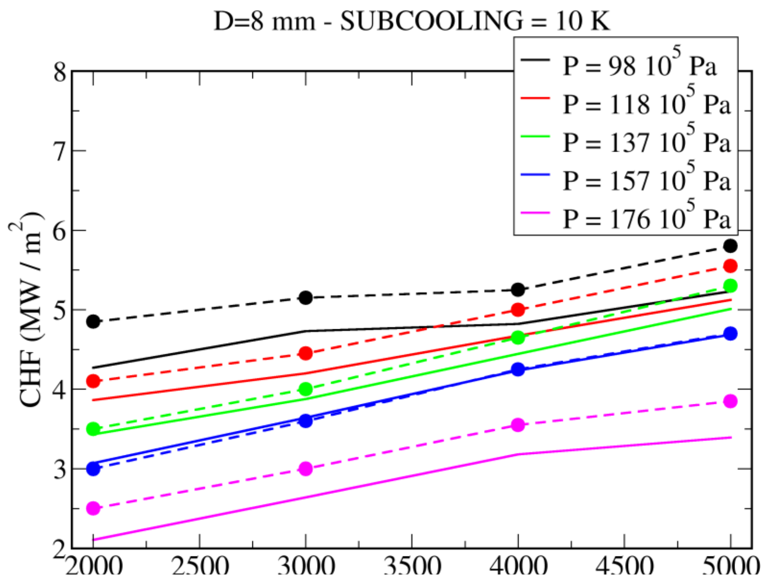

reproduce the tendencies

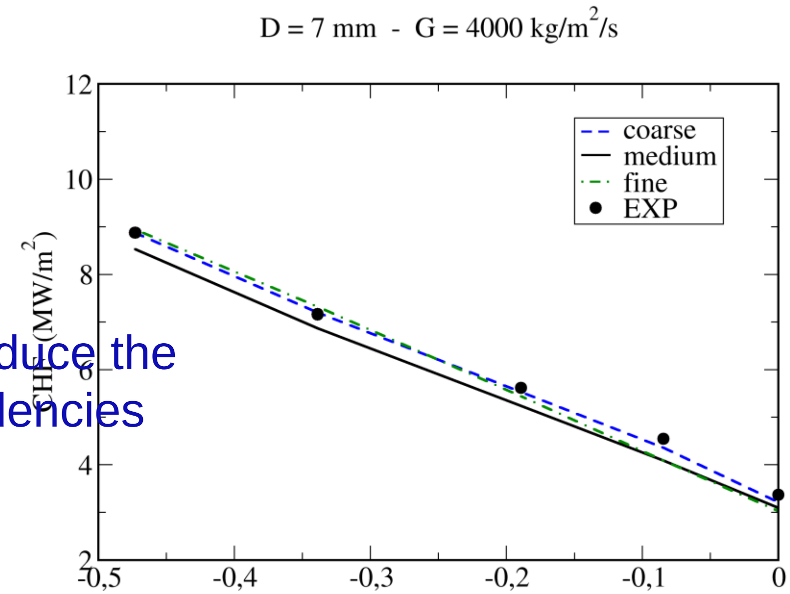

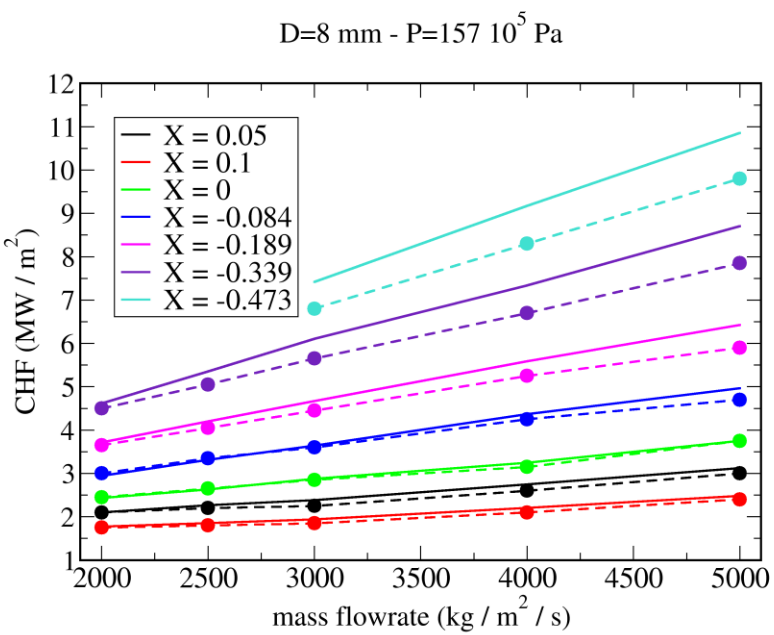

Tube diameter of 8 mm.

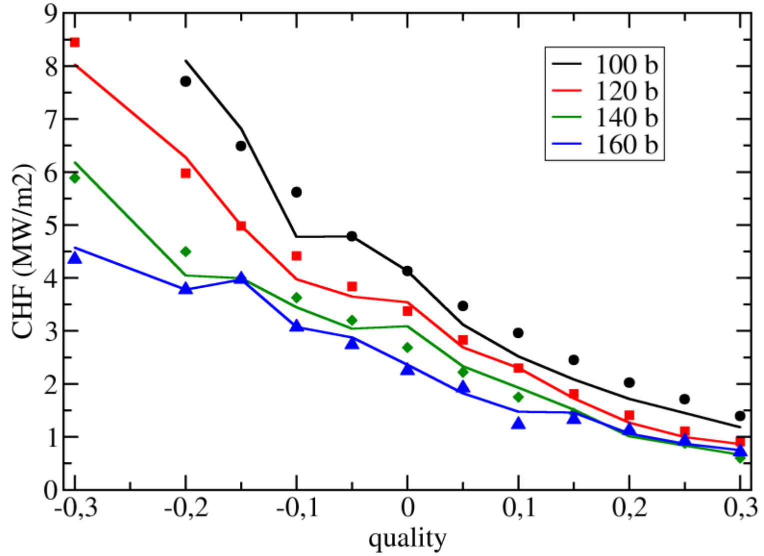

1500 VALIDATION CASES

Tendencies, P, G, X, tube diameter

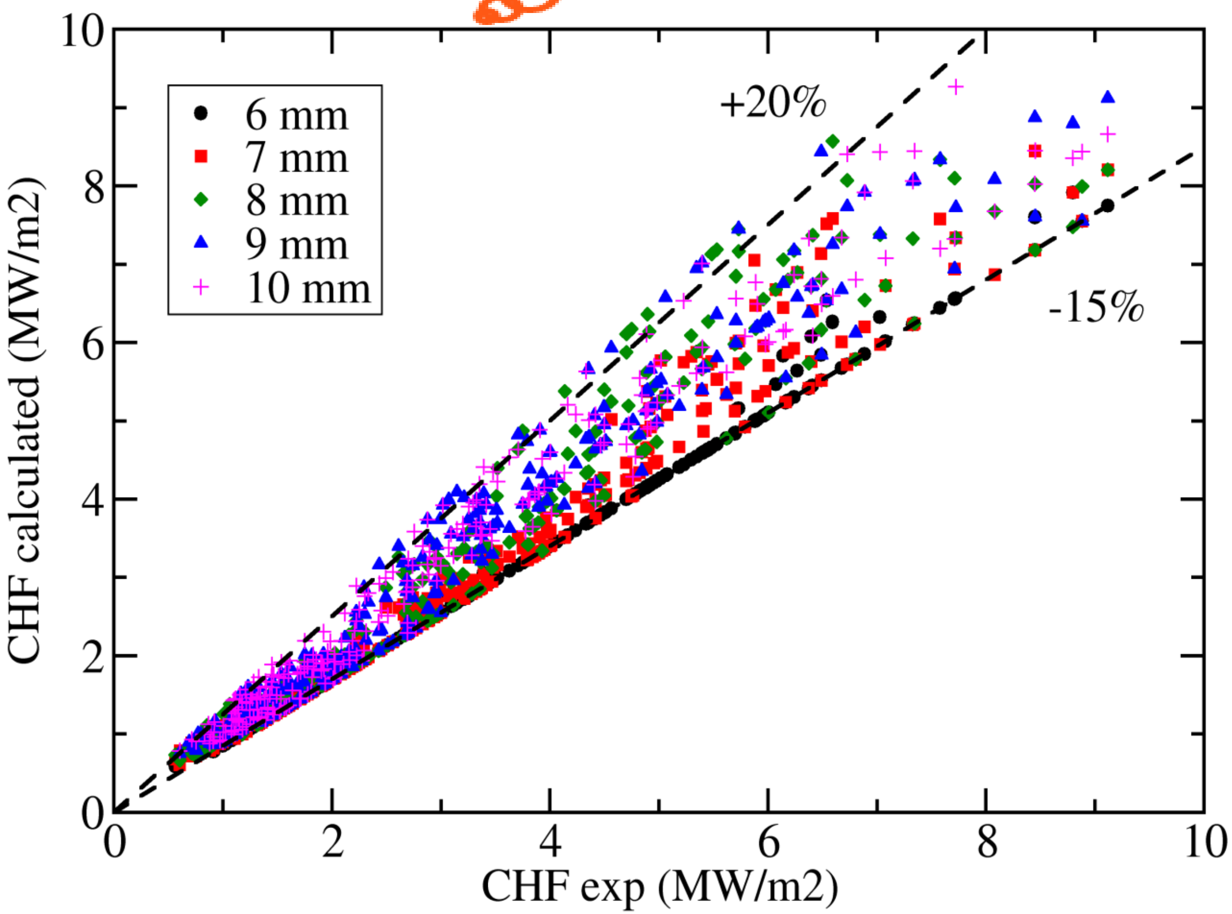

Stephane.Mimouni@edf.fr

Conclusion for the Critical heat flux

The objective of this work is to propose a new model in a computational multi-fluid dynamics tool leading to wall temperature excursion and onset of boiling crisis.

Critical heat flux is calculated against 1500 tests. The model tested covers a large physics scope in terms of mass flux, pressure, quality and channel diameter. Water and R12 refrigerant fluid are considered.

Furthermore, it was found that the sensitivity to the grid refinement was acceptable.

Neptune_CFD code with the DNB model is currently assessed in the nuclear industry for design optimization of rod bundles.

CFD results < empirical correlations based on experimental data

How can we improve the model ?

→Luc Favre, PhD 2023

NUCLEATION FREQUENCY

❑ *RPI*

$$f = \sqrt{\frac{4}{3}\frac{g|\rho_V - \rho_L|}{\rho_L D_b}}, \qquad t_q = \frac{1}{f}$$

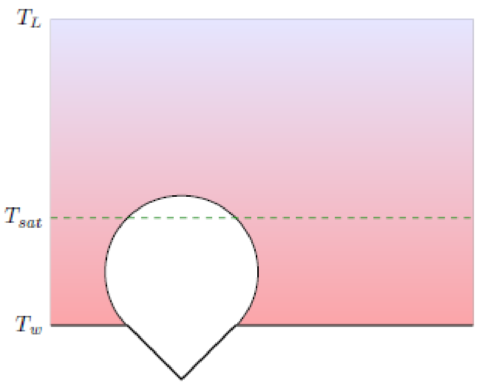

Growth to *Rd by pure conduction* : *t = tg,d*

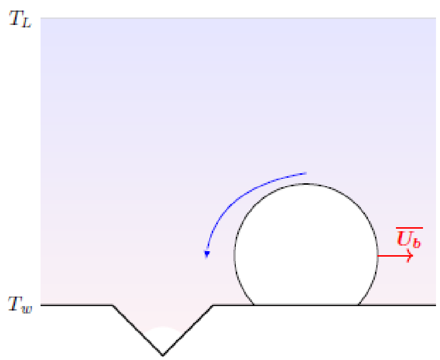

Departure by sliding: *t > tg,d*

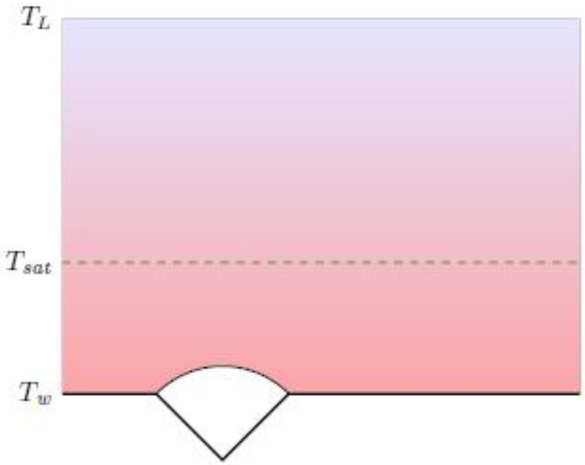

$$\rightarrow f = \frac{1}{t_g + t_{wait}}$$

Boundary layer reconstruction

New nucleation *t = tg,d + twait*

BUBBLE LIFT-OFF ½ : SLIDING LENGTH

Transient conduction induced by bubble sliding [Kossolapov, 2020]

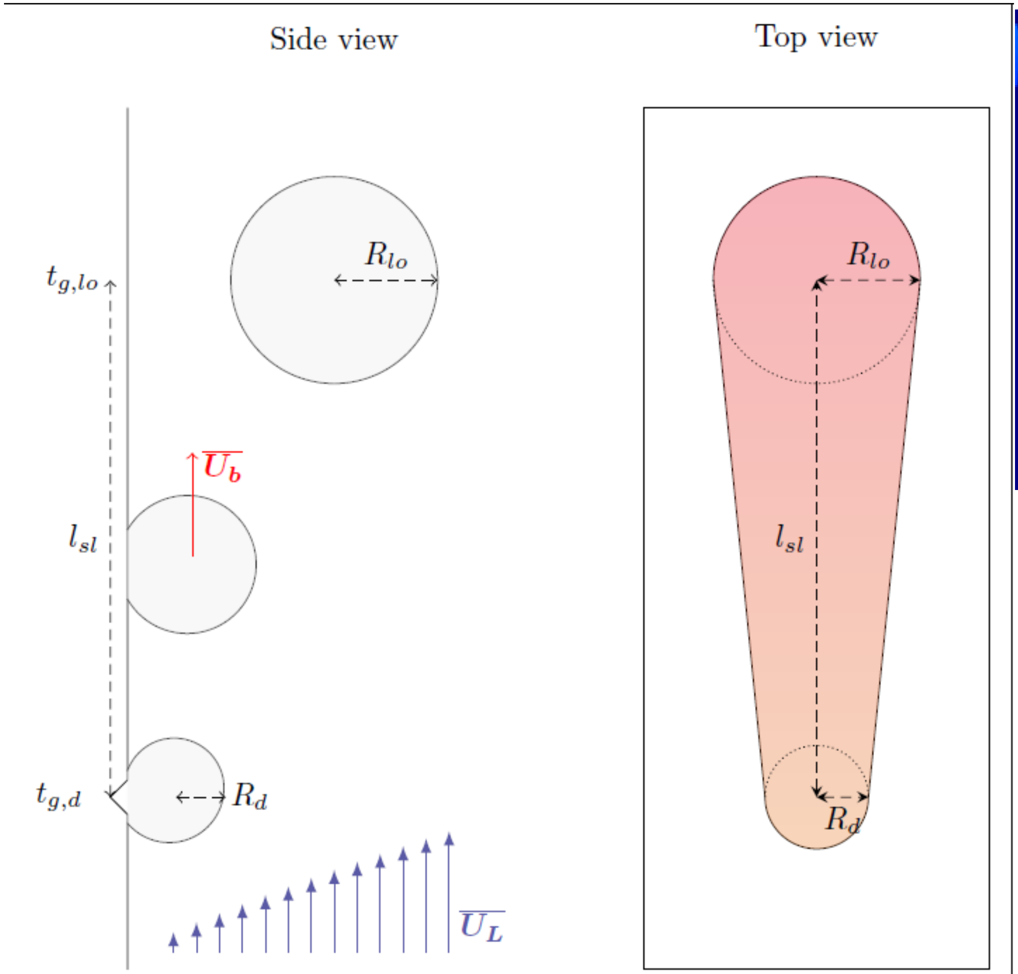

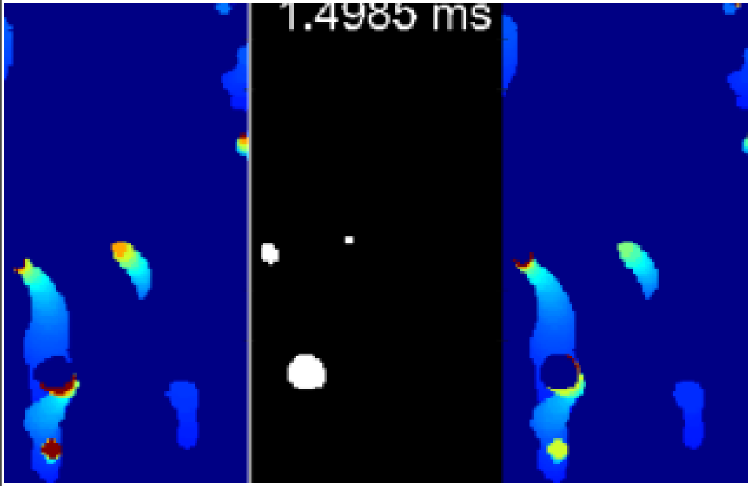

Rsl sliding diameter after *lsl : f(*Nucleating Bubbles Density)

- *RPI*

$$D_b = 2{,}42 \times 10^{-5} P^{0{,}709} \frac{a}{\sqrt{b\varphi}}$$

BUBBLE LIFT-OFF 2/2

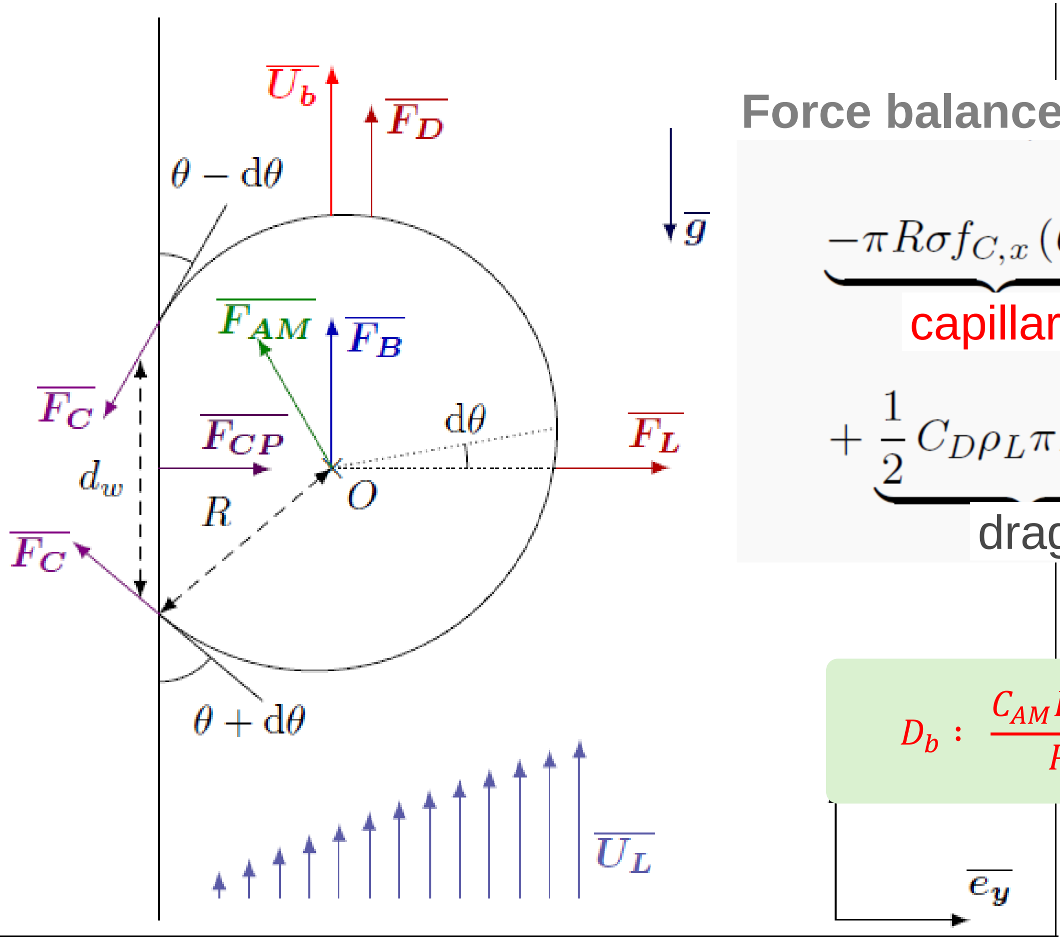

Force balance sketch

Force balance parallel to the wall

$$\underbrace{-\pi R \sigma f_{C,x}(\theta, \mathrm{d}\theta)}_{\text{capillary}} + \underbrace{\frac{4}{3}\pi R^3 (\rho_L - \rho_V) g}_{\text{buoyancy}}$$

$$+ \underbrace{\frac{1}{2} C_D \rho_L \pi R^2 U_L^2}_{\text{drag}} + \underbrace{\frac{4}{3}\pi R^3 \rho_L \, 3 C_{AM,x} \frac{\dot{R}}{R} U_L}_{\text{Added mass}} = 0$$

$$D_b : \frac{C_{AM} K^2 Ja_w^2}{Pr_L} + \frac{1}{3}\frac{Re_b}{Fr} + \frac{1}{8} C_D Re_b > \frac{1}{2}\frac{f_C(\theta, d\theta)}{Ca}$$

SITE DENSITY

❑ *RPI* : $N_{sit} = \left(210(T_w - T_{sat})\right)^{1,8}$

New phenomena are taken into account

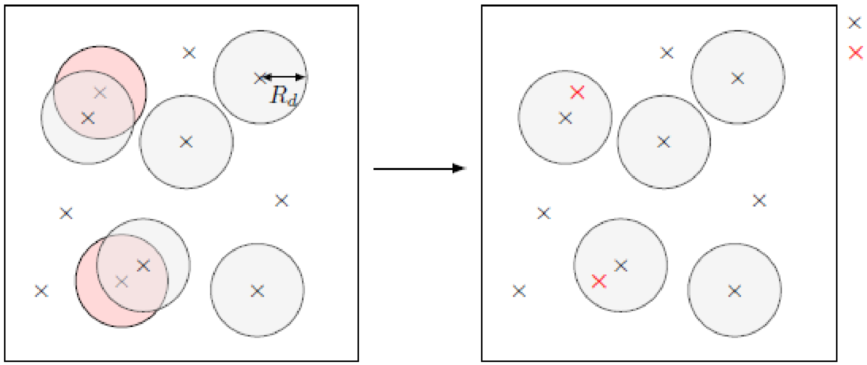

X Active site

× : Deactivated site

1. Nucleation Site Density Nsit : empirical relation f(Tw, Tsat, P, contact angle)
2. Static growing bubble <u>overlapping</u> probability : Pcoal,st
3. <u>Static coalescence</u> site density : Ncoal,st = Pcoal,st (Nb,Rd) Nsit,a
4. →Static & <u>Sliding Coalescing</u> Site Density Ncoal,st & Ncoal,sl (Rsl, …)

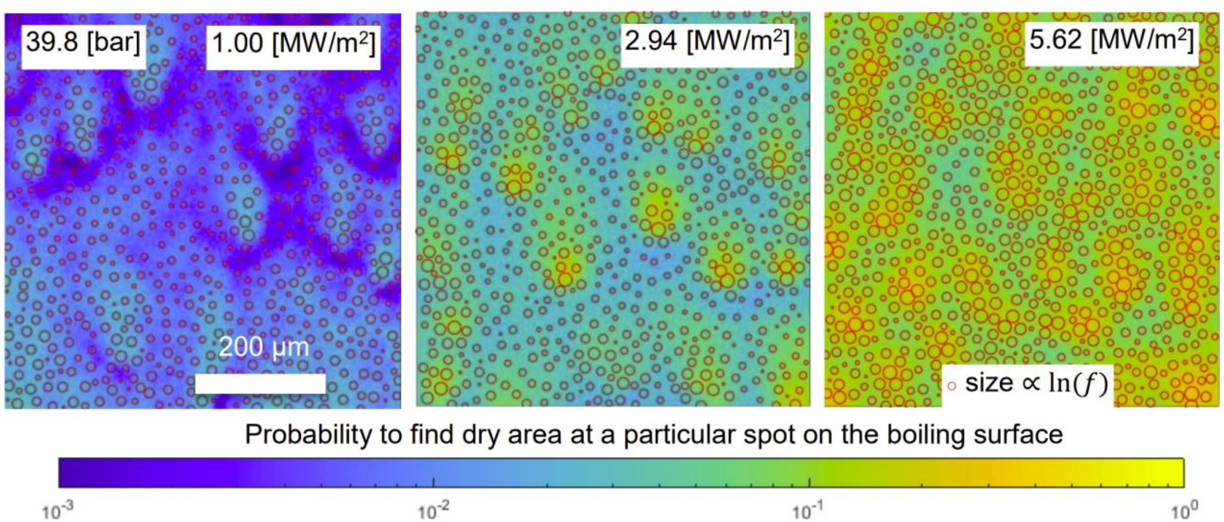

Nucleation site distribution

HEAT FLUX PARTITIONING CONSTRUCTION

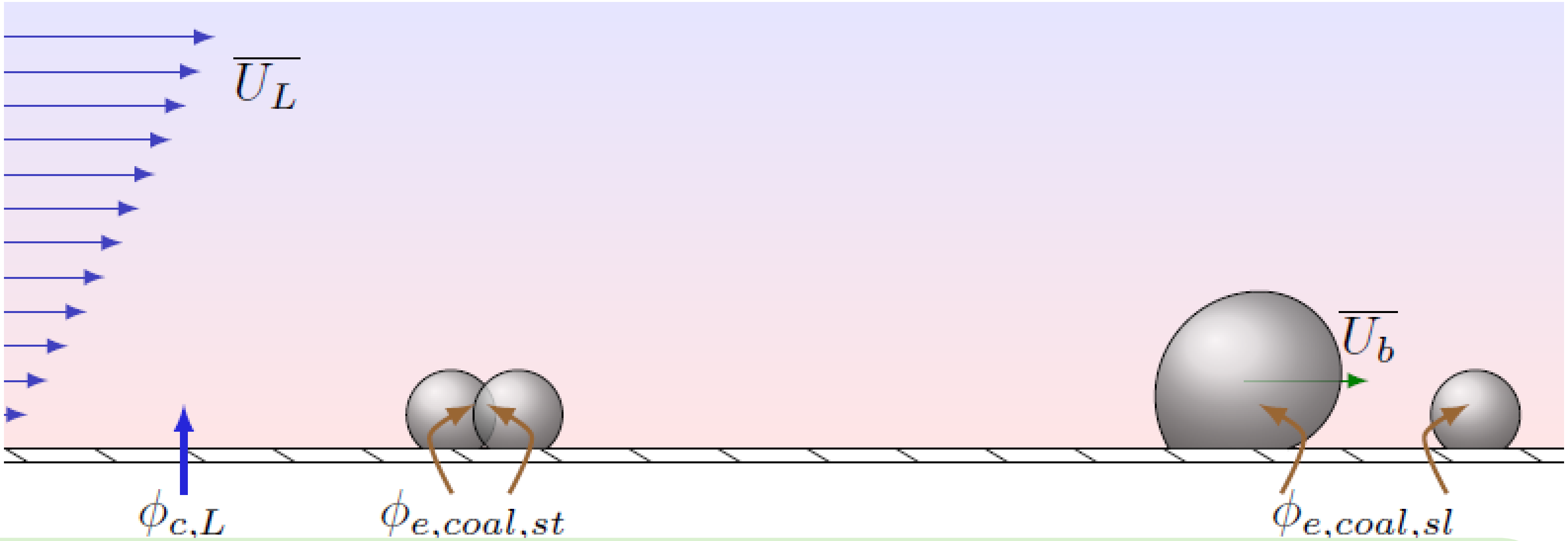

$$q''_w = q''_{cL} + q''_{e,coal\ st} + q''_{e,coal\ sl} + q''_q + q''_{cV}$$

- $q_{c,L} = Ac,l\ \ hc,l\ \ (Tw - TL)$ / $\phi c,V = Ac,V\ \ hc,V\ \ (Tw - Tsat)$
- *Static Coalescence Boiling Heat Flux :*

$$q''_{e,coal\ st} = \frac{N_{coal,st}}{2} f \rho_V h_{LV} \frac{4}{3} \pi R_d^3$$

- *Sliding Coalescence Boiling Heat Flux*

$$q''_{e,coal\ sl} = \frac{N_{coal,sl}}{2} f \rho_V h_{LV} \frac{4}{3} \pi (R_{sl}^3 + R_d^3)$$

QUENCHING HEAT FLUX

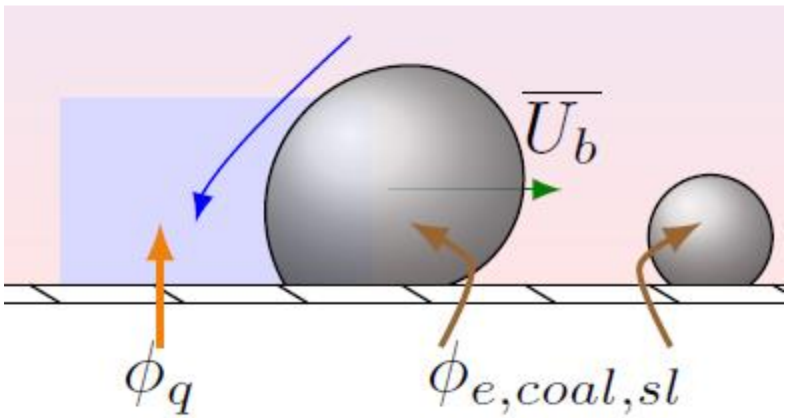

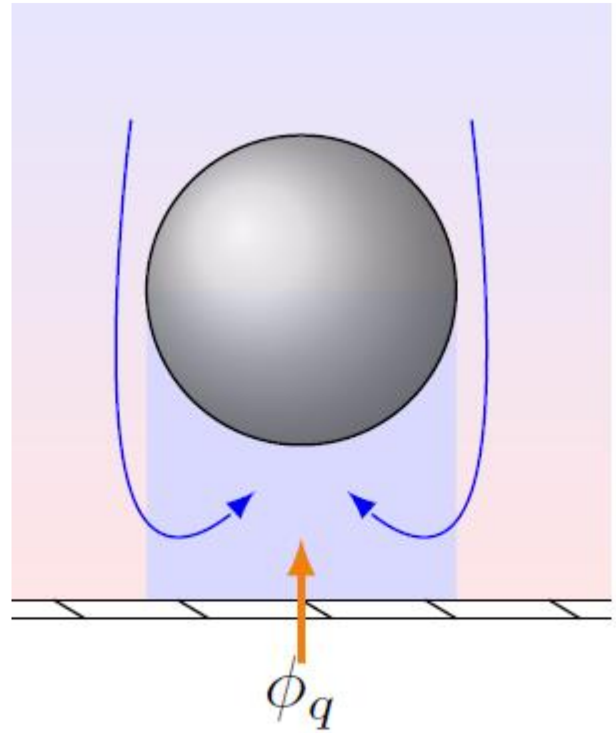

$$\phi_q = A_q t_q f \frac{2\lambda_L \left(\Delta T_w + \Delta T_L\right)}{\sqrt{\pi \eta_L t_q}}$$

Quenching area: $A_q = \underbrace{N_{coal,st} \pi R_d^2}_{\text{static coal.}} + \frac{N_{coal,sl}}{2} \underbrace{A_{q,1b}}_{\text{bubble sliding area}}$

NEW NUCLEATE BOILING : DEBORA EXP.

Test case	Deb5	Deb6
Inlet mass flow rate ($kg.m^{-2}s^{-1}$)	1996	1984.9
Inlet temperature (°C)	68.5	70.5
Wall heat flux ($MW.m^{-2}$)	1.2	0.8
Pressure (Mpa)	2.615	2.615
Quality	0.058	0.0848

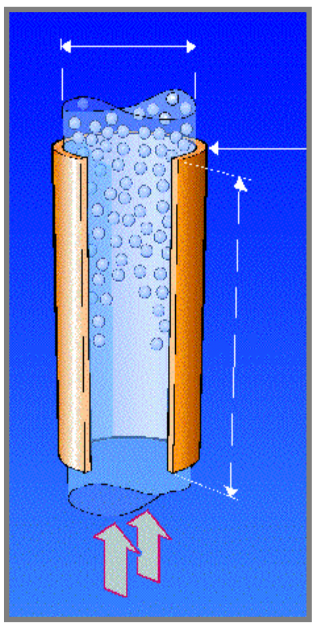

- 40 radial cells (～0.24 mm)
- 400 axial cells (～1 cm)
- Wall distance : *y+* ～100

Boundary Conditions:

◦ Axysymmetric simulation

◦ Outlet: uniform pressure

◦ Inlet: uniform velocity

◦ Wall: modified logarithmic law for bubbly flows [Mimouni et al., 2016] & uniform heat flux

◦ Other: Symmetry

C800

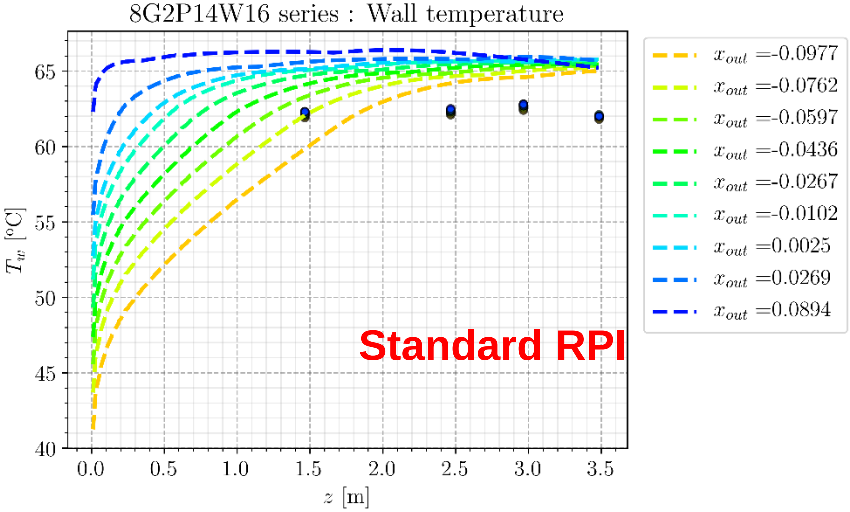

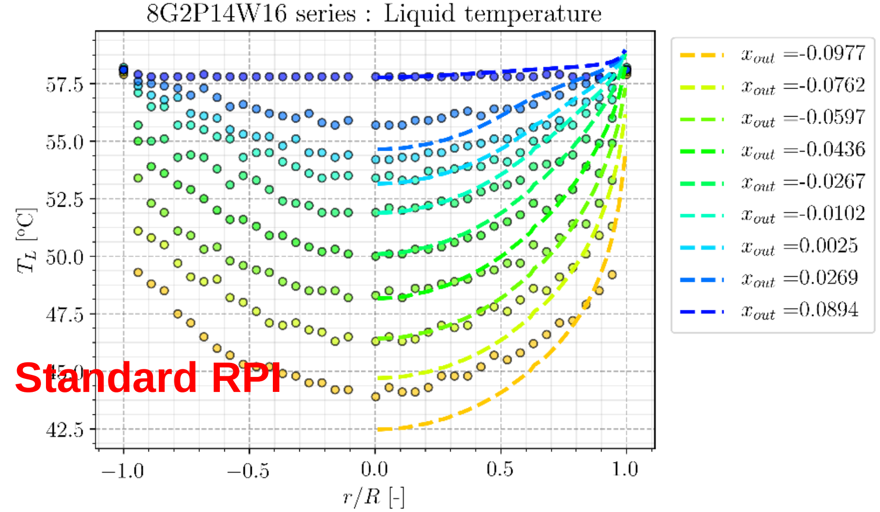

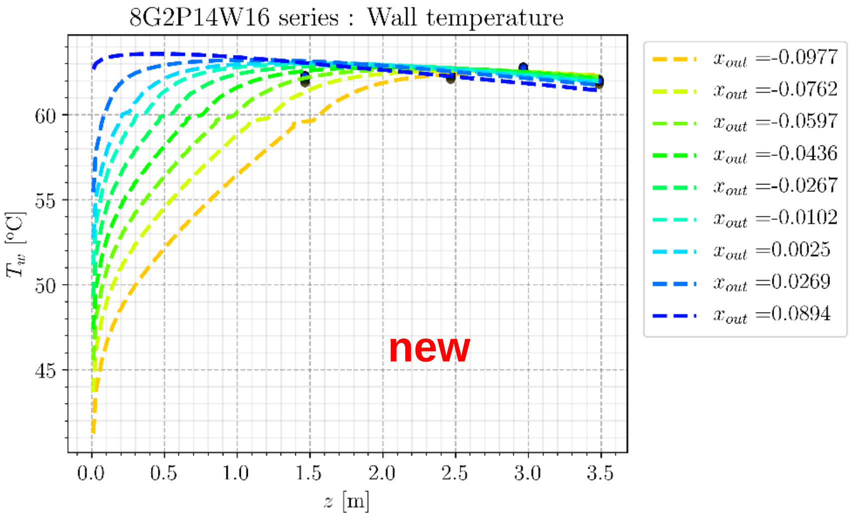

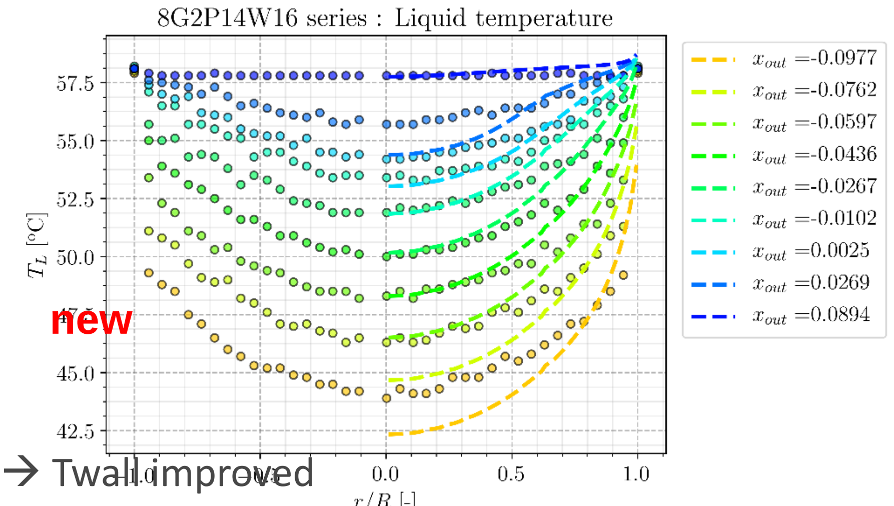

DEBORA exp : ~500 validation cases → Twall improved , other physical quantities are unchanged

→ Polydispersion bubble approach in further calculations

2. Multifield CFD calculations of industrial geometries

MSME, IMFT, CEA

FLOWS WITH LARGE INTERFACES LIQUID - GAS

Stephane.Mimouni@edf.fr

CONTEXT

Safety issues involved complex flows

Large range of bubbles diameters

Ex : Lift force coef $4 \le Eo_H \le 10 \quad C_L = 0.00105 Eo_H^3 - 0.0159 Eo_H^2 - 0.0204 Eo_H + 0.474$

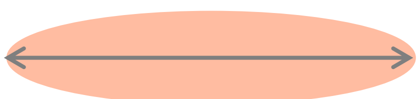

$$Eo_H = \frac{g(\rho_g - \rho_l) d_H^2}{\sigma}$$

$$d_H = D_b \sqrt[3]{1 + 0.163 Eo^{0.757}}$$

Wellek's correlation

$$Eo_H = \frac{g(\rho_g - \rho_l) D_b^2}{\sigma}$$

Db= mean Sauter Diameter

→ Large discrepancies for distorted bubbles

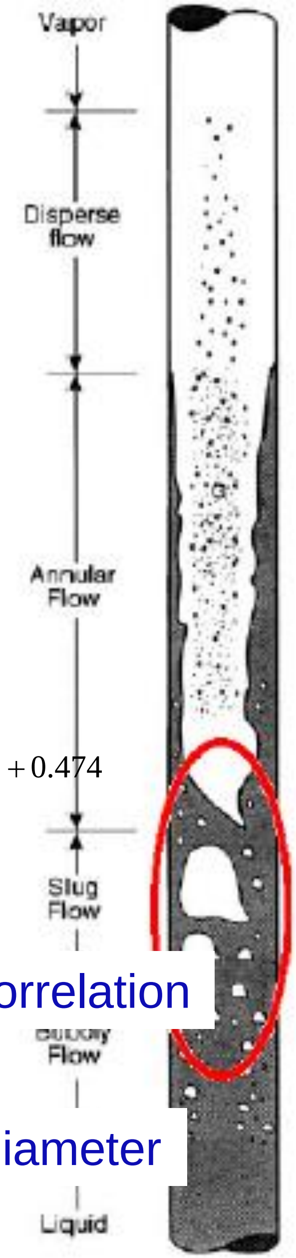

APPLICATION : COMPLEX FLOWS IN STEAM GENERATORS

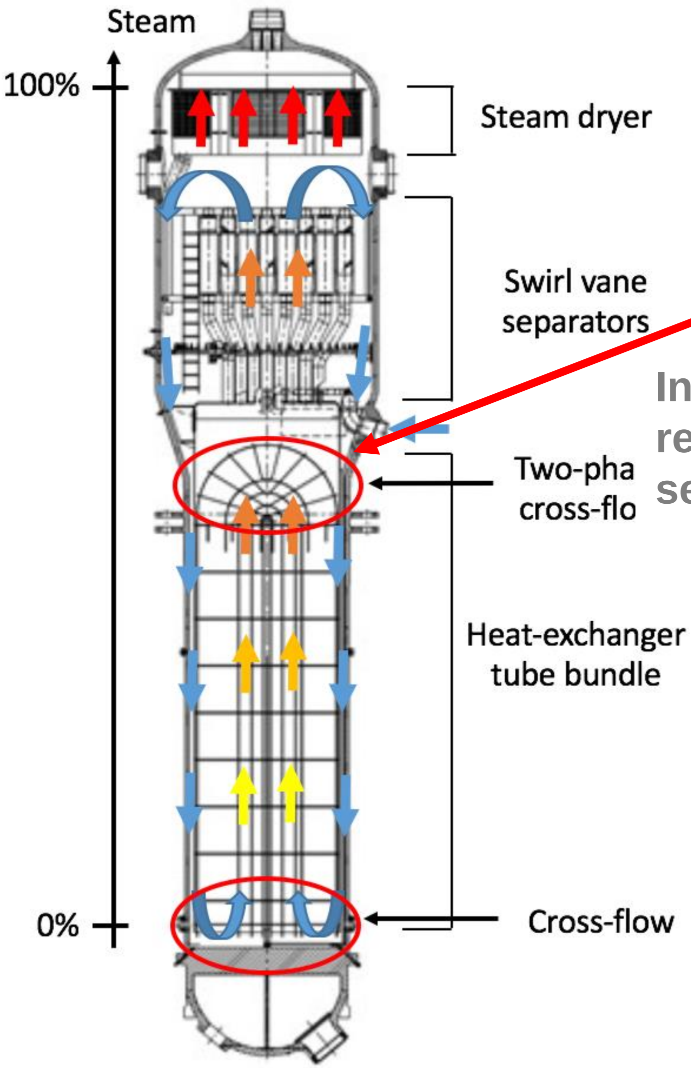

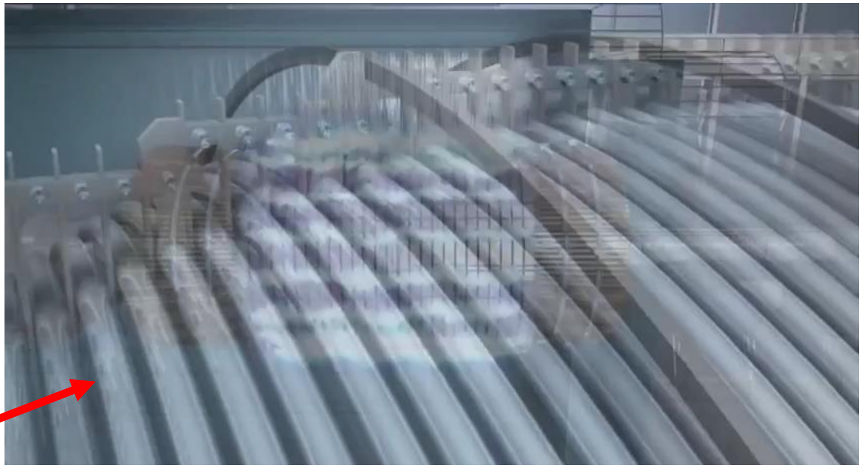

In the upper part, large vapor bubbles are created and are responsible of the vibrations of the tubes wich can cause severe mechanical damages

MODELLING STRATEGY: MULTIFIELD APPROACH

Denèfle et al., 2013
Fleau et al., 2017

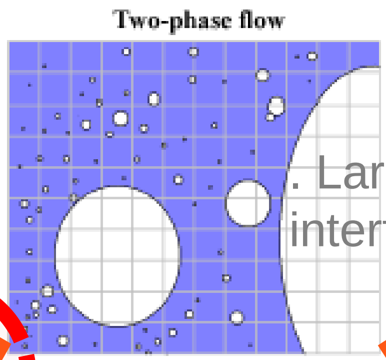

. Large bubbles are calculated by an interface tracking method

Large Bubble Model

Surface tension, drag force model, interface sharpening equation

Interfacial momentum closure laws (drag, lift, added mass,…)

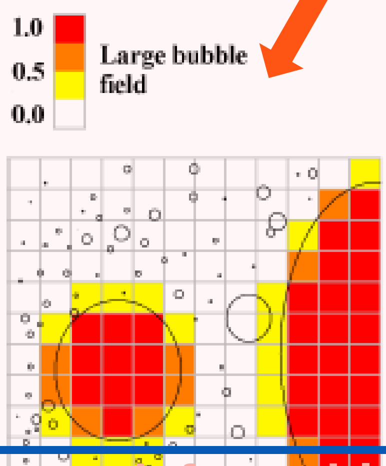

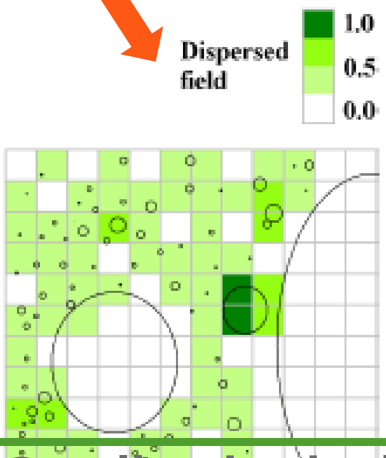

Mass transfers

Coalescence and breakup

Large deformable bubbles

Small spherical bubbles

LIQUID / VAPOR INTERFACE

Large Bubble Model

- Large deformable interfaces
- Two different velocity fields are defined at the interface
- Interface smearing caused by the two-fluid approach

Control the interface thickness

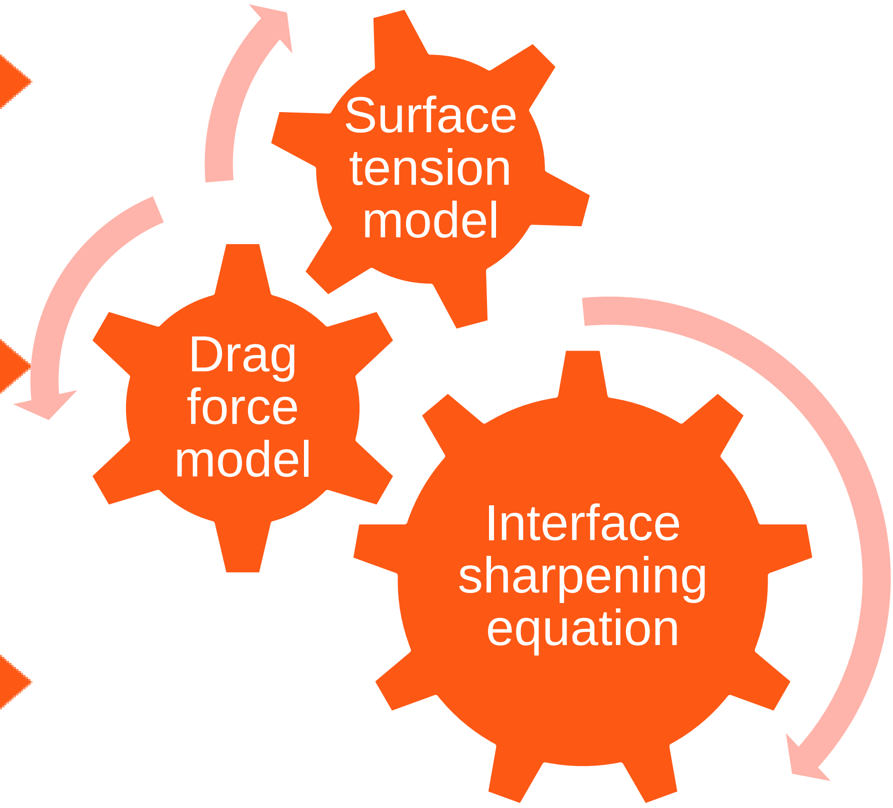

Denèfle et al., 2013
Fleau et al., 2017

LIQUID / VAPOR INTERFACE

Surface tension force, Brackbill et al. [1992]:

- For deformable interfaces with a finite thickness

$$F_{CSF} = \alpha_k \, \sigma \kappa \nabla \alpha_k \quad \text{with } \kappa = -\nabla . \left(\frac{\nabla \alpha_k}{||\nabla \alpha_k||} \right) : \text{theory}$$

Drag force law: To couple the velocity of each field at the interface: subgrid model

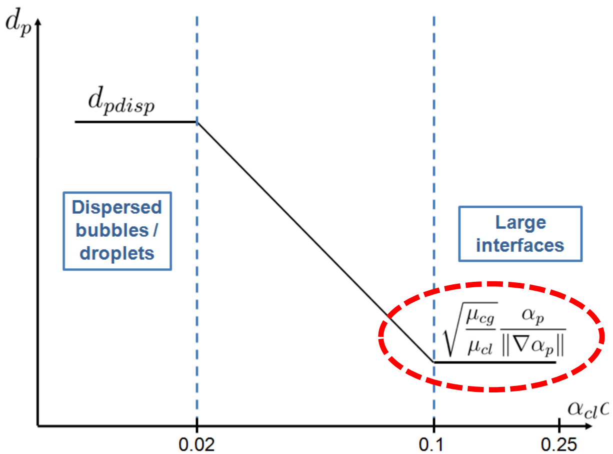

Bubbly flow

$$\alpha_{cg} < 0.3 : \qquad \mathbf{F}_{bubble} = \alpha_{cl}\alpha_{cg}\frac{18\mu_{cl}}{\alpha_{cl}d_p^2}\left(\mathbf{u}_{cl} - \mathbf{u}_{cg}\right)$$

Droplet flow

$$\alpha_{cg} > 0.7 : \qquad \mathbf{F}_{droplet} = \alpha_{cl}\alpha_{cg}\frac{18\mu_{cg}}{\alpha_{cg}d_p^2}\left(\mathbf{u}_{cl} - \mathbf{u}_{cg}\right)$$

Complex flow

$$0.3 \leq \alpha_{cg} \leq 0.7 : \quad \mathbf{F}_{mix} = \frac{0.7 - \alpha_{cg}}{0.7 - 0.3}\mathbf{F}_{bubble} + \frac{\alpha_{cg} - 0.3}{0.7 - 0.3}\mathbf{F}_{droplet}$$

[Brackbill, J.U. *et al.*, 1992, A continuum method for modeling surface tension, *J. Comput. Phys.*, Vol. 100, pp. 335-354]

NEED OF THE INTERFACE LIQUID/VAPOR MODELS : CASE OF A RISING BUBBLE

Complete LBMo | No sharpening | No surface tension | No drag force

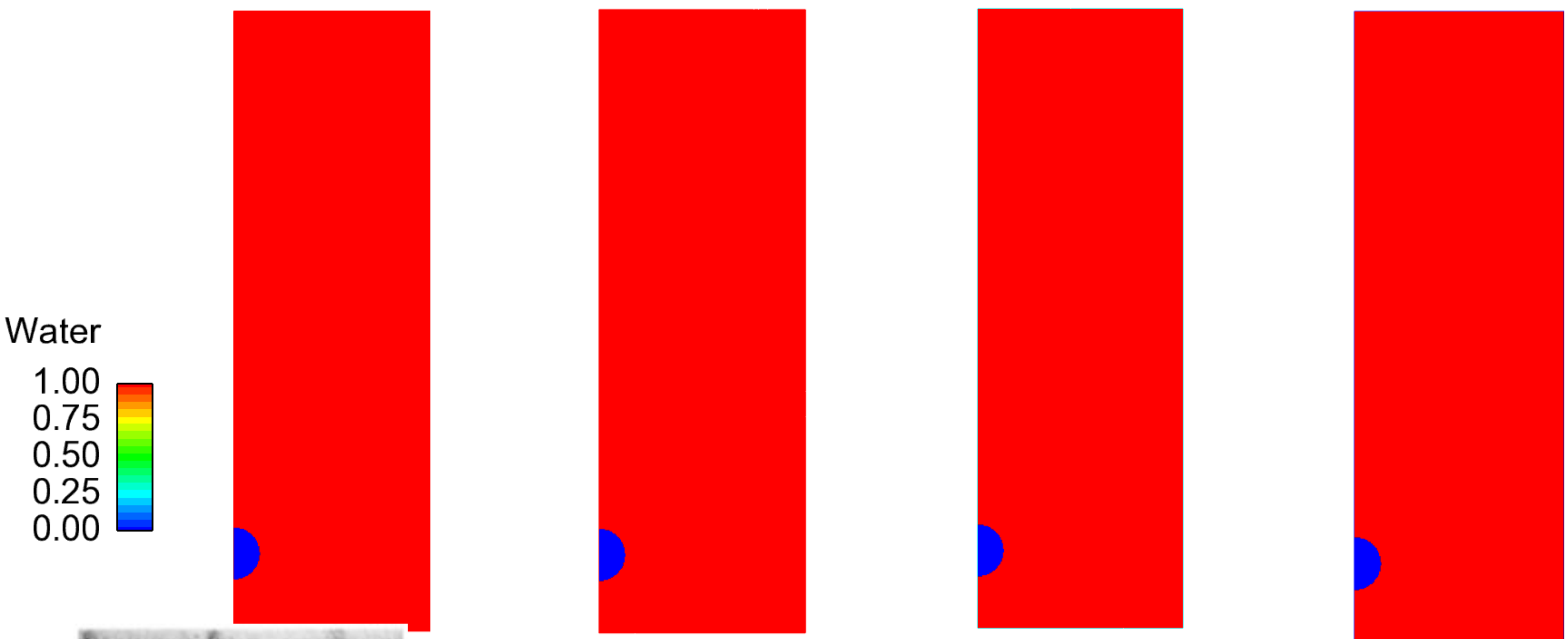

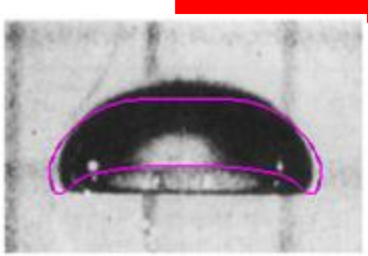

Time = 0.000000 s

The sharpening equation or the surface tension is sometimes forgot in industrial studies in order to save CPU time but the results could be not realistic.

METERO EXPERIMENT (CEA)

- M. Bottin, J.P. Berlandis, E. Hervieu, M. Lance, M. Marchand, O.C. Öztürk, G. Serre, “Experimental investigation of a developing two-phase bubbly flow in horizontal pipe”.

- This experiment has been developed in the frame of the NEPTUNE project, jointly developed by CEA, EDF, FRAMATOME and IRSN.

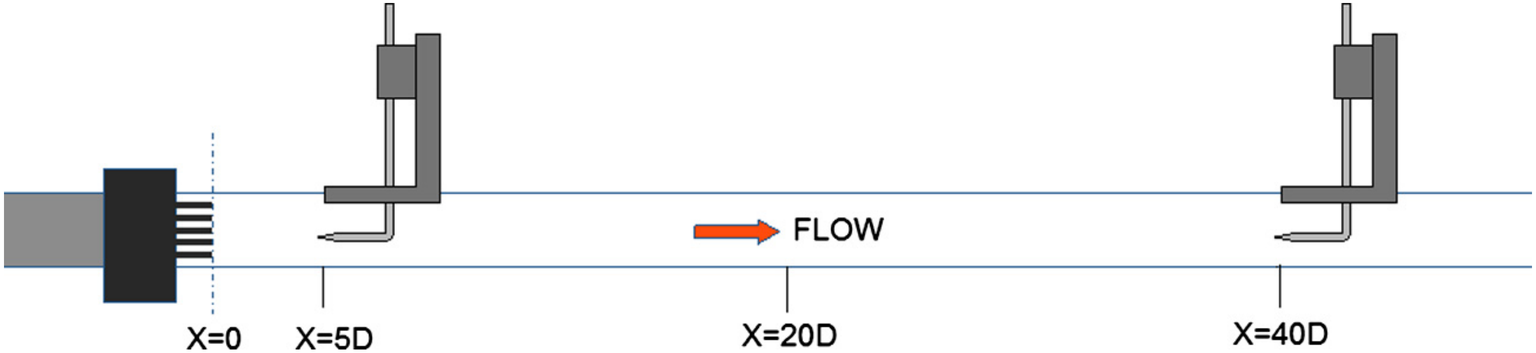

- The test section, 5.40 m long, has an inner diameter D = 0.1 m

- air injection tubes have been set to ensure uniform bubble injection in the inlet section.

- Inlet : water (0–5 m/s)+ air bubble (0–0.7 m/s).

- → provide a flow pattern map.

EXPERIMENTAL OBSERVATIONS

MSME, IMFT, CEA

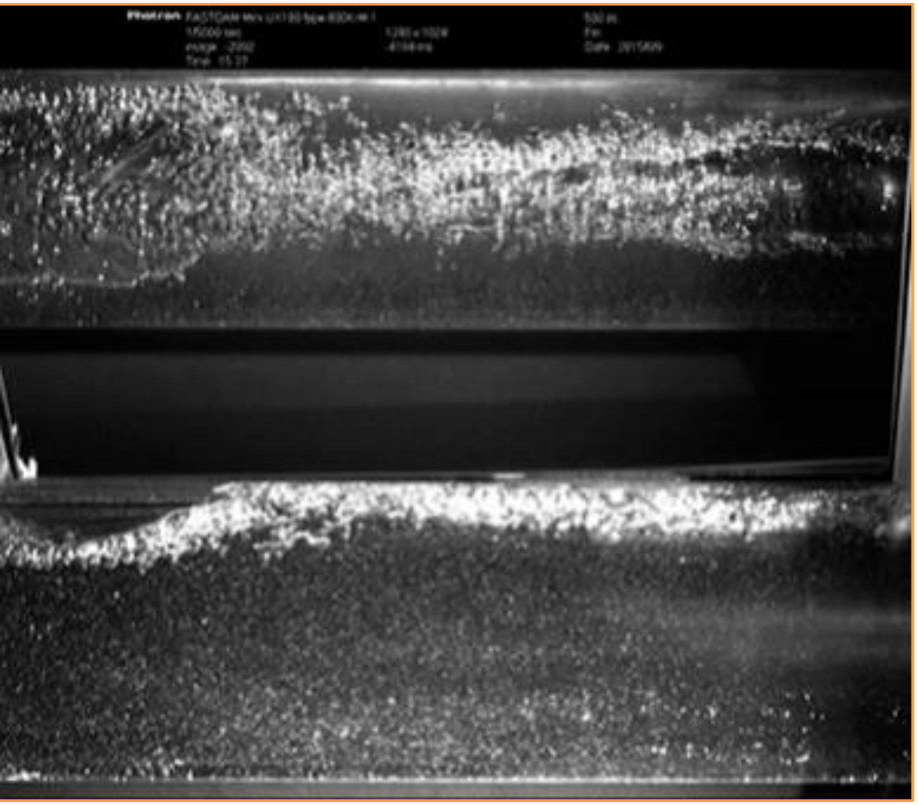

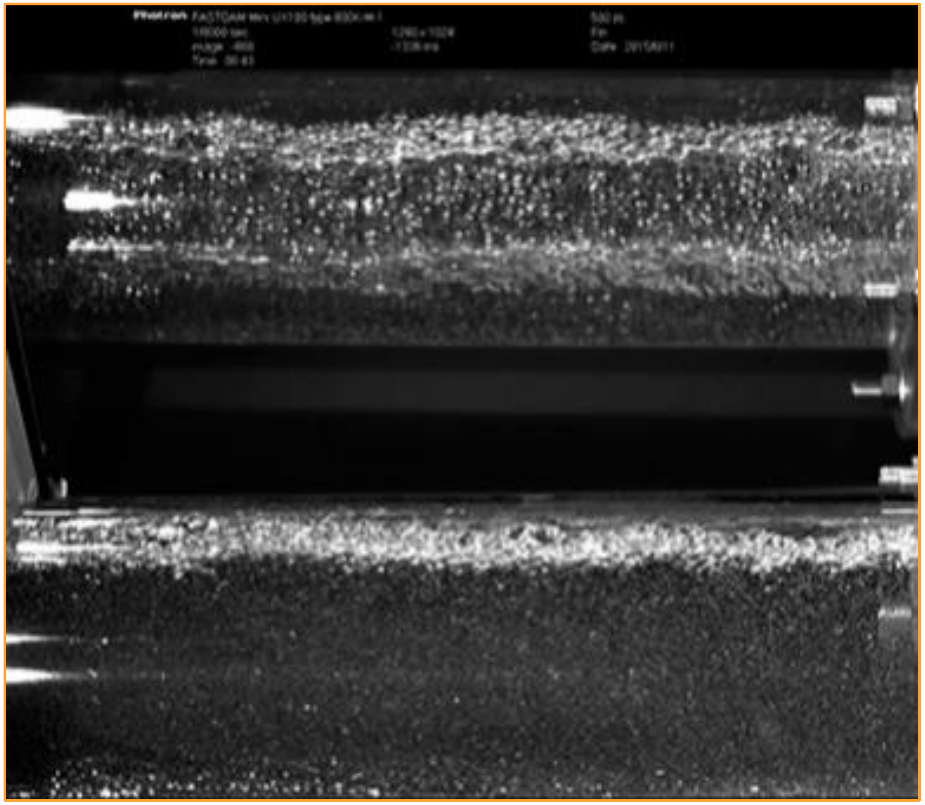

Stephane.Mimouni@edf.fr

METERO: FLOW PATTERN MAP FOR X/D = 40

Calculations : Jg is fixed and Jl increases

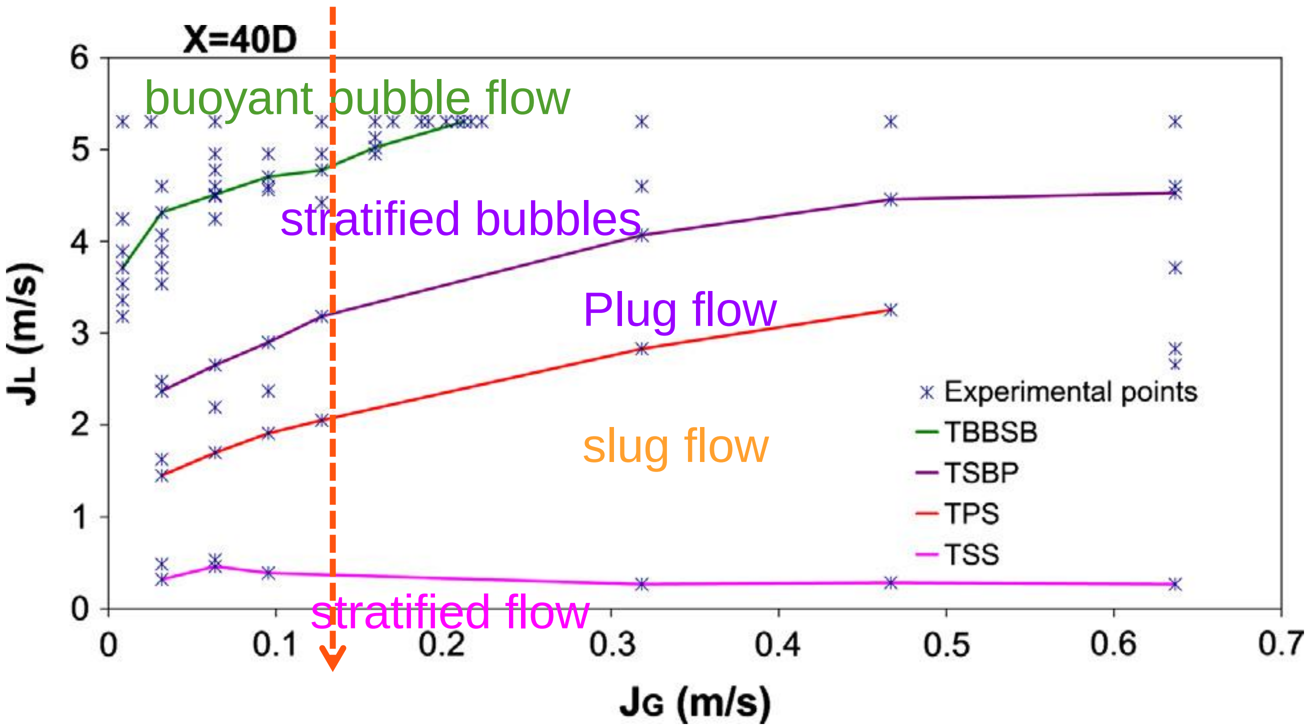

Transition from slug to stratified flow (TSS)
transition from plug to slug flow (TPS)
transition from buoyant bubble flow to stratified bubble flow (TBBSB)
transition from stratified bubbles regime to plug (TSBP)

PLUG FLOW REGIME: MEDIUM VALUE OF LIQUID MASS FLOWRATE

JL = 2.12 m/s; JG = 0.1273 m/s

JL = 2.4 m/s; JG = 0.03m/s

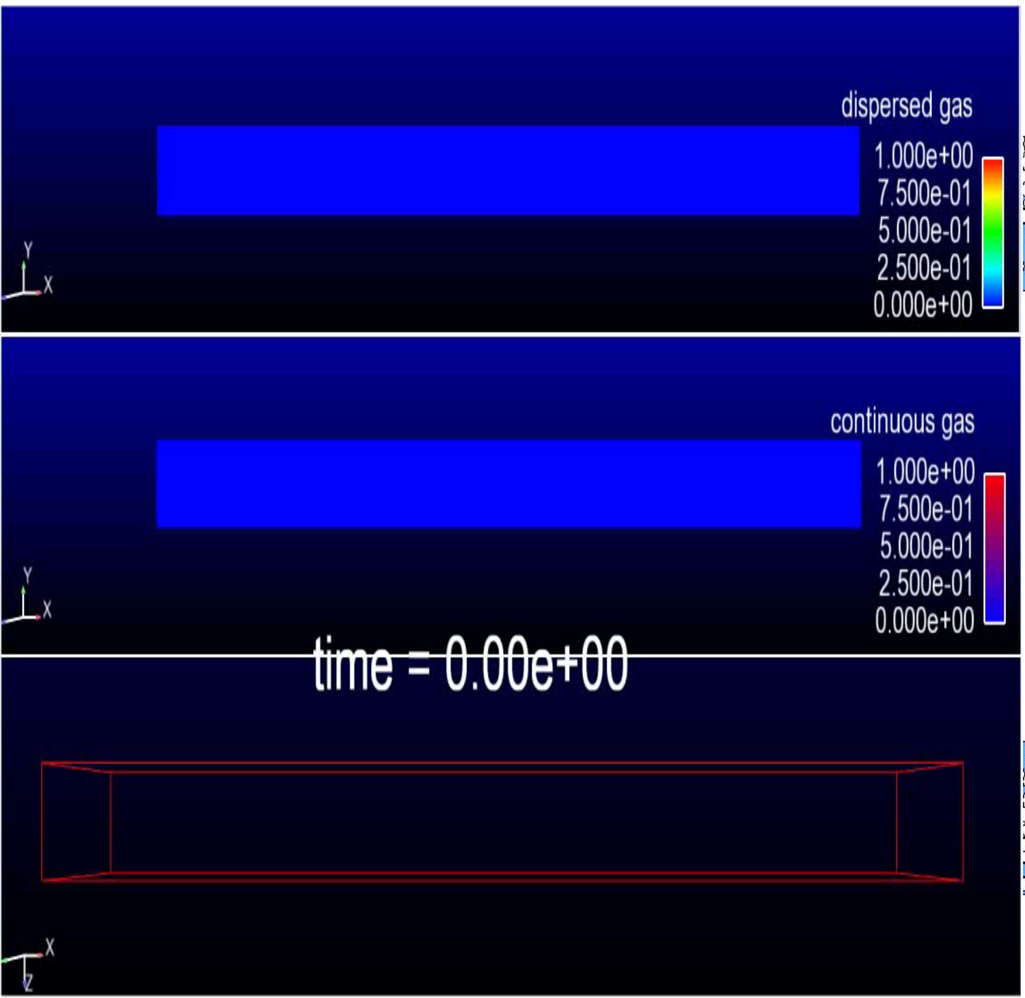

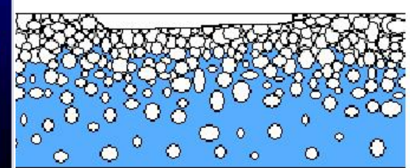

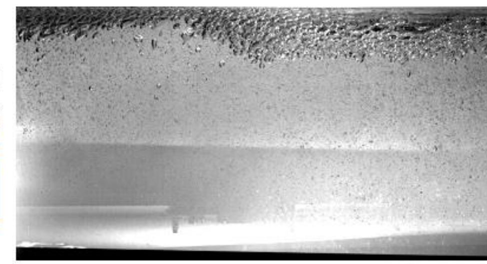

Side view

top bubbles coalesce to form plugs→ intermittent regime

Top view

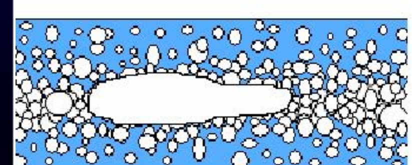

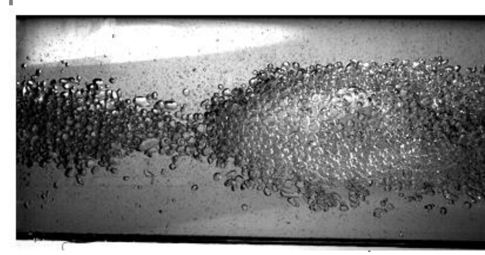

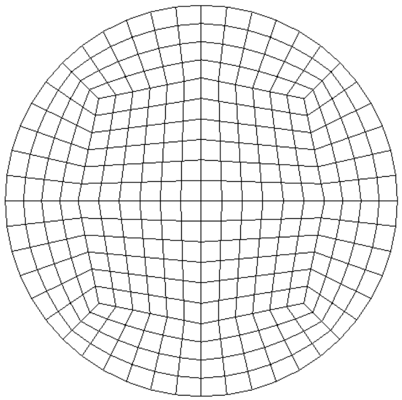

mesh 1 = 271000 cells

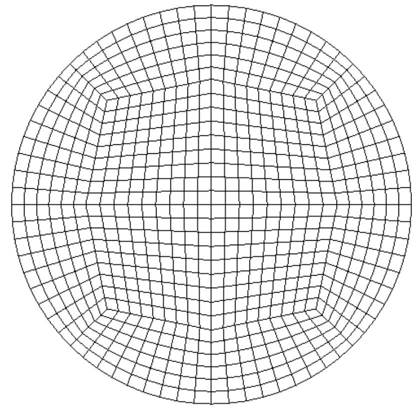

mesh 2 = 966000 cells

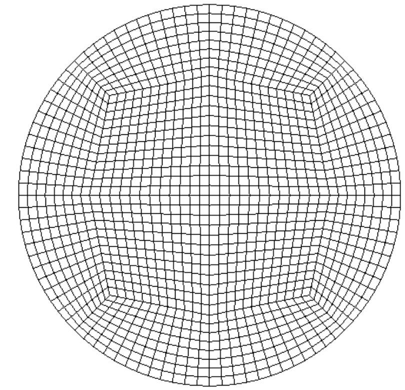

mesh 3= 2 327000 cells

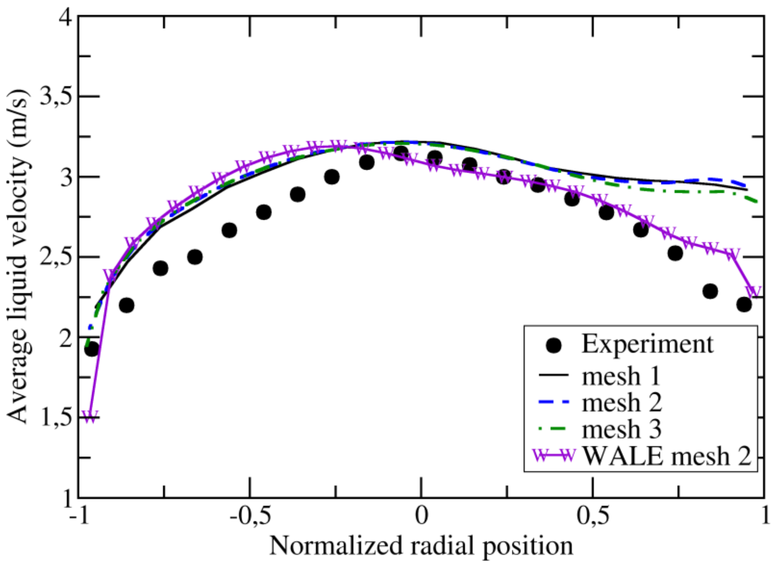

Figure 9c: Bubble velocity at 40D (plug flow).

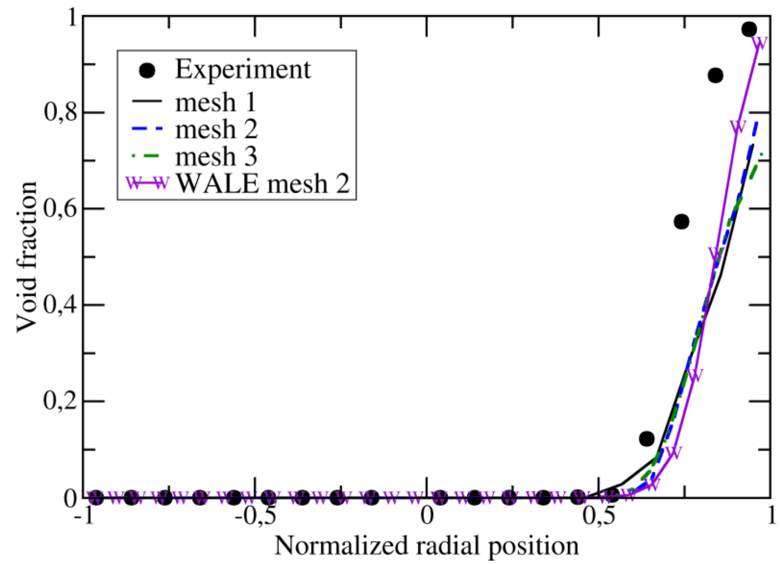

Figure 9d: Void fraction at 40D (plug flow).

SENSITIVITY TO THE MESH REFINEMENT

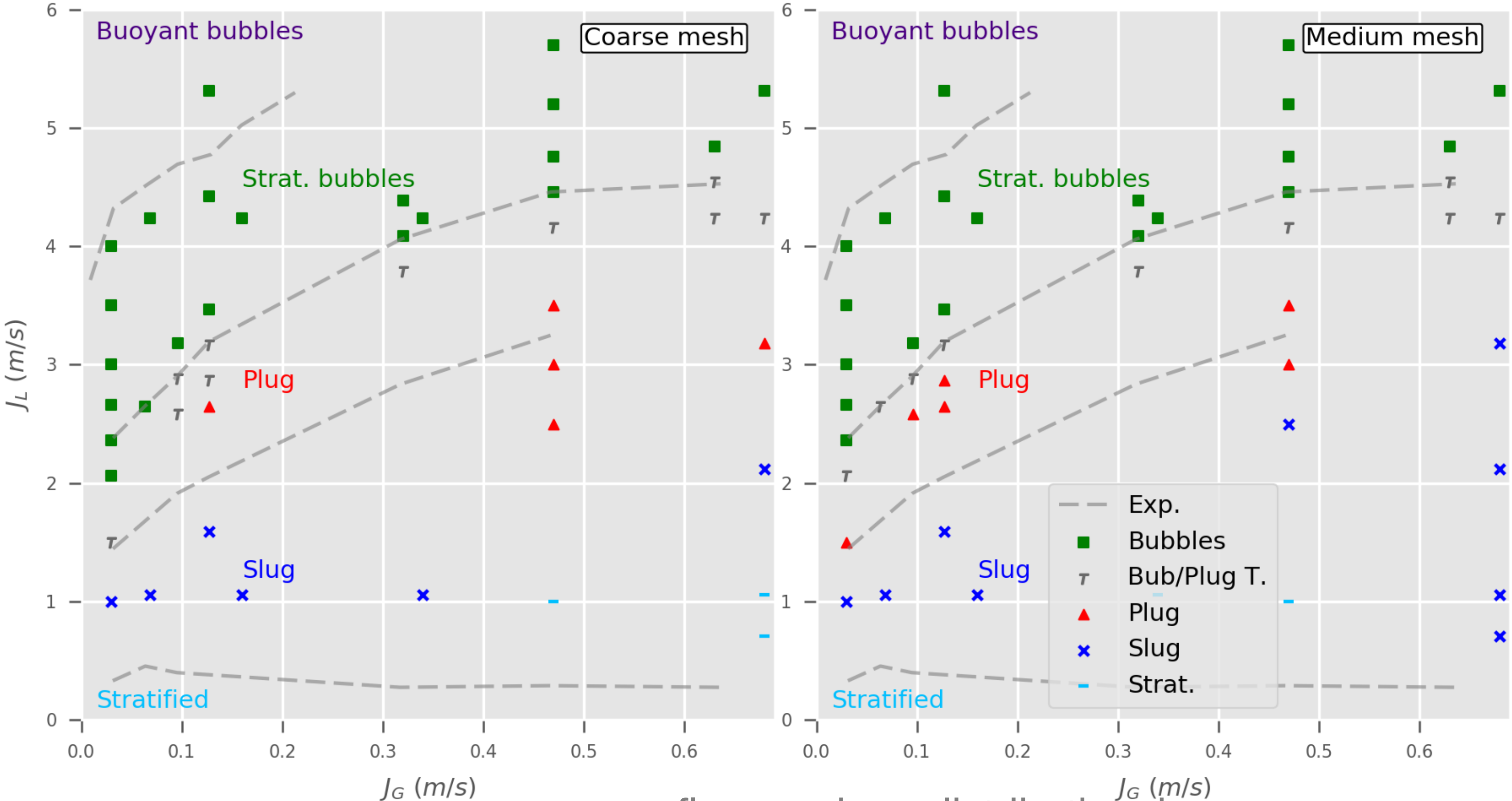

α critical = 30%

flow regime distribution is in good agreement with experimental data, especially for the bubble/plug transition.

Sensitivity to the mesh refinement

Stephane.Mimouni@edf.fr

TOWARD AN DIMENSIONLESS-NUMBERS-BASED MODEL

large bubble of a given length scale L.

Several mechanisms can destabilize the bubble :

- **Effect of gravity on bubble deformation can be described by EOTVOS number:**

$$Eo = \frac{\Delta \rho g L^2}{\sigma}$$

- **WEBER number: relative importance of the fluid's inertia compared to its surface tension**

$$\mathrm{We} = \frac{\rho_l v^2 L}{\sigma}$$

- **HINZE introduces a turbulent WEBER value, comparing eddies kinetic velocity to surface tension cohesion of a bubble :**

$$\mathrm{We} = \frac{\rho_l (u')^2 L}{\sigma}$$

→ Eddies which scale is the same as the bubbles can lead to distortion and breakup of the bubbles.

Stephane.Mimouni@edf.fr

TOWARD AN DIMENSIONLESS-NUMBERS-BASED MODEL

surface tension energy of bubble $\sigma 4\pi \left(\frac{d}{2}\right)^2$

is

the turbulent kinetic energy of a sphere which diameter is the same as the bubble, able to destabilize it, is : $\frac{1}{2}\rho_l \frac{4}{3}\left(\frac{d}{2}\right)^3$

Bubble breakup is possible when these quantities are of the same order of magnitude → $\mathrm{We}_{turb} \sim 12$

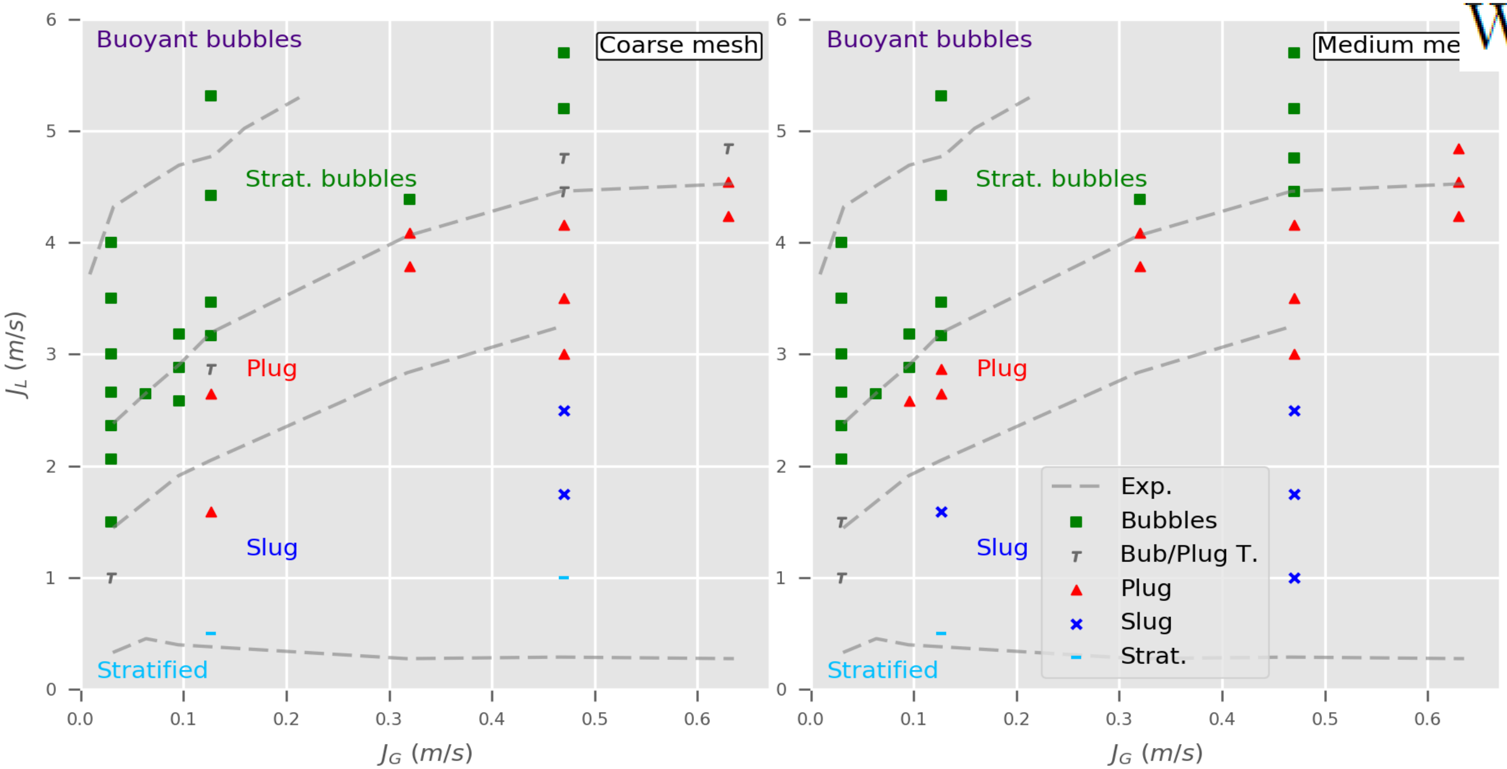

criterion based on non-dimensional numbers can be more easily generalized to different fluids and different thermalhydraulics conditions

APPLICATION TO TUBES VIBRATION ANALYSIS IN STEAM GENERATOR : MAXI 2 EXPERIMENT (CEA)

- **3D two-phase R114 Freon (**simulant fluid for water at high pressure)
- **40 rows of 5 tubes (adiabatic) inclined of 30° with the horizontal .**
- **Void fraction and gas velocity are measured along the line NS defined by x = 48.75mm and z = 276.36mm, and the line WE defined by y = 48.75mm and z = 276.36mm, i.e. between the 7th and 8th row tubes.**

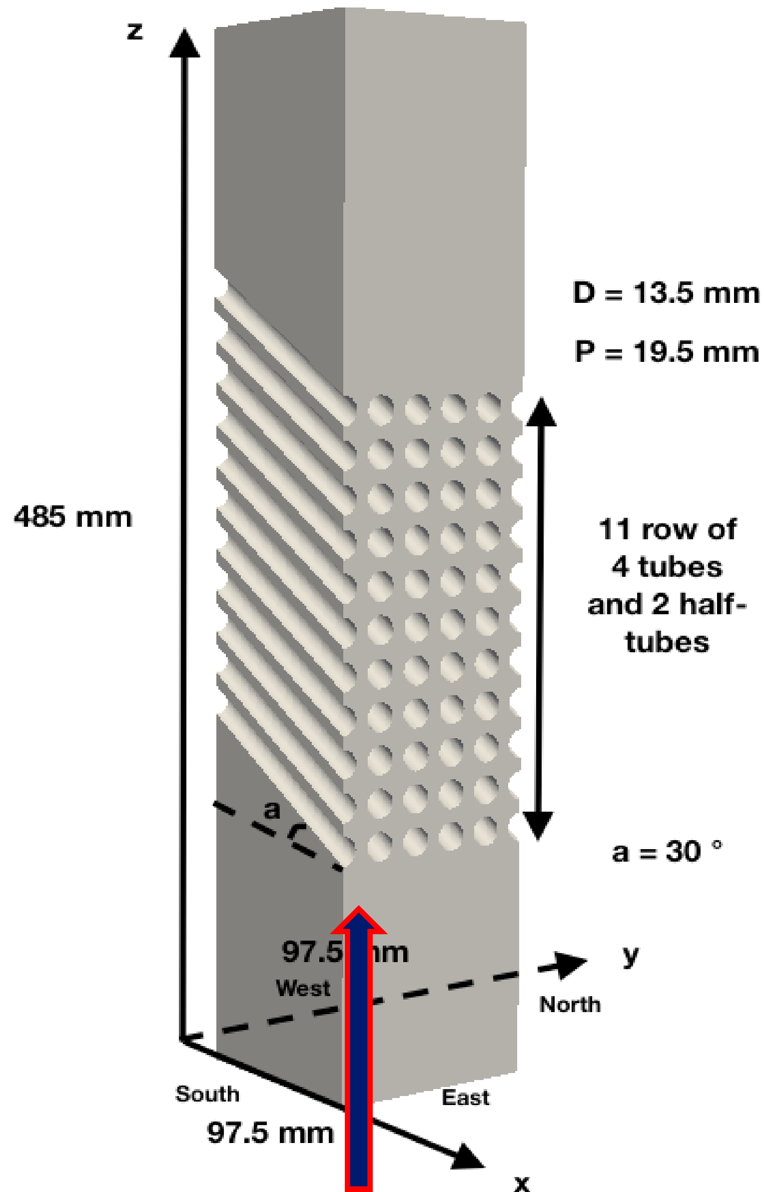

At inlet : Liquid + vapor

Validation of the two-phase numerical model
MAXI2 Experiment Freon/Freon

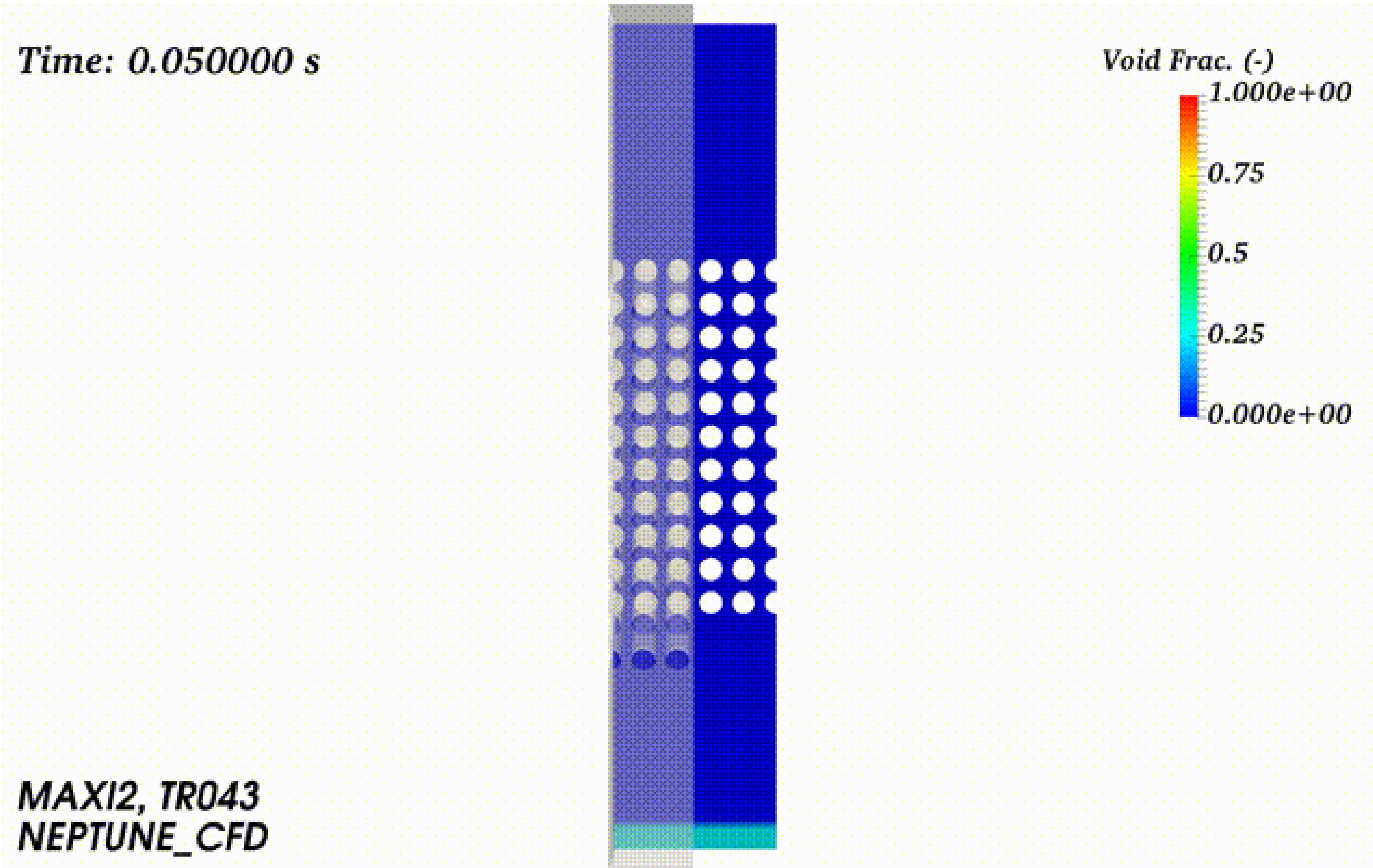

MAXI : 3 FIELDS → QUITE ENCOURAGING

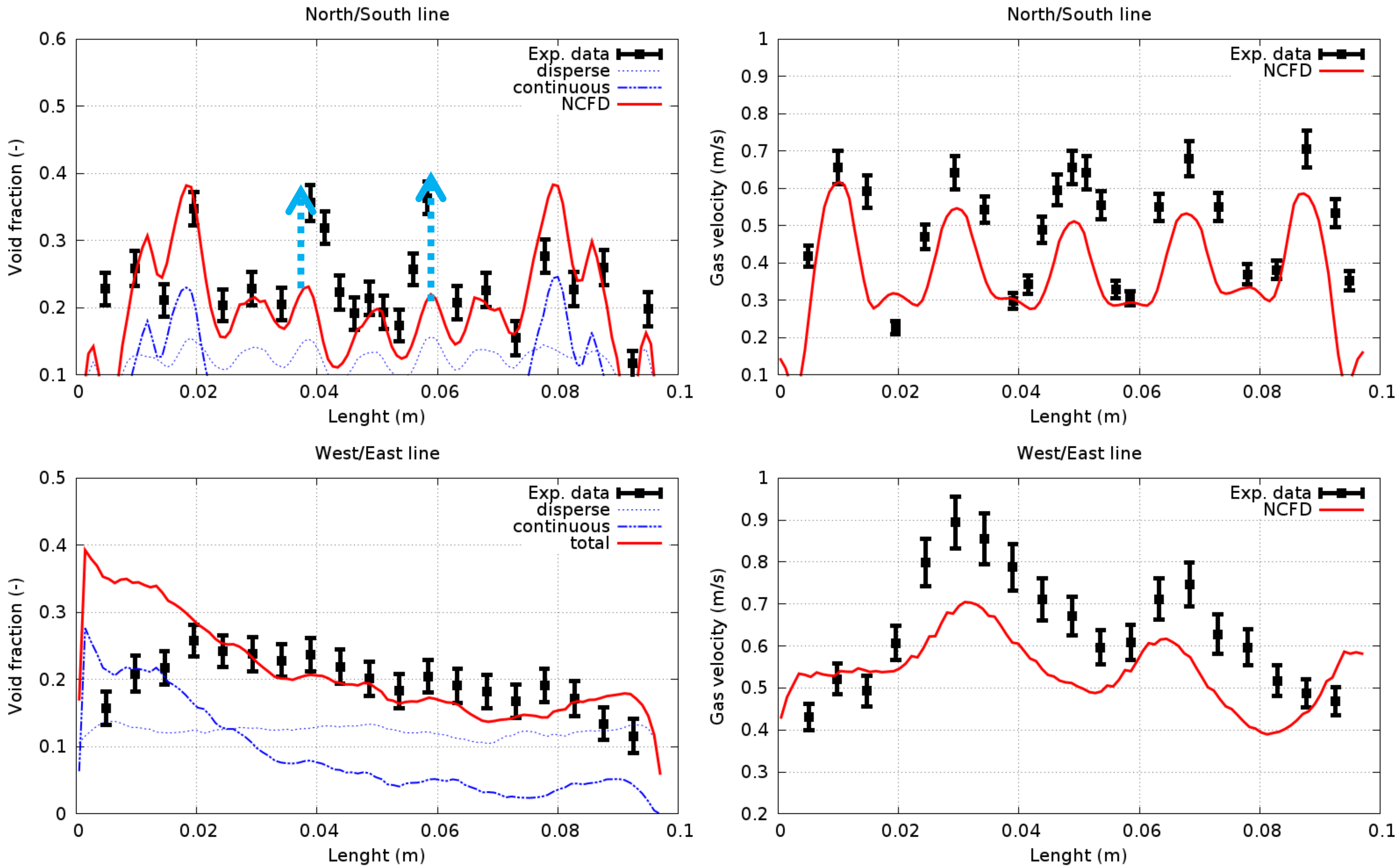

INTERFACE LOCATING METHODS→ LES

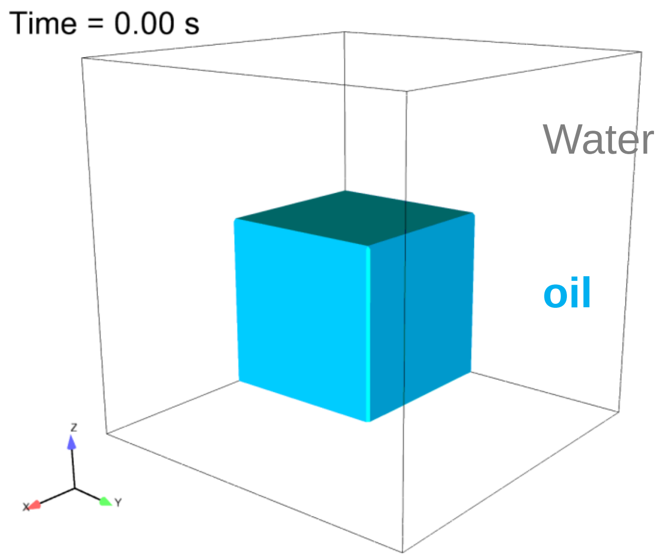

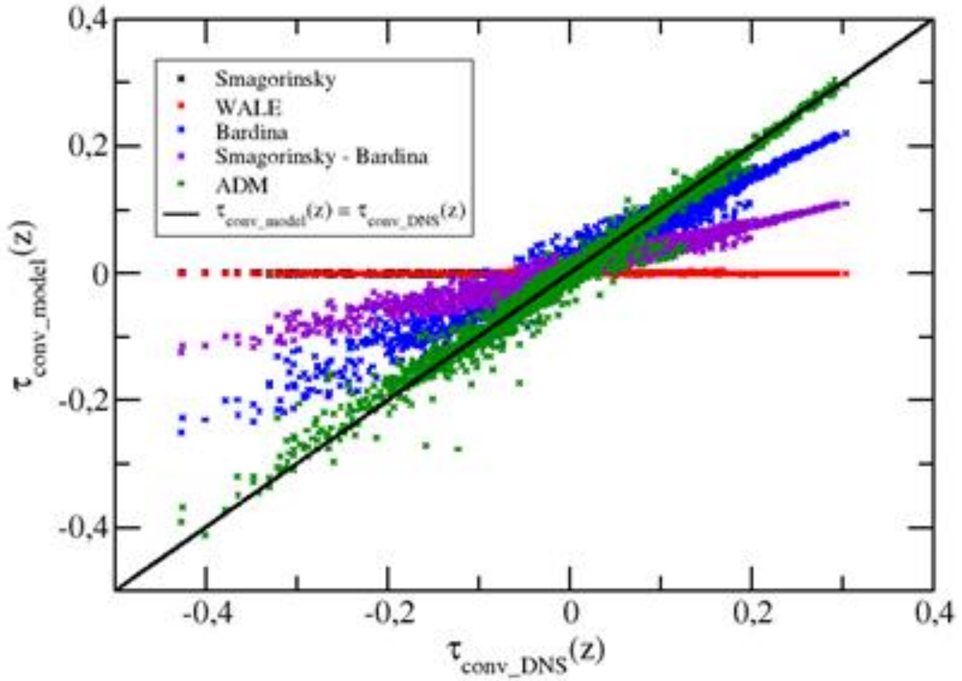

- Filtered momentum balance equation:

$$\rho_k \partial_t(\overline{\alpha_k}\,\overline{\boldsymbol{u}_k}) + \boxed{\tau_{time}} + \rho_k \nabla.(\overline{\alpha_k}\,\overline{\boldsymbol{u}_k}\otimes\overline{\boldsymbol{u}_k}) + \boxed{\tau_{conv}} = \mu_k \nabla.\left(\overline{\alpha_k \underline{\underline{S_k}}}\right) + \boxed{\tau_{diff}}$$
$$-\overline{\alpha_k}\nabla\overline{P} - \boxed{\tau_{pressure}}$$
$$+\overline{\alpha_k}\rho_k \boldsymbol{g} + \widehat{\boldsymbol{F}_{CSF}} + \boxed{\tau_{superf}} + \widehat{\boldsymbol{F}_{Drag}} + \boxed{\tau_{drag}}$$

[Vincent, S., Tavares, M., Fleau, S., Mimouni, S. *et al.*, 2016, *A priori* filtering and LES modeling of turbulent two-phase flows Application to phase separation, *Comput. Fluids*]

CONCLUSION FOR MULTIFIELD FLOWS

- **Large interfaces and dispersed bubbly + droplets in the same calculations.**
- **Reasonable accuracy for industrial cases with reasonable grid size (1mm) and reasonable CPU.**
- **Sensitivity to mesh refinement → reasonable.**
- **dimensionless numbers → encouraging results for the transition regimes**
- **<u>Turbulence → transition regimes : How to calculate all subgrid terms ?</u>**
- **<u>How to combine LES for large interfaces (deterministic approach) + RANS for dispersed flow (stochastic approach) ?</u>**
- **<u>Transition regimes → large interface calculated accurately → AMR (adaptive Mesh refinement) : which degree of maturity?</u>**

PHASE CHANGE : « BRACKBILISATION »

$$\boldsymbol{\Gamma}_{\boldsymbol{Steam}} = \frac{Q_{Liq\rightarrow Steam} + Q_{Steam\rightarrow Liq}}{H_{Liq} - H_{Steam}}$$

Where:

$$Q_{Liq} = \alpha_{Liq}\,\lambda_{Liq}\,\boldsymbol{\nabla T_{Liq}} \cdot \boldsymbol{\nabla \alpha_{Liq}}$$

$$Q_{Steam} = -\alpha_{Steam}\,\lambda_{Steam}\,\boldsymbol{\nabla T_{Steam}} \cdot \boldsymbol{\nabla \alpha_{Steam}}$$

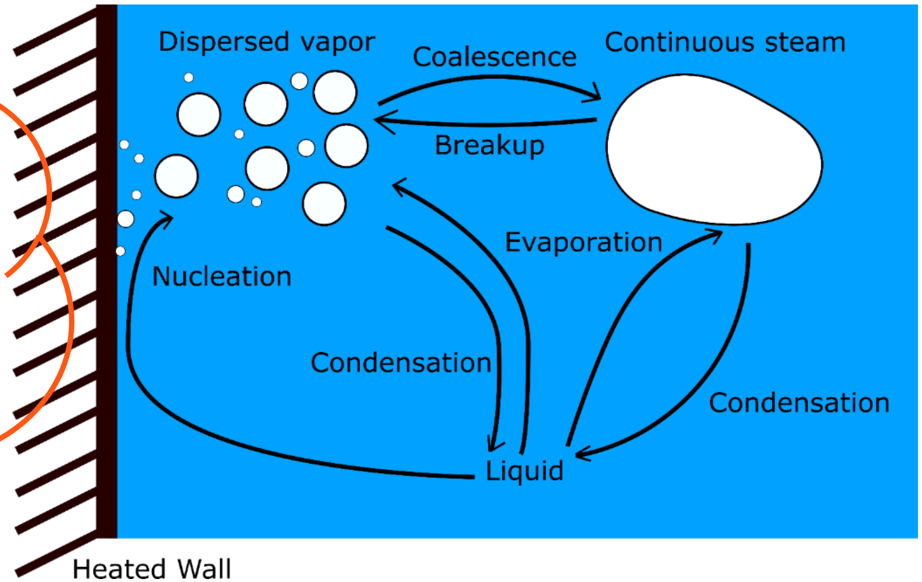

VALIDATION : VAPOR FRONT

1D tube with a heated wall . The liquid is overheated, and the wall temperature is equal to T_{sat} → steam is at the saturation temperature

Sucking pb

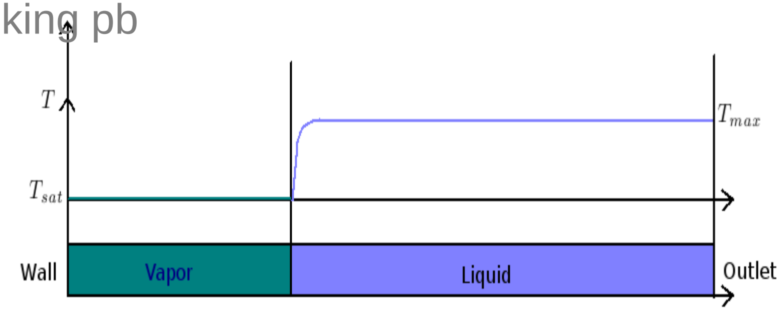

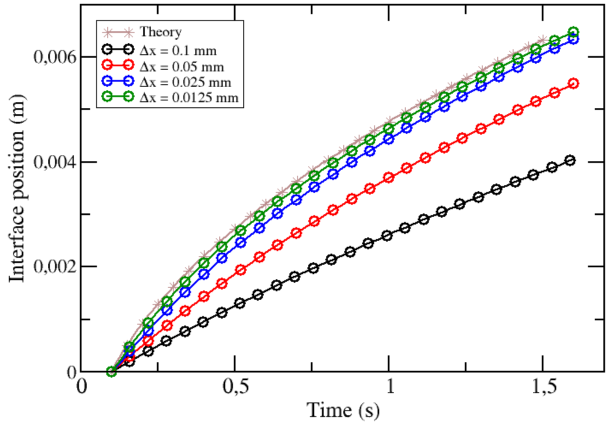

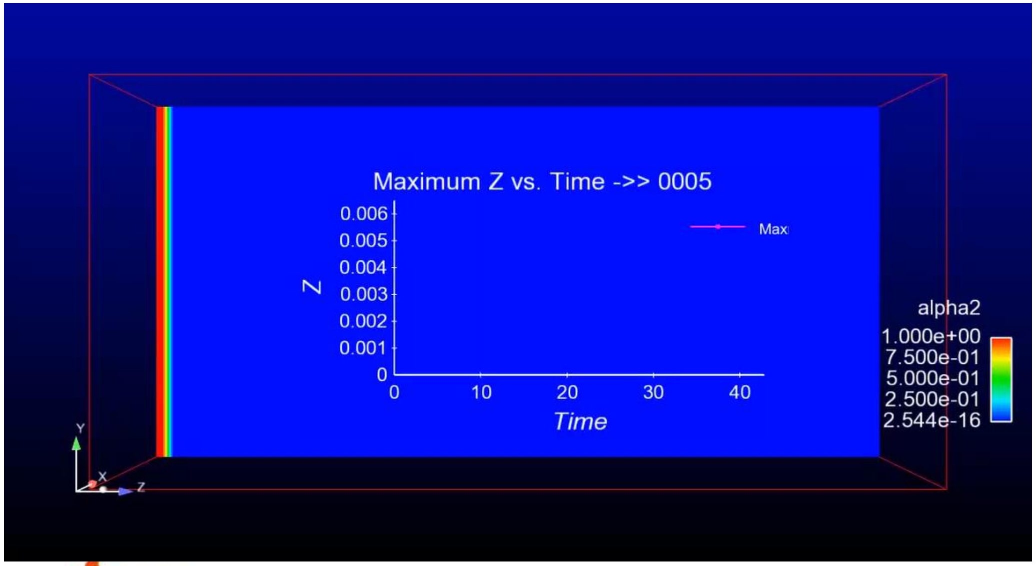

the liquid begins to boil at the interface, which induces a displacement of the steam/water interface

SODIUM FAST REACTOR : GR19→KNS 37

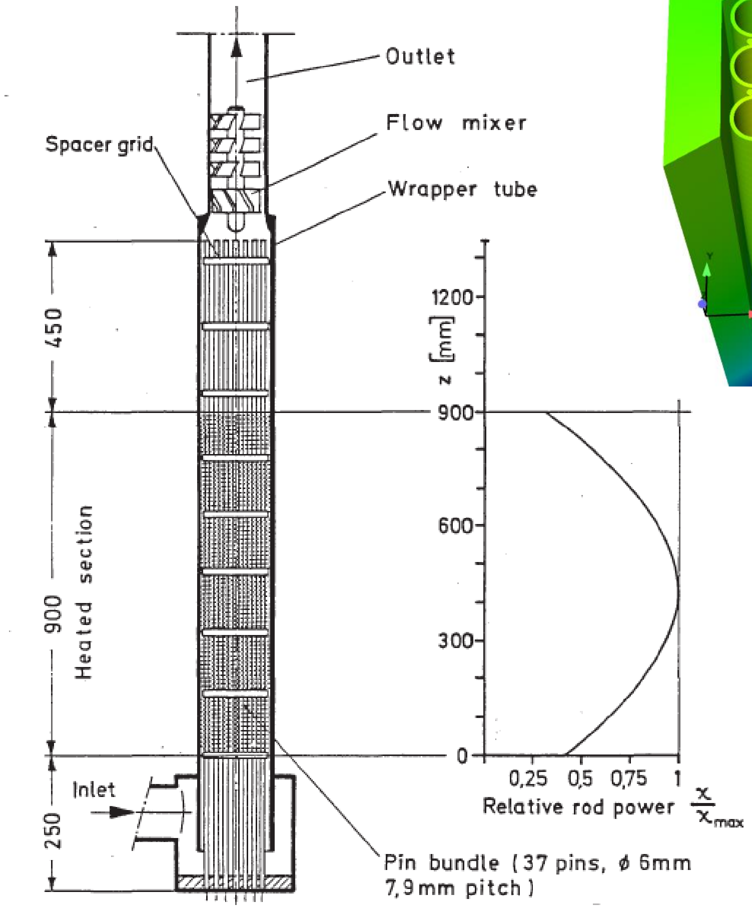

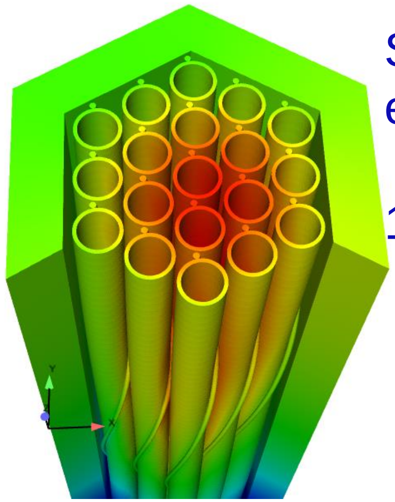

Small bubbles if void fraction <1% experimental observations

19M cells

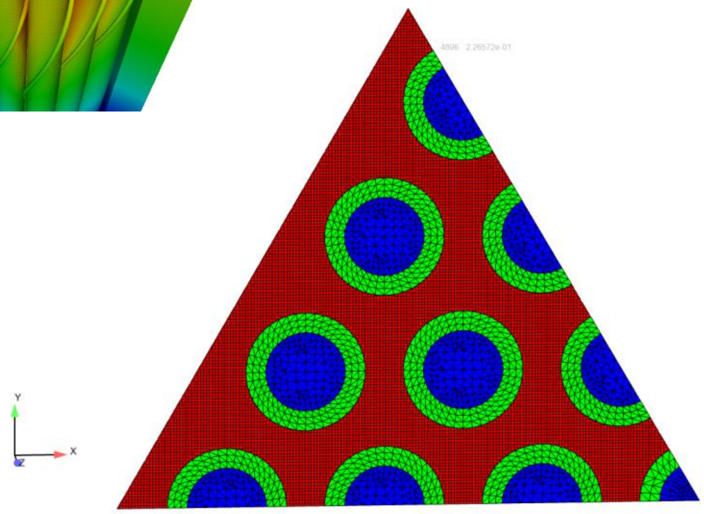

σ sodium 1 bar=157, σ water 1 bar=73, σ water 150bar = 12 → large bubbles

ρl / ρv = 2776 (sodium) 1620 (water 1 bar) 6 (water 150 bar)

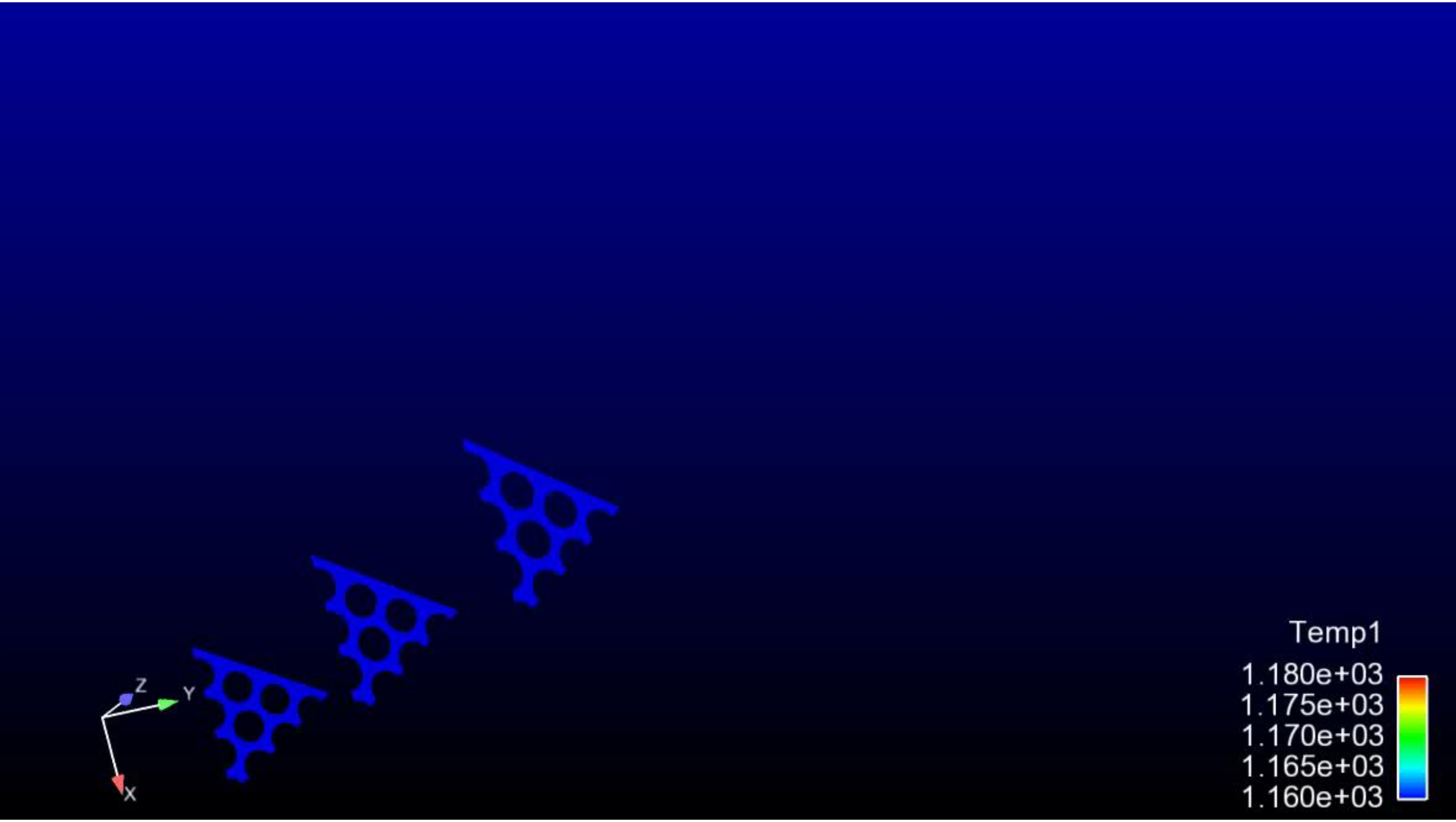

Stephane.Mimouni@edf.fr

3. Multifield CFD calculations of industrial geometries

WALL CONDENSATION, WETTING, CAPILLARITY AND DYNAMIC OF THE TRIPLE LINE

MSME, EDF (ERMES-MMC), ESPCI
ANR MACENA 2 : I2M Bordeaux, INP Grenoble, SIAME Anglet

CAPILLARITY EFFECTS

the height of liquid depends on the tube diameter

Source: P-G. de Gennes

Surface tension force: $F_{CSF} = \alpha_k\, \sigma \kappa \nabla \alpha_k$ with $\kappa = -\nabla.\left(\frac{\nabla \alpha_k}{||\nabla \alpha_k||}\right)$

In order to compute more precisely the interface curvature, we diffuse the interface:

$$\frac{\Delta \alpha_k}{\Delta \tau} - \nabla.D\nabla \alpha_k = 0 \longrightarrow \kappa = -\nabla.\left(\frac{\nabla \alpha_{k,diff}}{\|\nabla \alpha_{k,diff}\|}\right)$$

eDF

WETTING EFFECTS

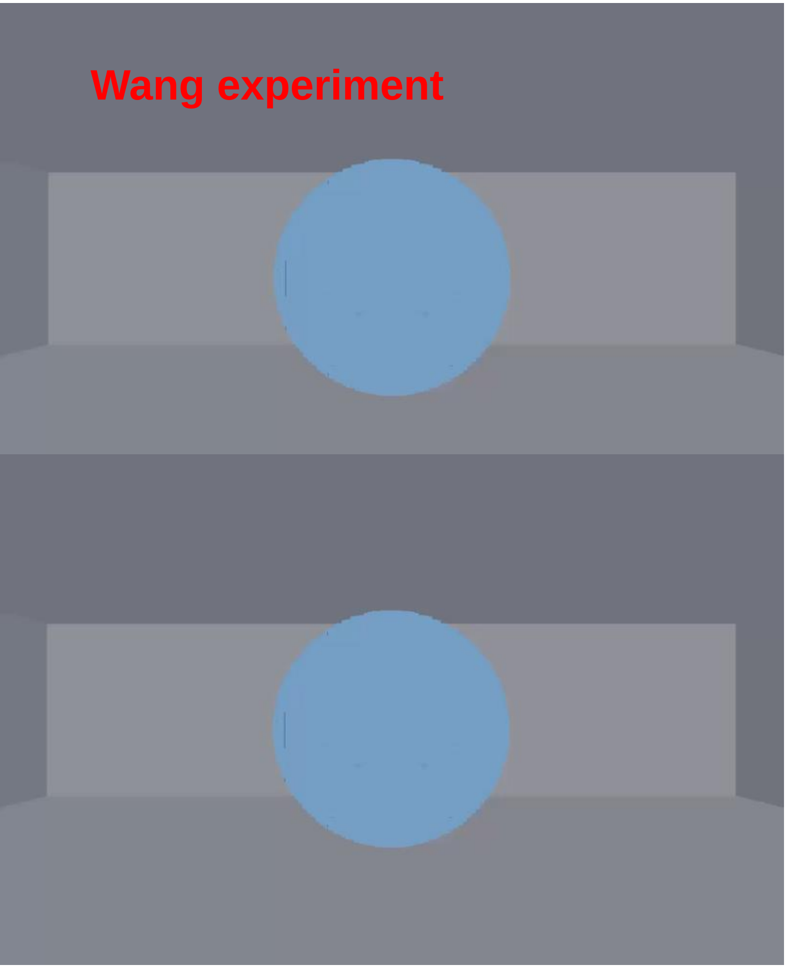

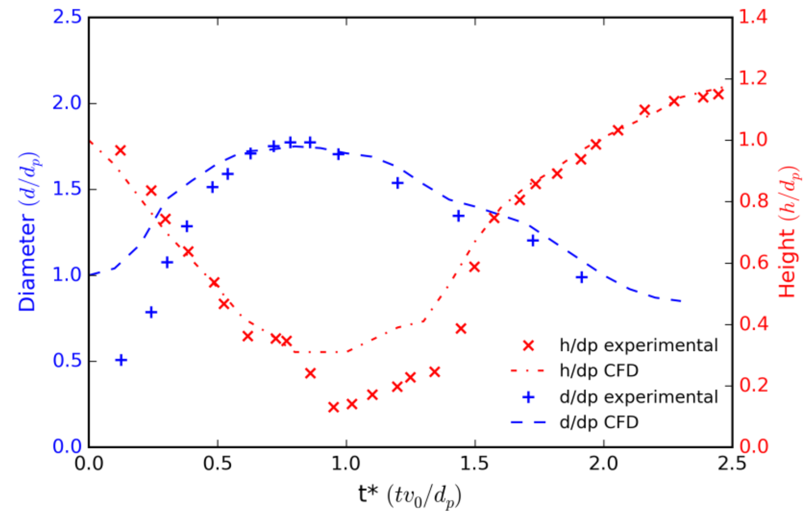

Source: P-G. de Gennes

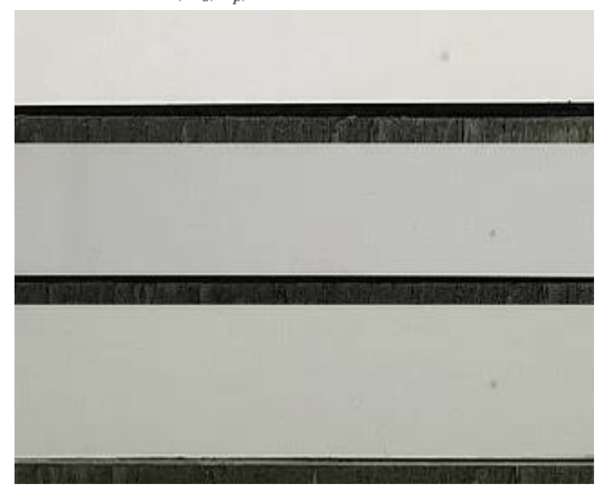

Diffusion equation generalized : $$\frac{\Delta \alpha_k}{\Delta \tau} - \nabla . D \nabla \alpha_k + B^S (\alpha_k^{n+1} - \alpha_p) = 0$$

At the wall : B → ∞
Penalty term

$\alpha_{k;diff} \rightarrow \alpha_p$ at the wall.

CONCLUSION

- Models for disperse fields (bubbles and droplets) are available
- validation of the multifield approach : Verification cases, Validation cases, Integral validation cases
- Sensitivity to mesh refinement
- Phase changes : dispersed gas phase and continuous gas phase → SFR … DNB, Steam Generator, …
- Wettability and capillarity effects → Dynamics of capillary bridges in a crack

→ new challenges ?

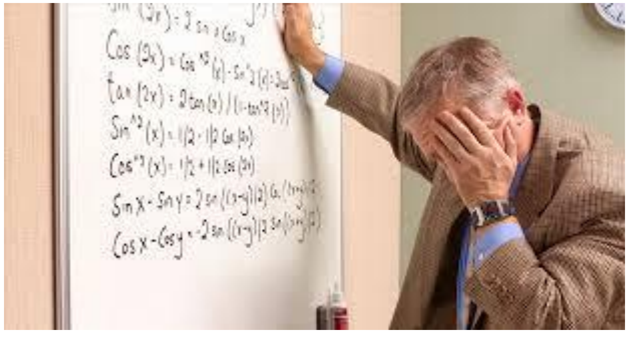

ALL regime flows
for nuclear power plant

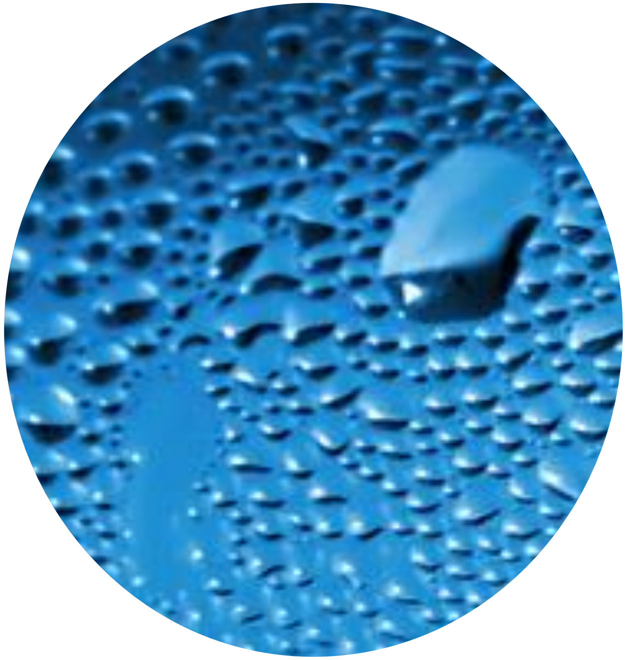

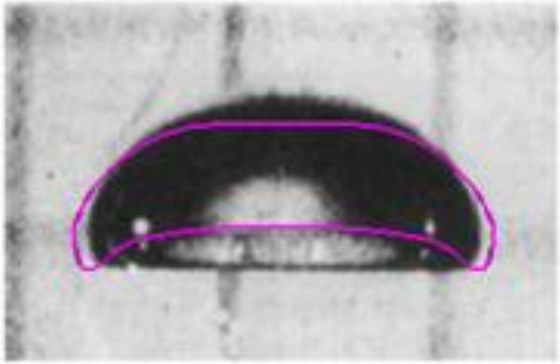

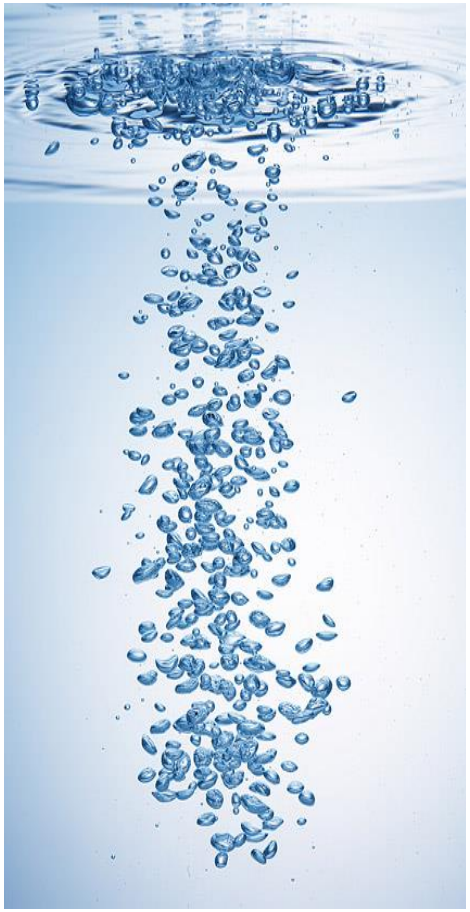

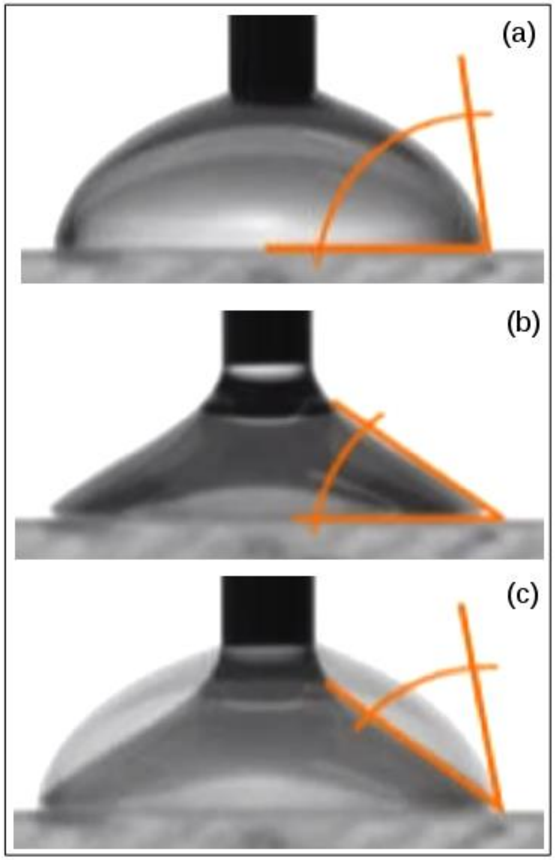

models presented previously work together.

TWO-PHASE FLOWS IN CRACKS

During the course of hypothetical accidents in a PWR → large mass and energy releases into the containment (Steam Line Break, Loss of Coolant Accident, etc.),

Vapor → P increases → mass flow rate through the concrete ?

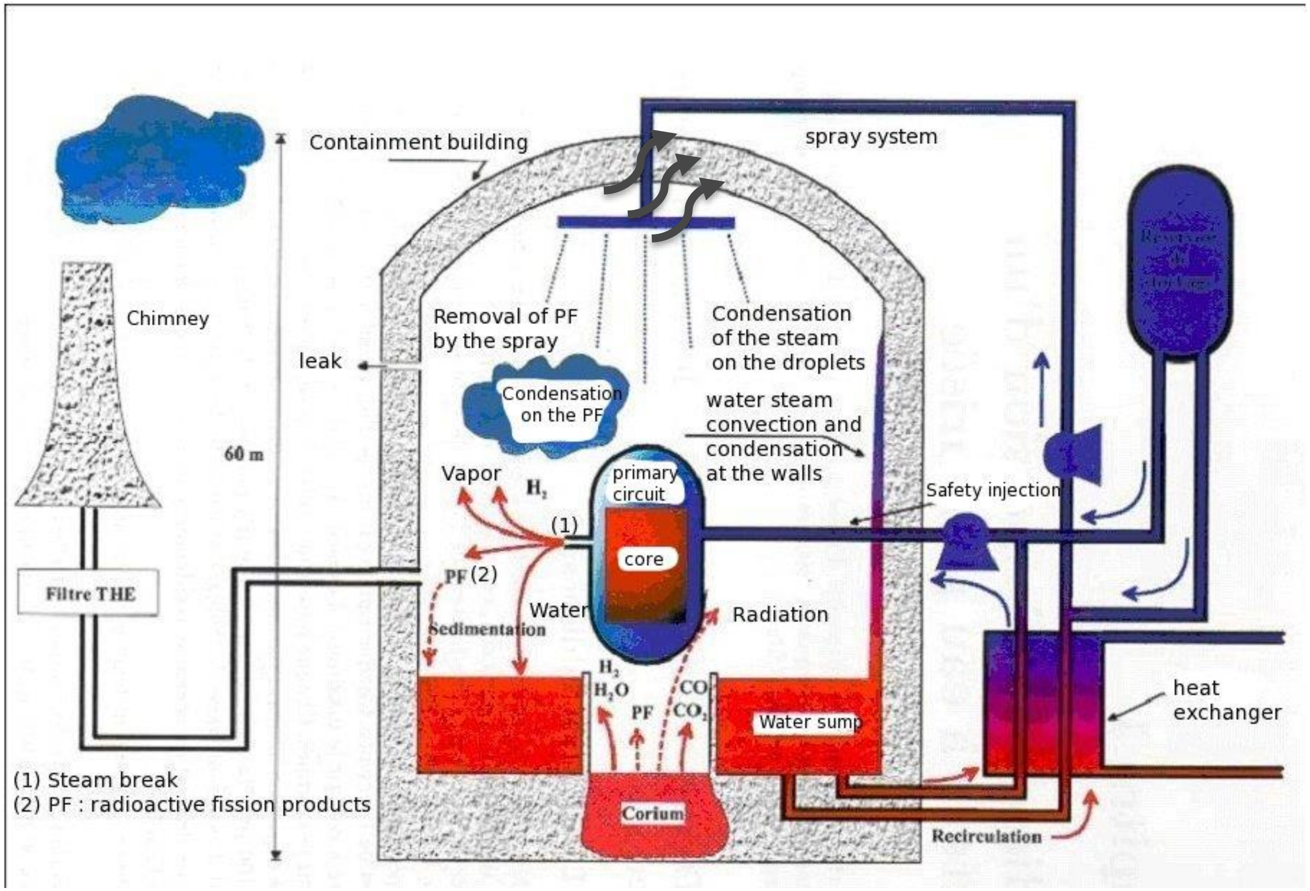

ALL MODELS WORK TOGETHER: CRACKS IN THE CONCRETE

Head losses increase→ flow rate decrease

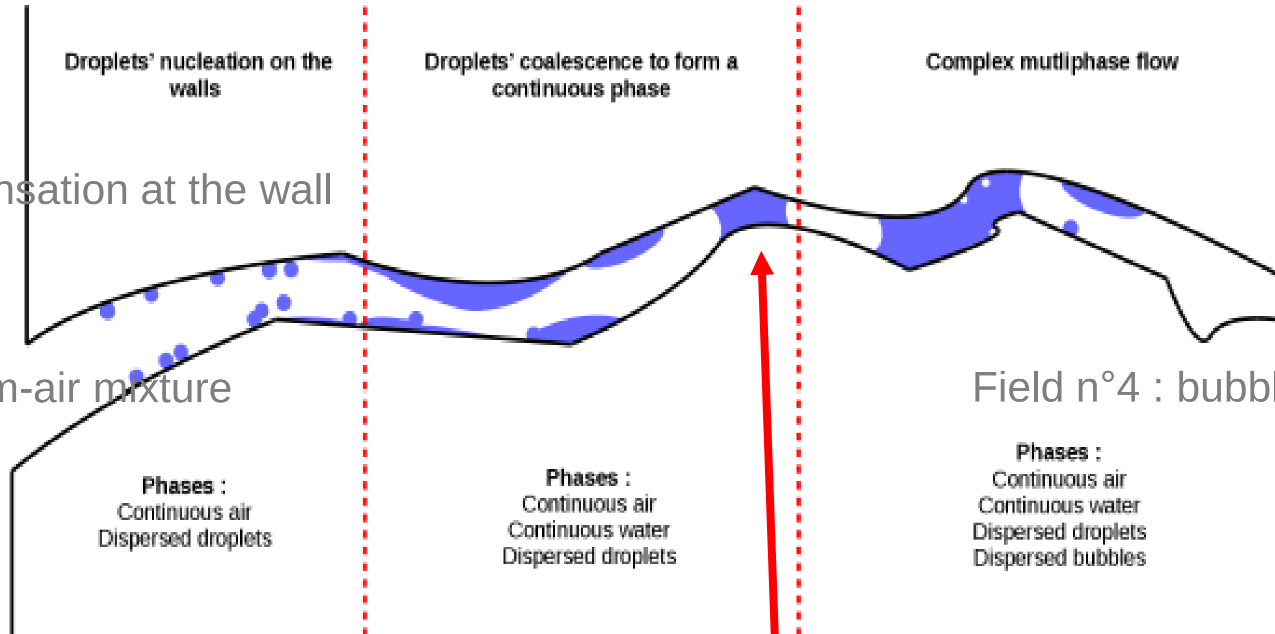

Condensation at the wall

Field n°1: Steam-air mixture

Field n°4 : bubbles

Field n°3 : liquid film

Field n°2 : droplets

Calculation of the mass flow rate through cracks in the concrete.

Dynamics of capillary bridge: wetting + capillarity models

TWO-PHASE FLOWS IN CRACKS : VALIDATION CASE

different regime flows → all the models detaillled work together.

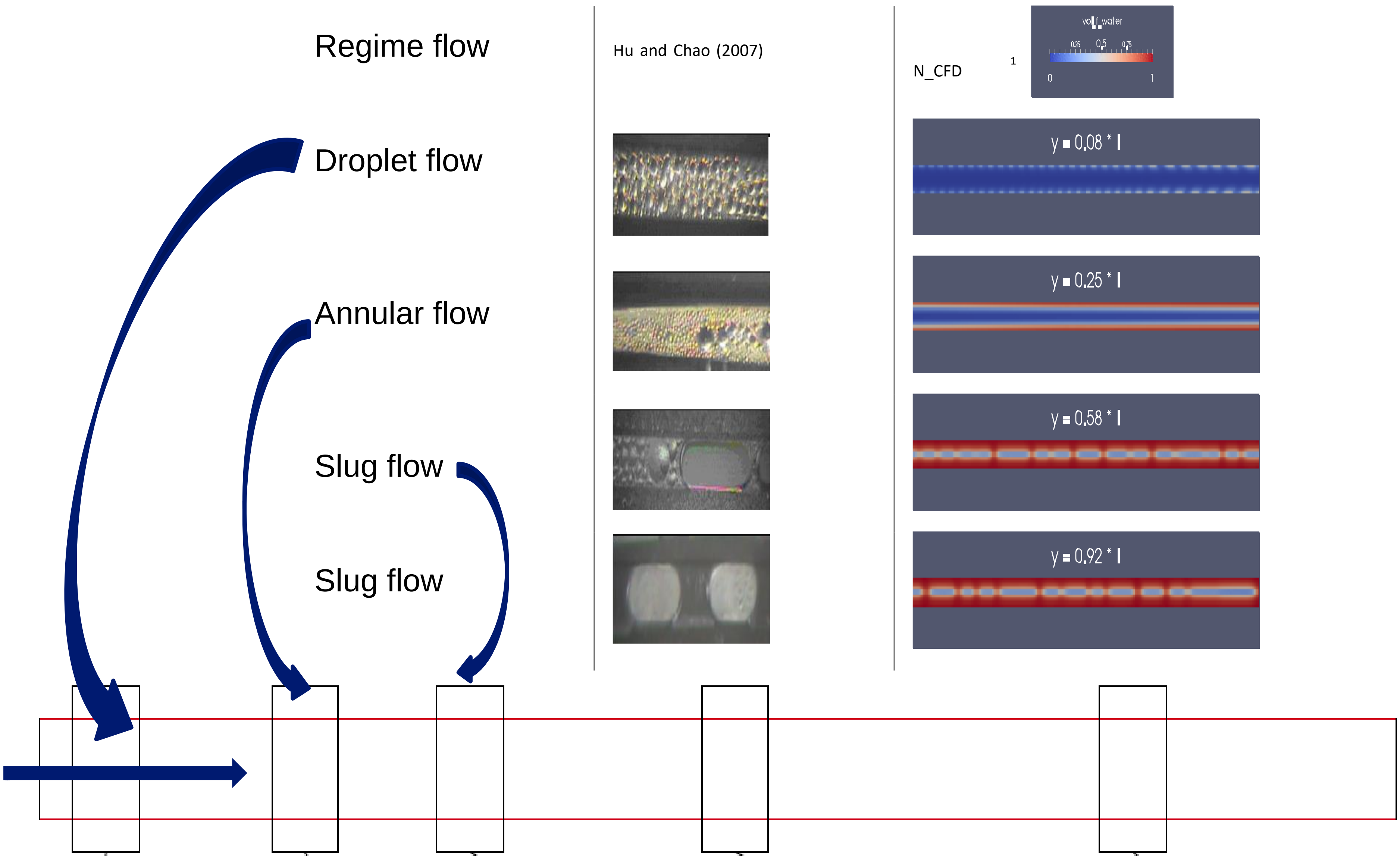

I. STUDY CONTEXT: LEAKY RODS

- About ten rods crack each year in France.

Inside a rod

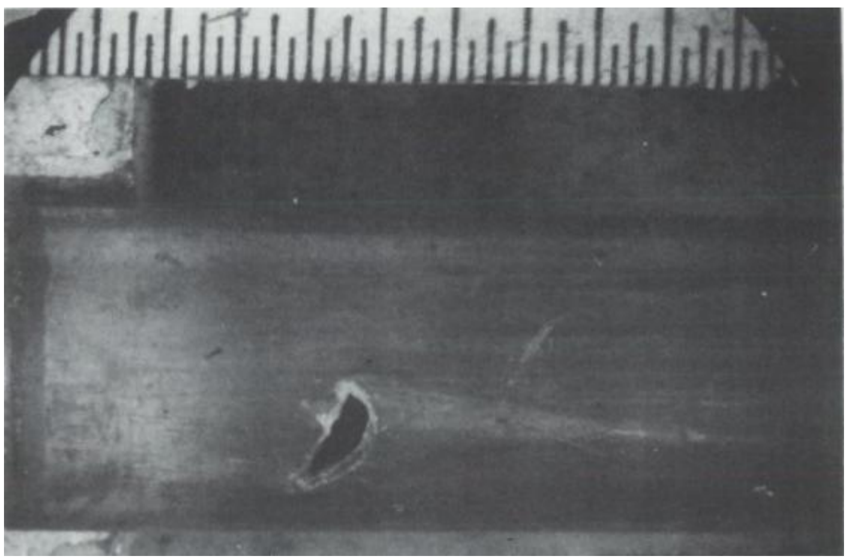

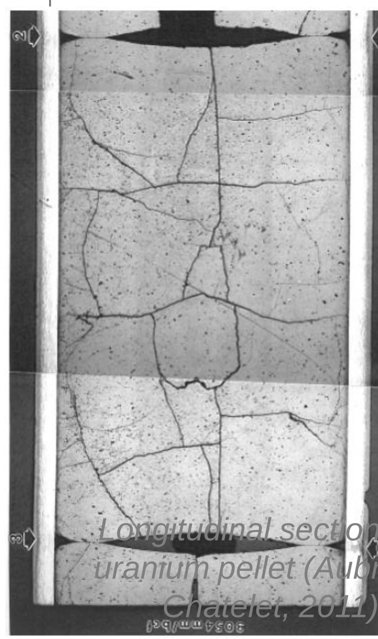

Longitudinal section of a uranium pellet (Aubrun & Chatelet, 2011)

- **Filling the free spaces of the leaky rods with water.**
- **Potential hydrogen risk (explosion) during the evacuation of spent fuel to La Hague:**

$H_2O \rightarrow H_2 + ½ O_2$

II. NUMERICAL STUDY: WETTABILITY

Experimental case of Mukherjee (2005) – representative of microchannel boiling (drying of leaky rods)
Microchannel size 200 µm x 260 µm x 1200 µm.
Boundary conditions: Inlet (uin = 0.127 m/s and Tint = 102°C) – Outlet (P = 1 bar).
Contact angle θ = 30°.

II. NUMERICAL STUDY: WETTABILITY

DNS Mukherjee | Experiment Mukherjee | neptune_cfd : coupe 2D | neptune_cfd : vue 3D

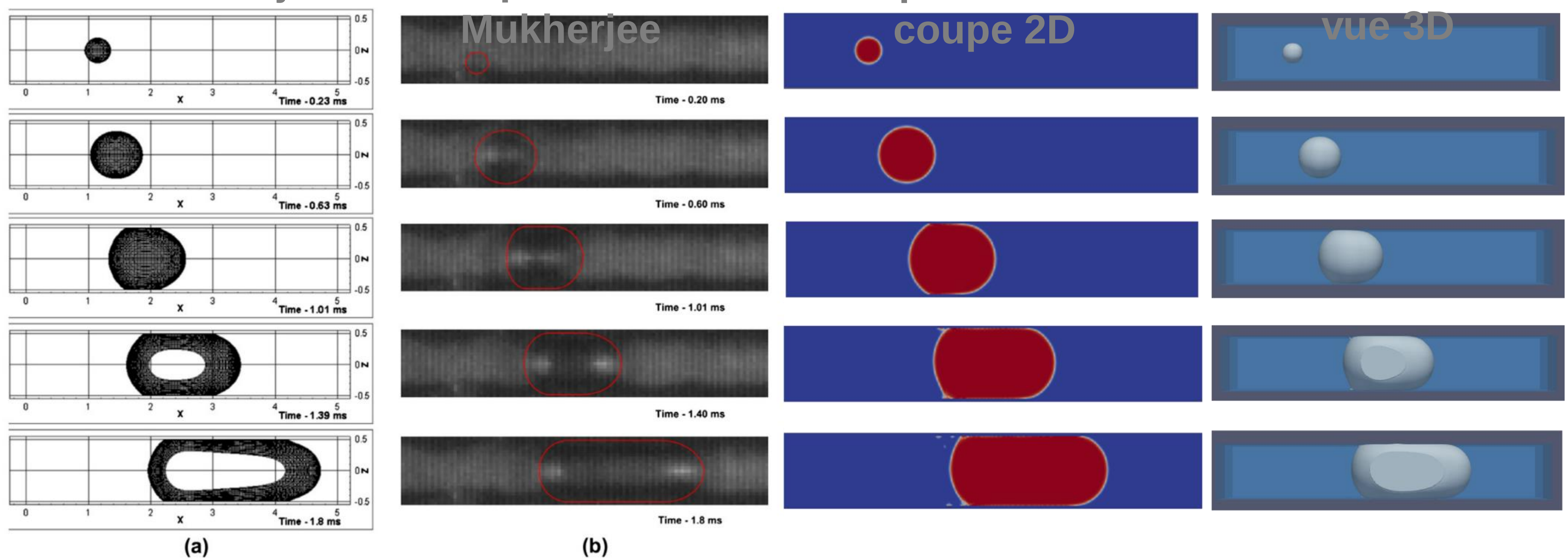

II. NUMERICAL STUDY: WETTABILITY

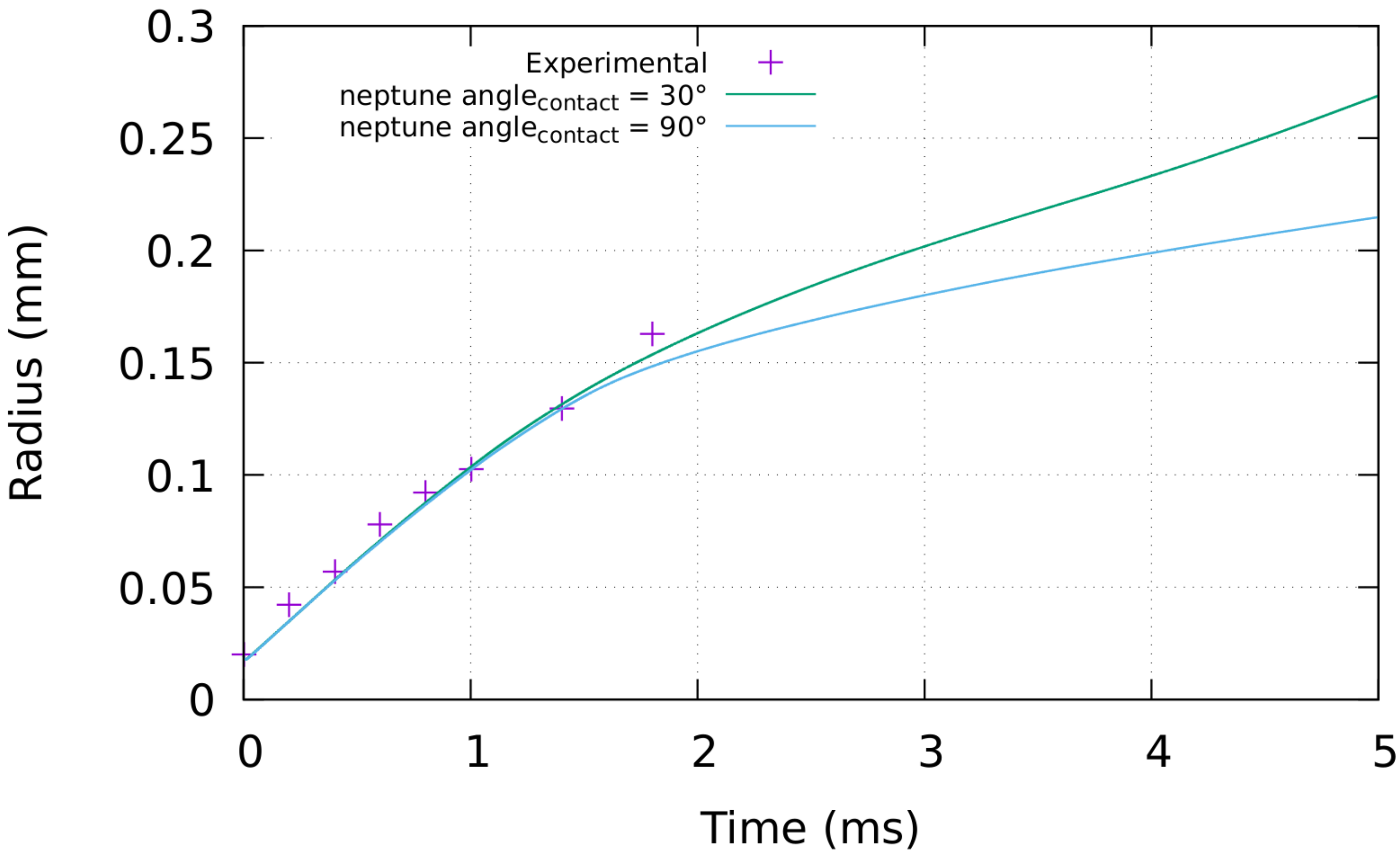

- Quantitative results in accordance with experience.
- Show the importance of considering wettability.

III. EXPERIMENTAL STUDY → SLUG regime

- Periodic nucleation of steam bubbles.
- Growth of bubbles by interfacial boiling as predicted by numerical simulations.

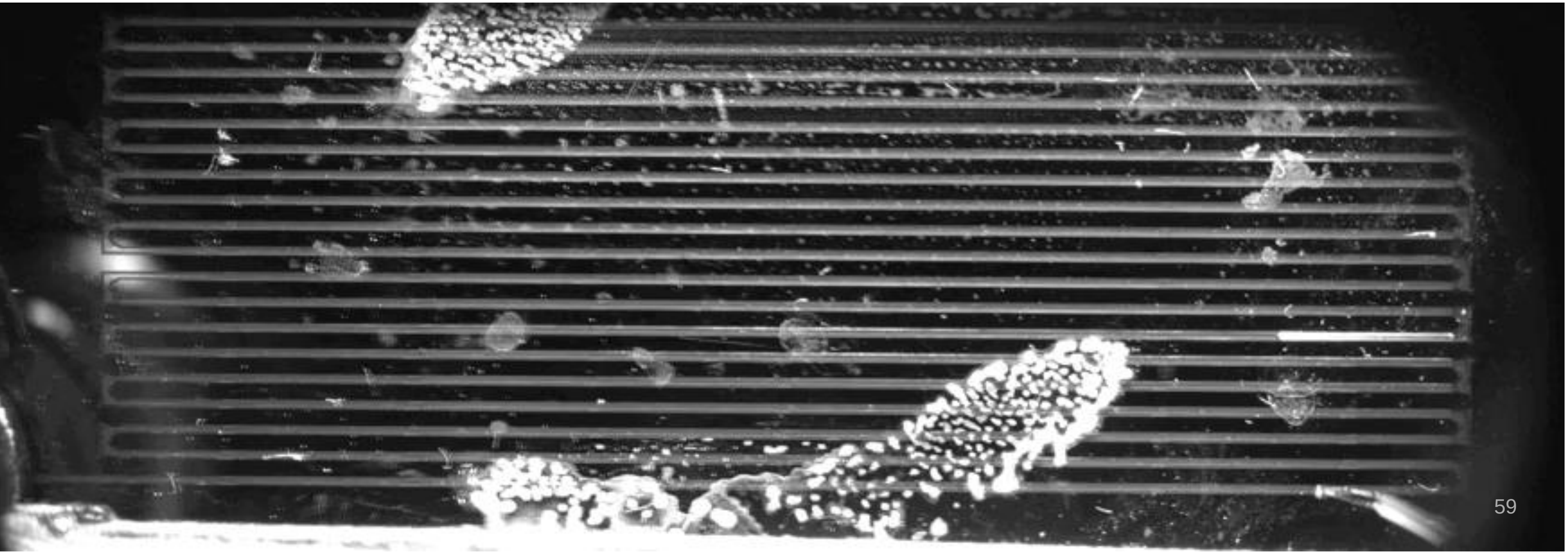

IV. Upscaling

- The calculations presented in Part II. are very expensive numerically.
- Need a very fine mesh.
- The Δt time steps are very small (in the order of 10-6 to 10-8 s) because of the CFL constraint : $.CFL = \frac{u\Delta t}{\Delta x} < 1$

Simulation of one hour of drying of a leaky rod:

3.2 billion cells.

11,415 years on 64,000 processors.

The objective is to transform a 3D simulation into an equivalent 1D simulation.

Simulation 3D

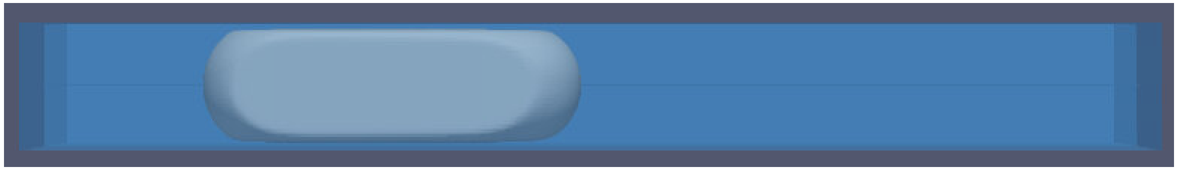

Simulation 1D

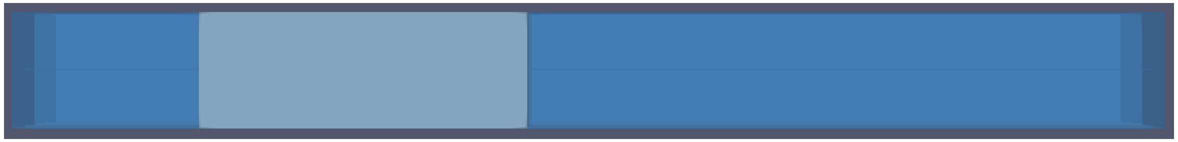

Conclusion

Scaling up microfluidics: a fight against computational time

Numerical calculation time at the beginning of the study ≈ 100,000 years

Simulation 3D (computational time≈ 10,000 years) **Experimental work**

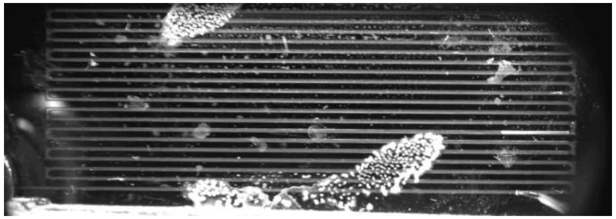

Simulation 1D (calculation time≈ 1 year)

Simulation 1D → two-phase flow effects can be neglected under assumptions → Industrial Model 0D (computation time ≈ 1 minute)

4. CFD modelling of dispersed two-phase flow for nuclear power plant

MODELLING OF SPRAYS IN A MULTI-COMPARTMENT GEOMETRY WITH A CMFD CODE

IMFT, IRSN, ESPCI
European projects : PSI, UCL, JSI, Becker T., KFKI, U. Pisa, CEA, …

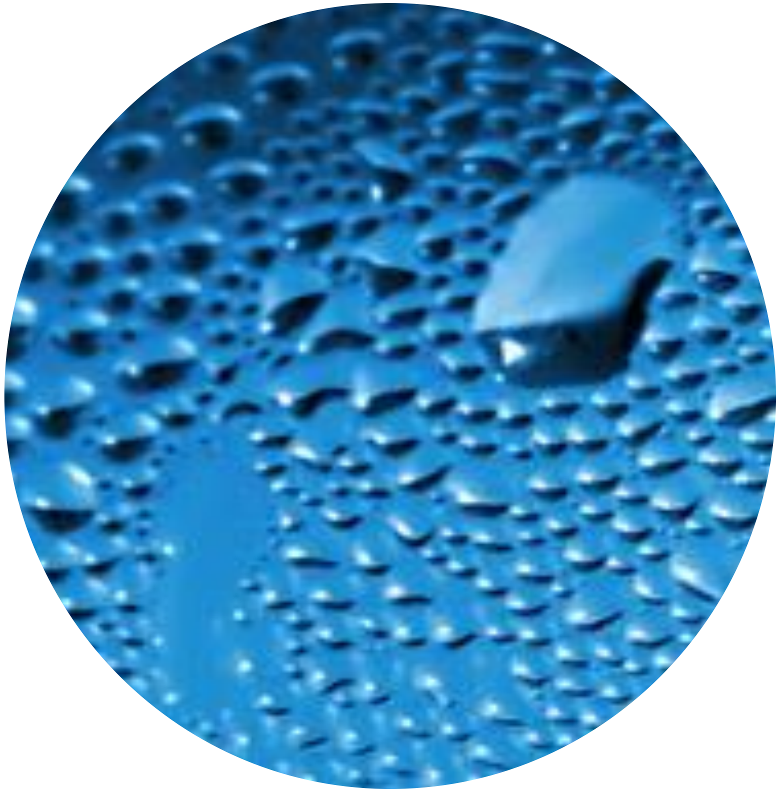

BACKGROUND

hypothetical accidents in a PWR : Steam Line Break → lead to large mass and energy releases into the containment

→ spray systems are used in the containment:

- in order to limit overpressure
- to enhance the gas mixing in case of the presence of hydrogen
- to drive down the fission products

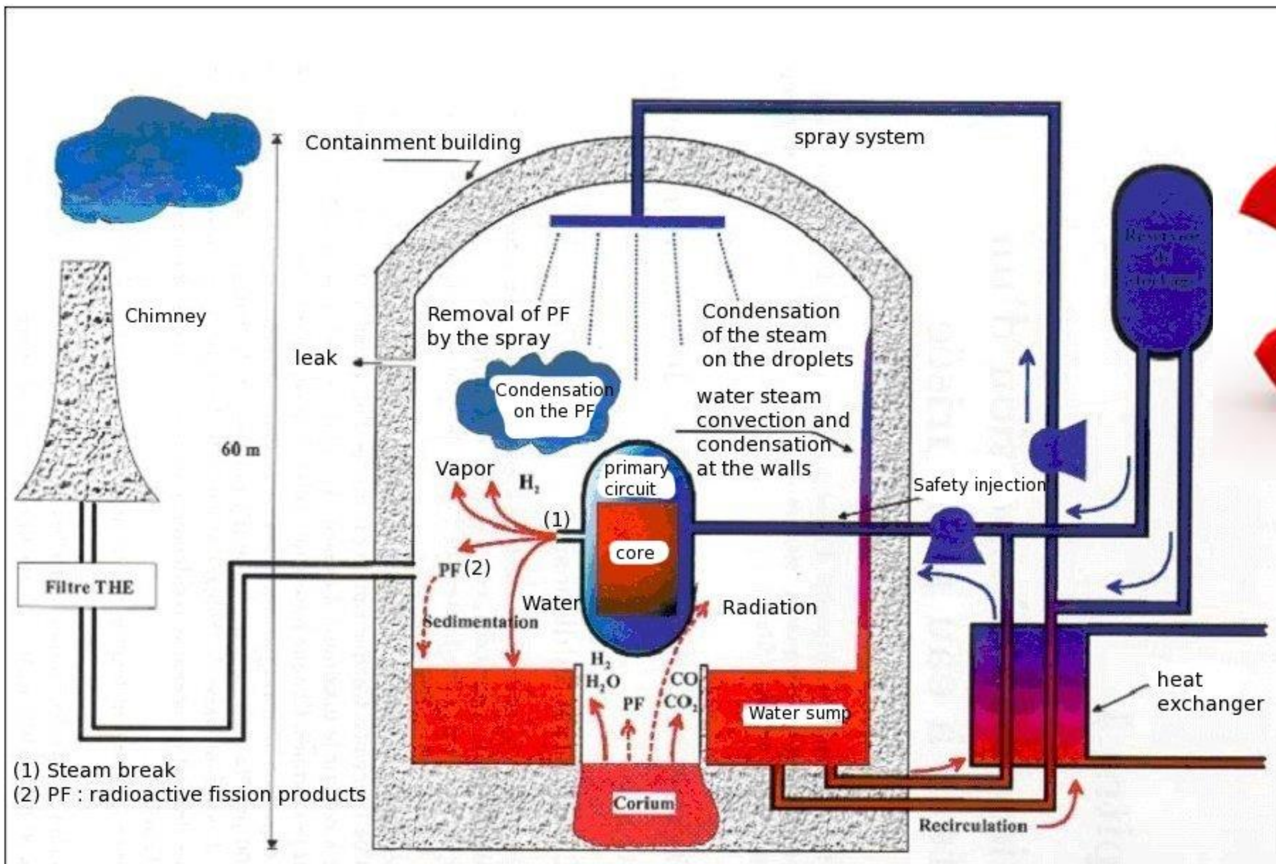

DROPLETS CONDENSATION/EVAPORATION

$$T_{liq} \neq T_{gas}$$

$$V_{liq} \neq V_{gas}$$

Vapor density at saturation state at $T_{droplet}$

diffusion coefficient

Vapor density at T_{gas}

d : droplet

g : gas

$$\begin{cases} mass\_transfer : \Gamma_g^c = \dfrac{6\alpha_d}{d_d^2} Sh.D(T_m).\left\{\rho_{sat}(T_d) - \rho_g y_v\right\} \\ heat\_transfer : \Pi'_g = \dfrac{6\alpha_d}{d_d^2} Nu.\lambda_g(T_m)\left\{T_d - T_g\right\} \end{cases}$$

Vapor mass fraction

thermal conductivity

$$\Gamma_1^c = -\frac{\Pi'_1 + \Pi'_2}{H_2^\sigma - H_1^\sigma}$$

$$\begin{cases} Sh = 2 + 0{,}56\,\mathrm{Re}^{1/2}\,Sc^{1/3} \\ Nu = 2 + 0{,}56\,\mathrm{Re}^{1/2}\,\mathrm{Pr}^{1/3} \end{cases}$$

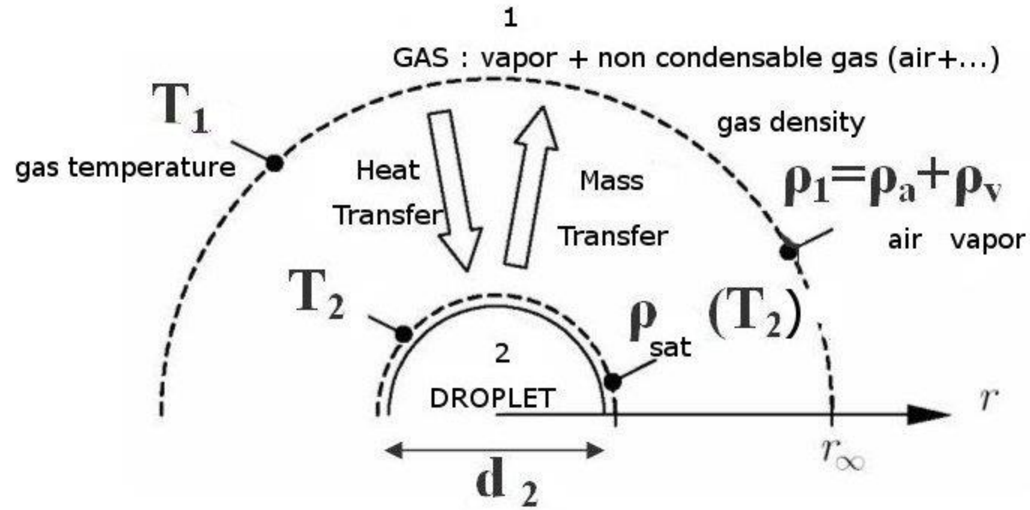

Computation of Sh and Nu numbers : relations of Frössling / Ranz-Marshall

Tabulated laws : $D(T_m)$, $\rho_{sat}(T_2)$, $\lambda_1(T_m)$

PANDA EXPERIMENT (PSI)

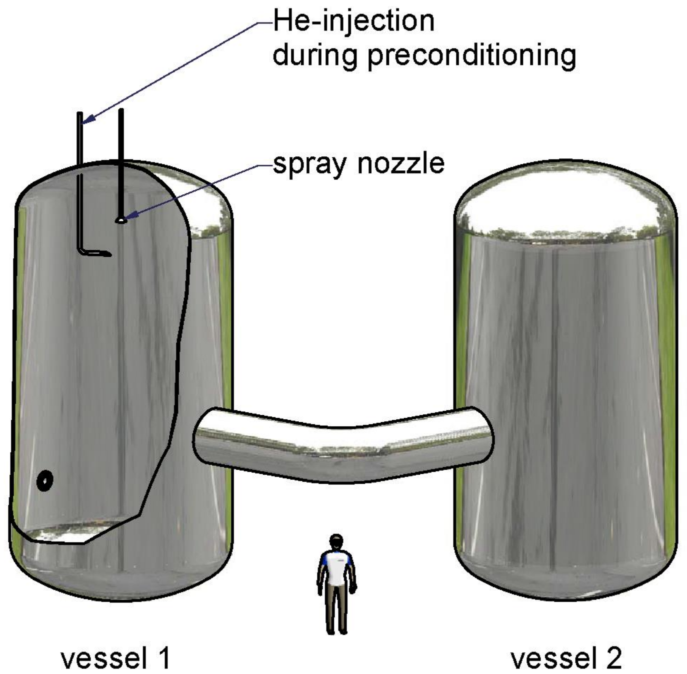

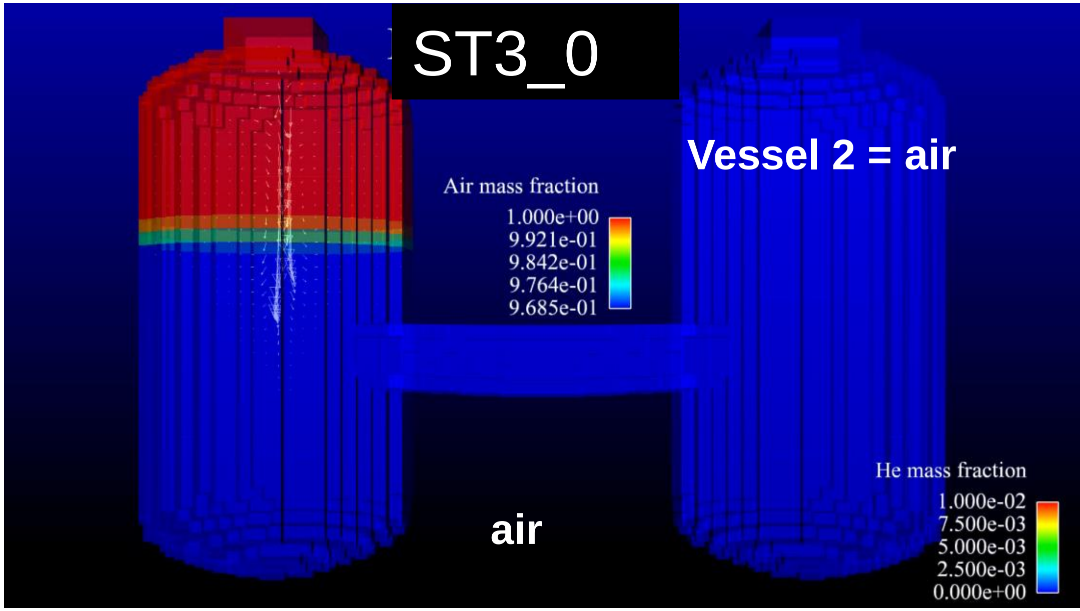

The spray nozzle is oriented vertically downward in vessel 1.
It produces a conical solid spray pattern.
The two vessels are connected with a 1 m diameter pipe (IP).
Ddroplet=0.582mm

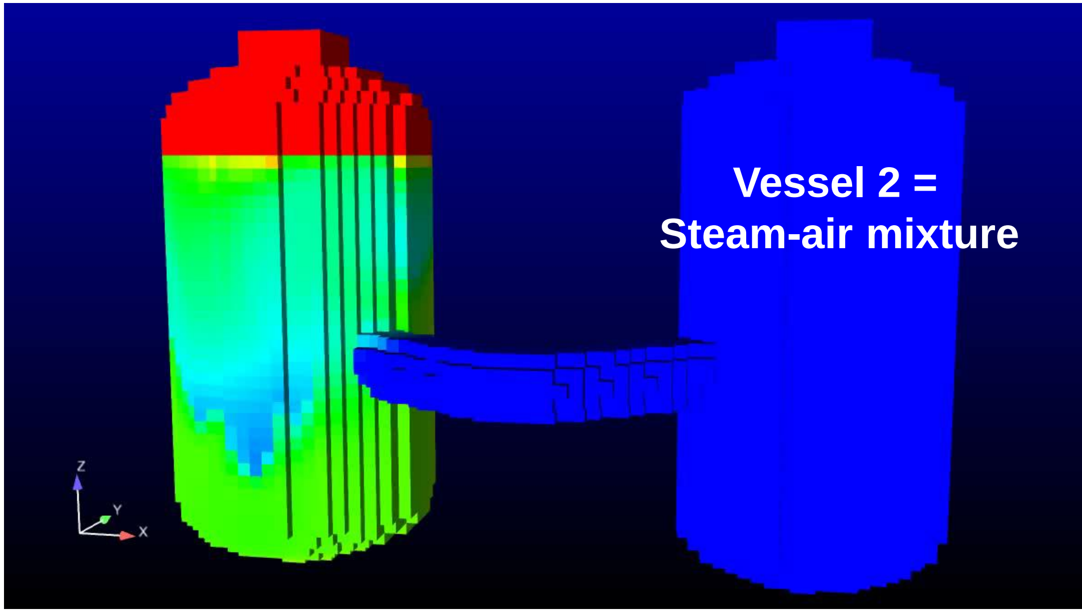

Sectional method developped in NEPTUNE_CFD code

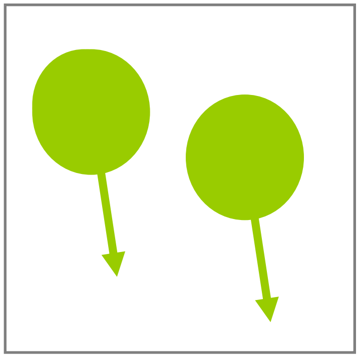

← Monodispersed

Polydispersed→

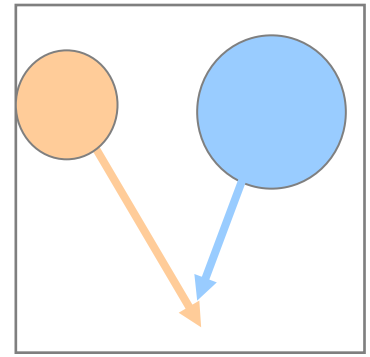

Cutting the size distribution into sections

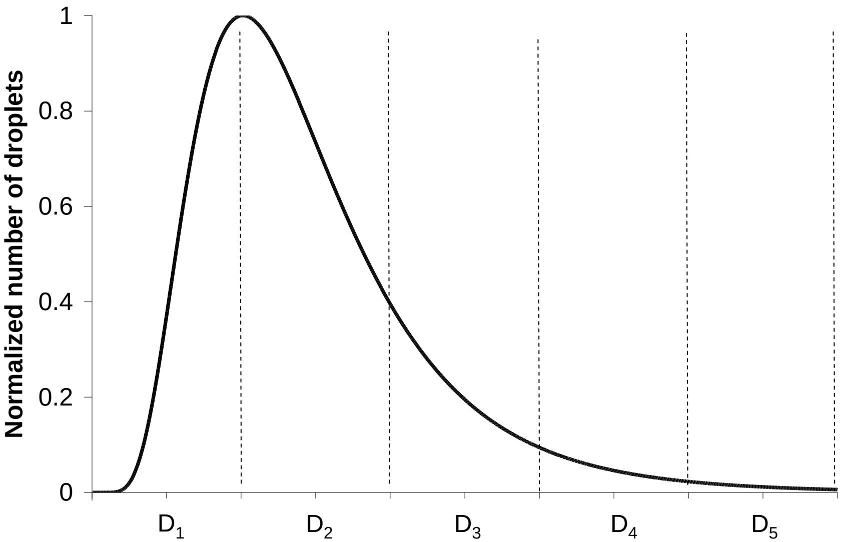

Solving the equilibrium equations for each section:

- mass
- momentum
- enthalpy

Equation closure terms:

- turbulence (+ inverse coupling)
- drag (between sections and gaseous phase)
- collision terms (mass and momentum transfers)

1 size <-> 1 velocity

Development of the sectional approach into the NEPTUNE_CFD code

Stephane.Mimouni@edf.fr

Droplet size

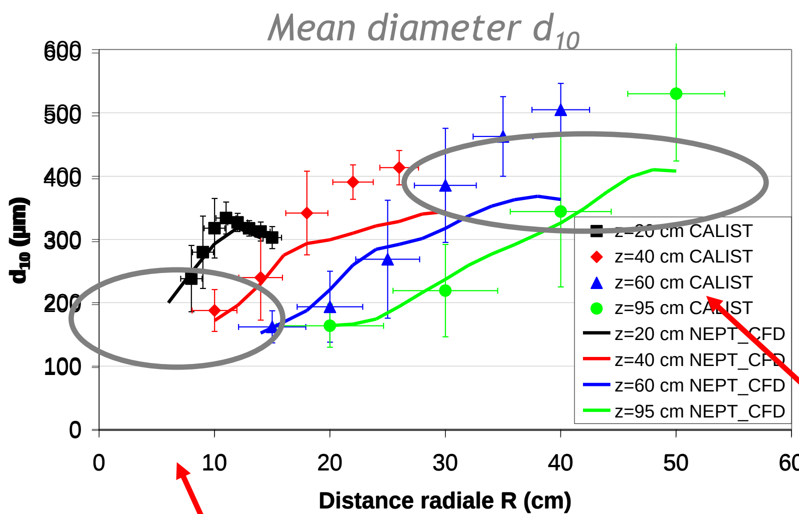

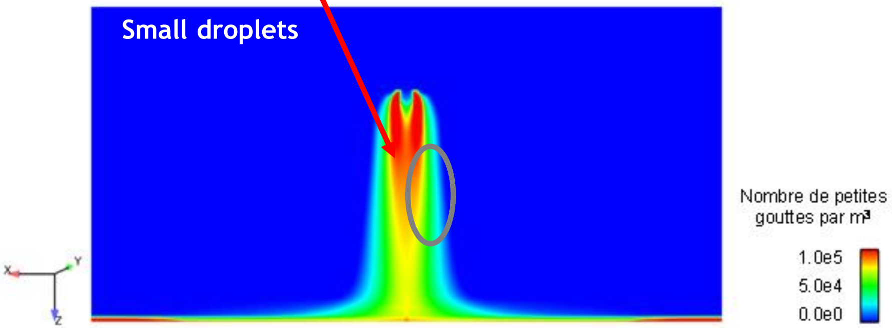

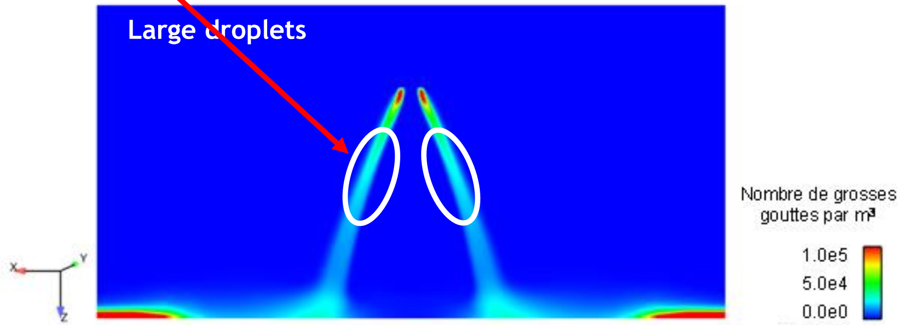

Monodispersed approach : 44 % *polydispersed approach : 8,9 %*

Stephane.Mimouni@edf.fr

COLLGATE : Modeling the droplet collision outcome

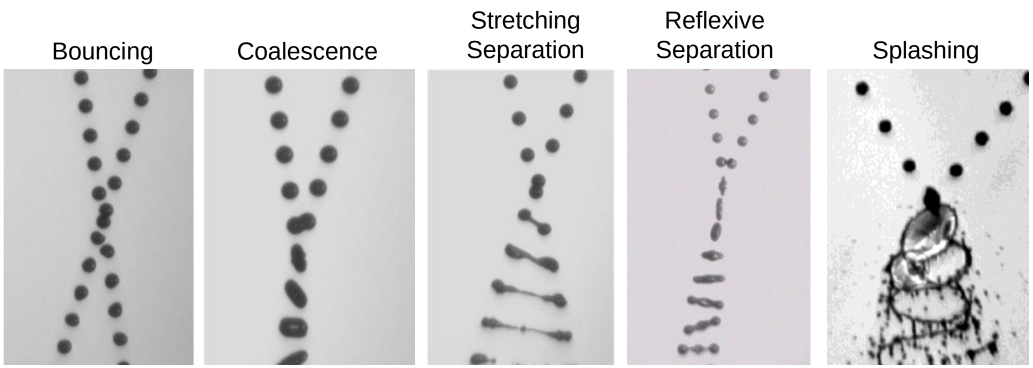

(Rabe et al. 2010)
(Foissac et al. 2011)

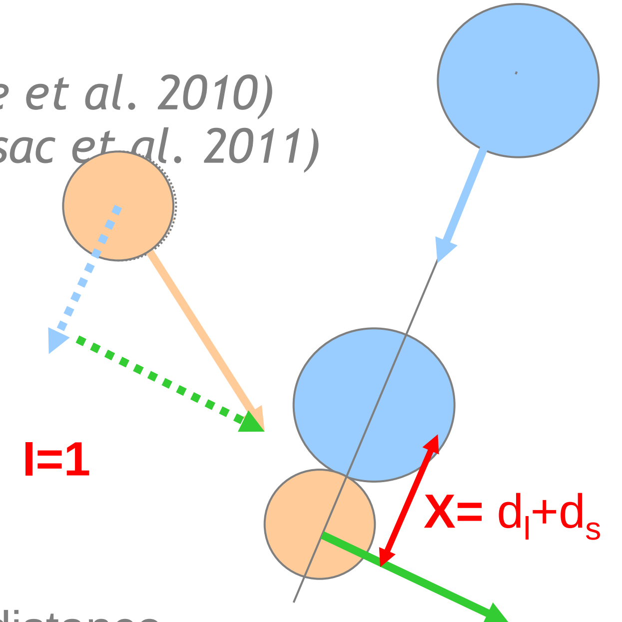

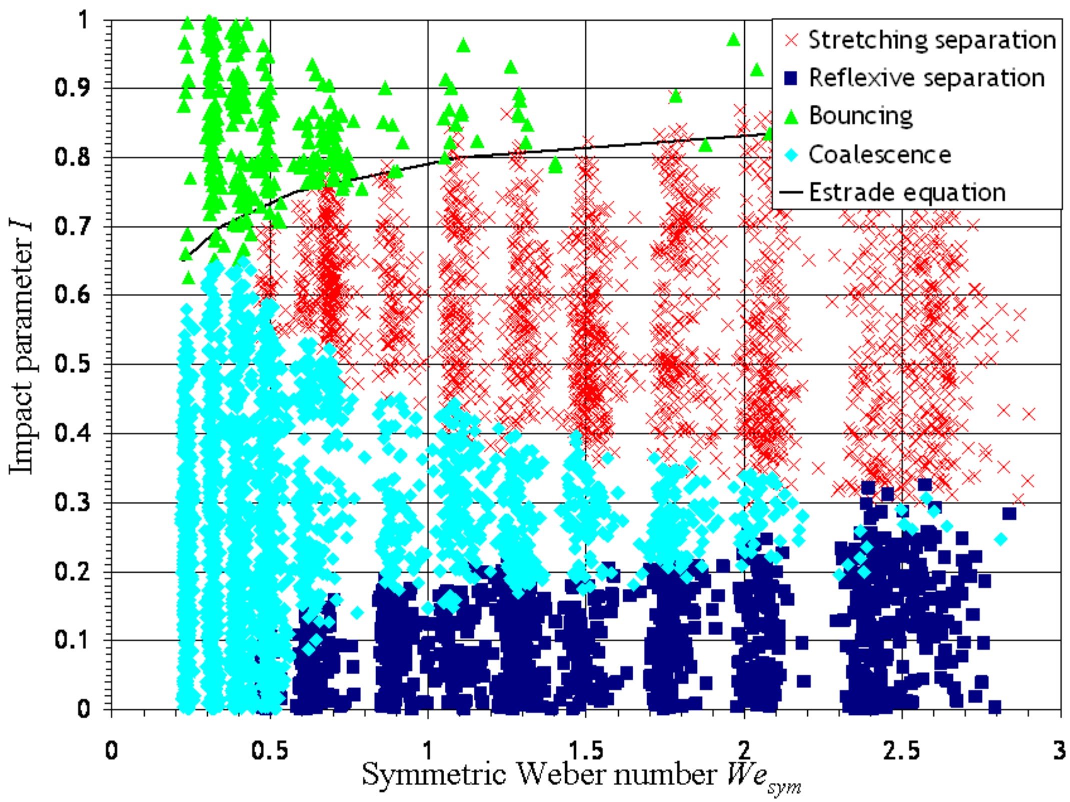

X : distance between large droplet center and relative velocity applied on small droplet center.

Δ : diameter ratio

$$I = \frac{2X}{d_s + d_l}$$

$$We = \frac{\rho}{12\sigma} \frac{d_s^3 \left\|\vec{v}_s\right\|^2 + d_l^3 \left\|\vec{v}_l\right\|^2}{d_s^2 + d_l^2}$$

BC of the simulation

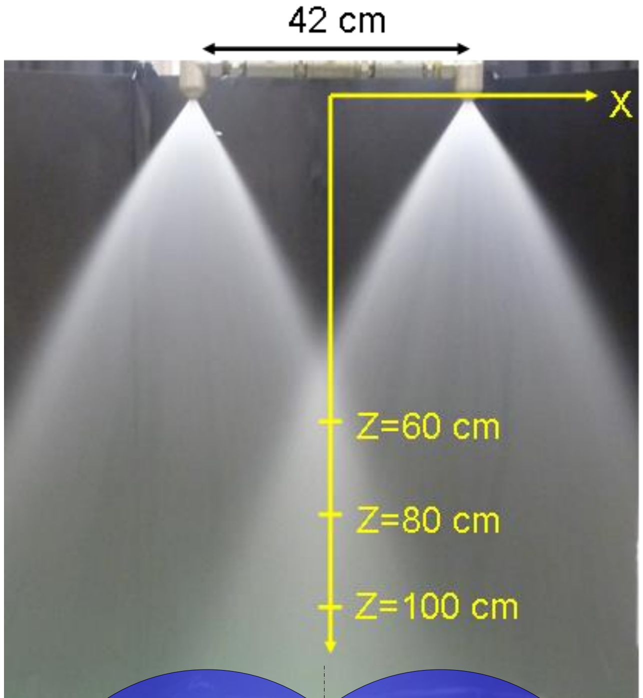

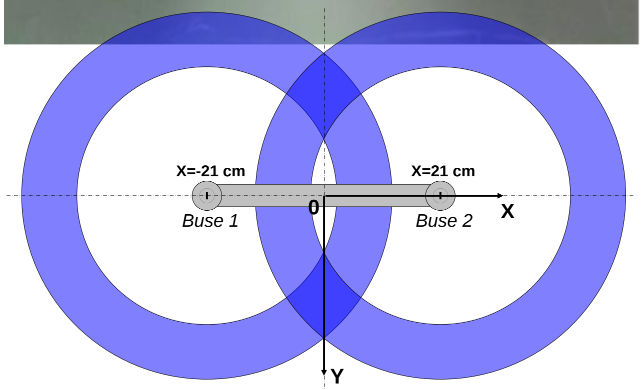

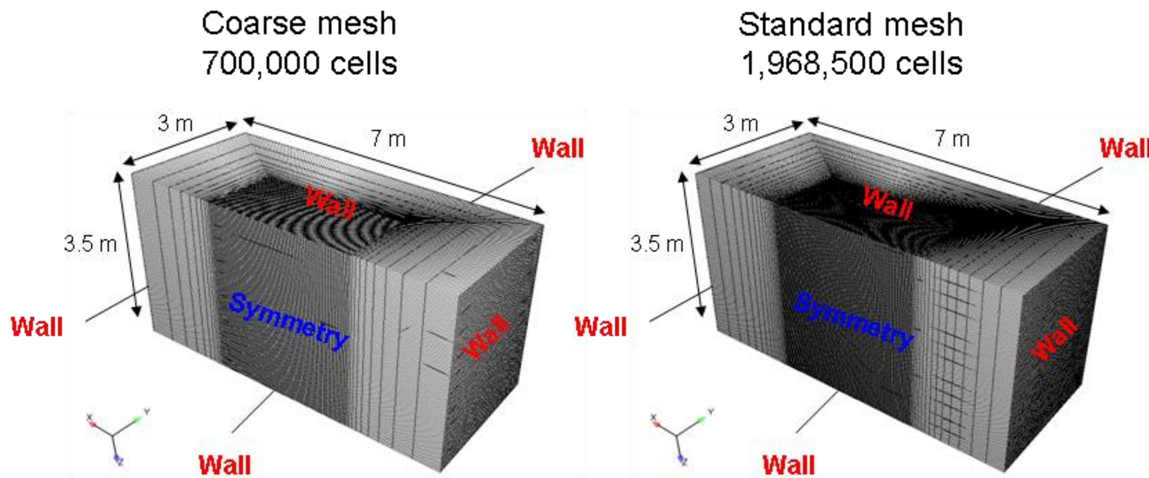

Experimental and numerical local size distributions obtained for two interacting sprays are compared for different positions along the symmetrical axis :

<u>**Inlet conditions:**</u> definition of 9 sections for each nozzle

Section	Diameter	Flowrate
1	55 µm	1.42 10^{-5} kg/s
2	166 µm	2.67 10^{-2} kg/s
3	277 µm	1.28 10^{-1} kg/s
4	388 µm	1.91 10^{-1} kg/s
5	500 µm	2.02 10^{-1} kg/s
6	611 µm	1.72 10^{-1} kg/s
7	722 µm	1.29 10^{-1} kg/s
8	833 µm	8.87 10^{-2} kg/s
9	944 µm	6.35 10^{-2} kg/s

Stephane.Mimouni@edf.fr

Two PWR interacting sprays: some results

•The smallest droplets are drifted away in the air flow.
•The biggest droplets, having more inertia, are not altered in the spray interacting area.

Small droplets

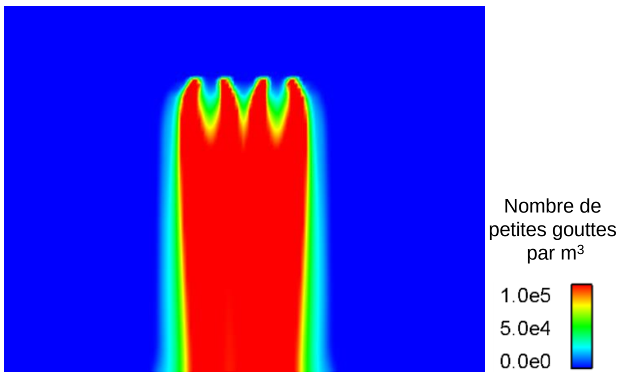

Large droplets

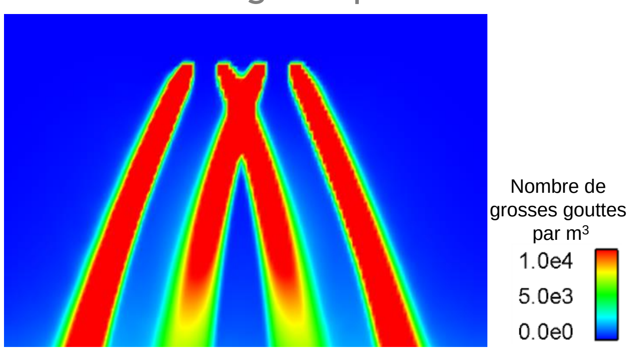

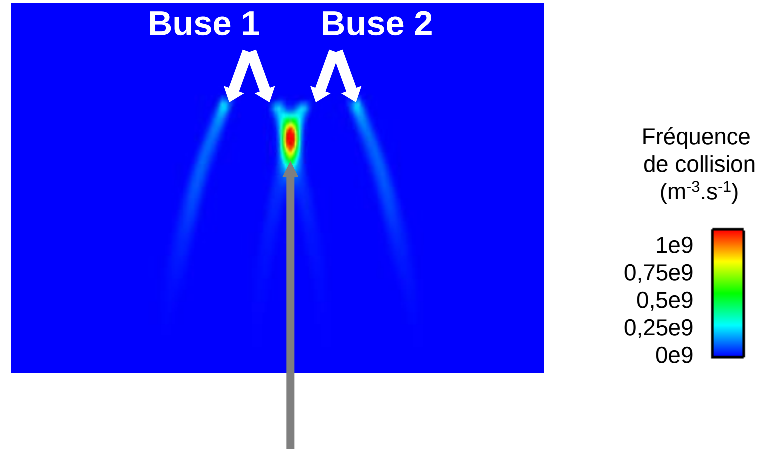

10^9 collisions.$m^{-3}.s^{-1}$

Collisions lead to break up

The droplet size decreases: the mean geometric diameter is about 300 µm before spray interaction and about 200 µm after spray interaction.

Stephane.Mimouni@edf.fr

VERCORS EXPERIMENT, A 1/3 MOCK-UP OF A 1300 MWE NUCLEAR REACTOR CONCRETE CONTAINMENT BUILDING

- Built by EDF in order to investigate the behaviour of concrete containment building in scenarios where a large amount of vapor is released in the containment
- The containment is inially filled with air only at 1 bar. A steam mass flow rate is imposed at the bottom (6 tons/hour) in the internal containment. But, this vapor mass flowrate evolves during the transient in order to maintain a pressure equal to 5 bar in the containment
- The concrete width for the wall containments is about 40 cm

COUPLING BETWEEN 3 CODES : NEPTUNE CFD + NEPTUNE_CFD FOR TWO DISCONNECTED FLUID COMPUTATIONAL DOMAIN AND SYRTHES IN THE WALLS

fluid flow in the internal containment

fluid flow in the space inter-containment

thermal exchanges in the wall (3D) is solved with the code SYRTHES

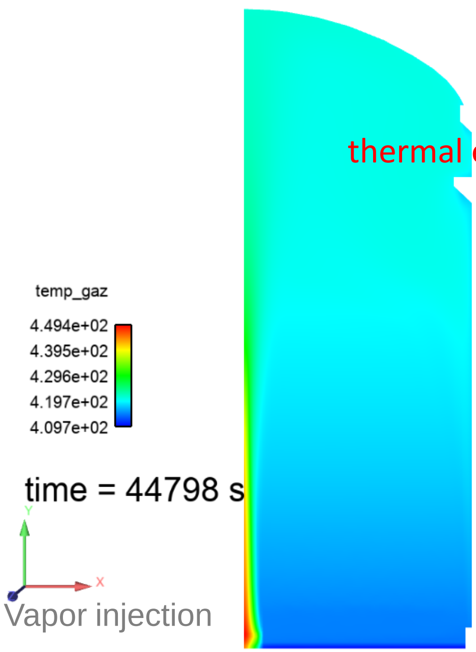

Cell size ~ 2 cm

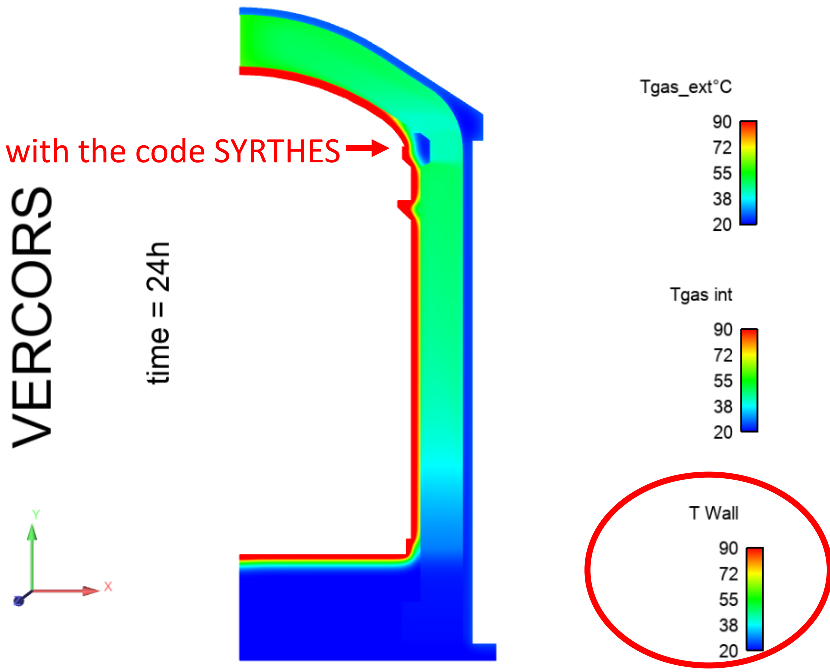

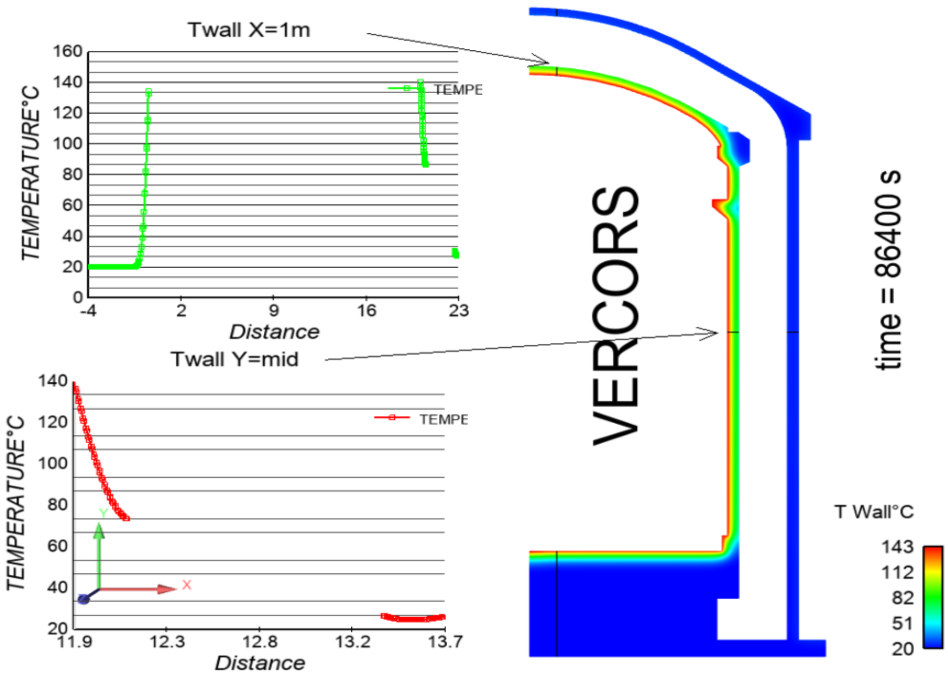

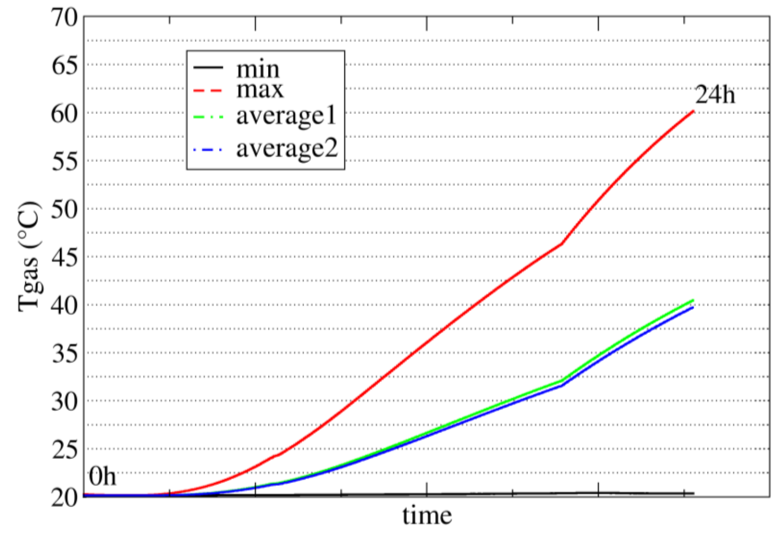

Upper part of the inter-containment :gas temperature reaches 60 C after only 24h
→ detrimental for temperature sensors;
Mid-level, the temperature is about 40 C at time = 24h which is acceptable.

Before launching the experimental test, CFD calculations have been performed to assess the evolution of the wall temperature in the internal containment and the wall temperature of the external containment.

- Moreover, the calculation demonstrates the feasibility of the tests regarding the vapor mass flow rate injected during the tests.
- The calculation estimates also the amount of liquid from condensation in the wall that needs to be evacuated.

CONTAINMENT BUILDING OF A 1300 MWE FRENCH PWR

- **cylindrical shape with a maximum height of 59 m, a maximum diameter of 40 m and a volume of 70 437 m3.**
- **local mesh refinement have been performed in this study in the region of spray aspersion in order to reach a cell size of about 1 cm.**
- **One-dimension fluid-structure heat transfer model has been applied to several structures : enclosure covering the building (90 cm), handling bridge (70 cm) and internal walls (40 cm).**

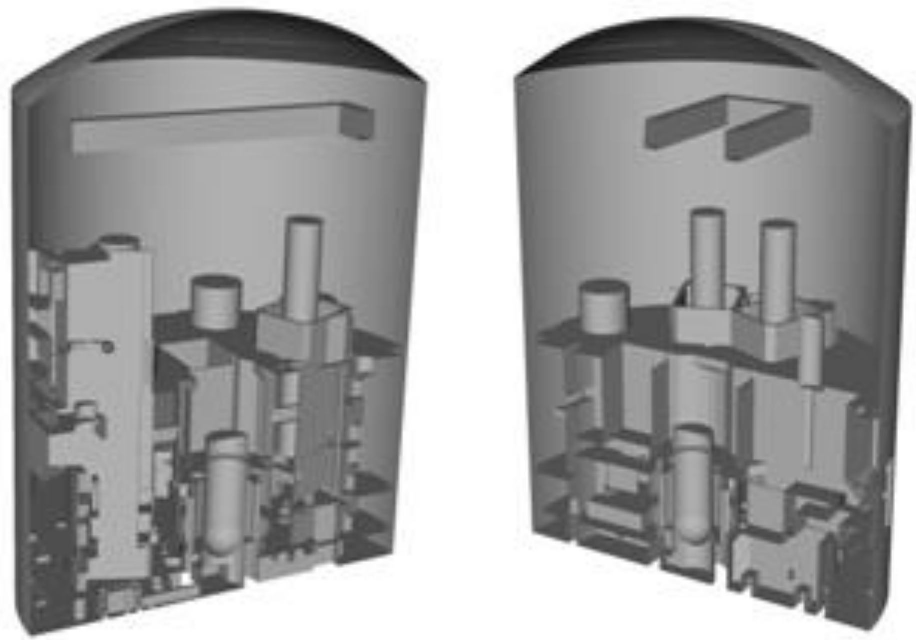

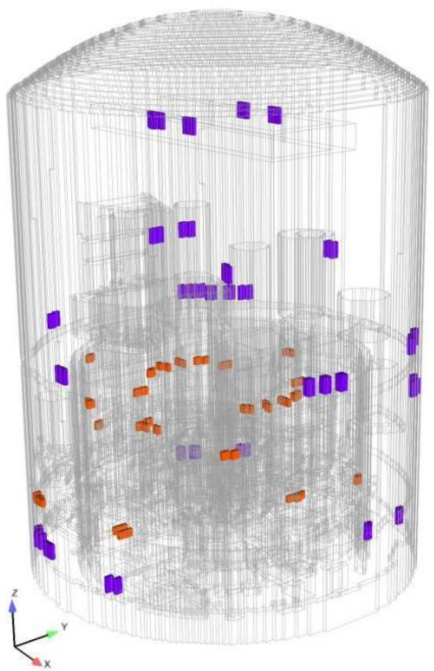

Location of the recombiners of the 1300MWe unit

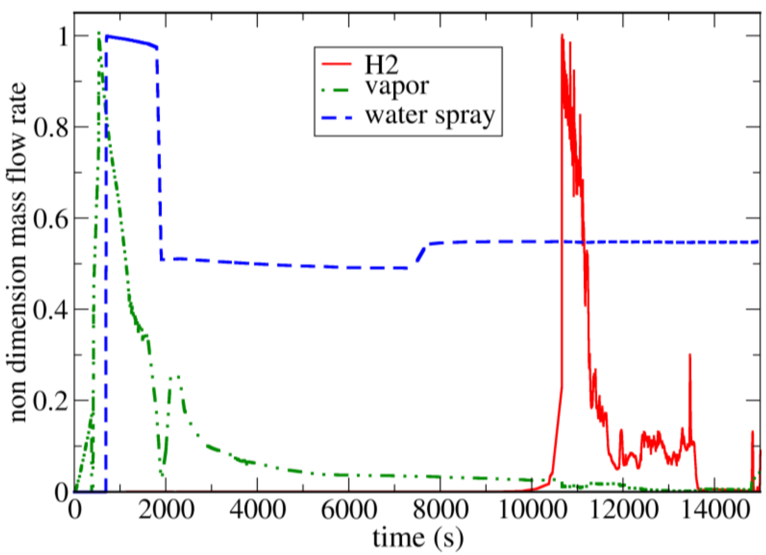

Hydrogen, vapor and water spray mass flowrate injected at the boundary condition.

The mitigation of the hydrogen risk is ensured by a set of hydrogen recombiners installed in the enclosure.

$$H_2 + \frac{1}{2}O_2 \quad \rightarrow \quad H_2O$$

Droplet diameter is injected at 2 mm to avoid being in a situation favorable to the pressure drop, because small drops of the order 100 micrometers increase the surface of exchange in the thermal transfer. Vapor condenses onto droplets which modifies the droplet diameter as a function of time and space

SENSITIVITY TO THE MESH REFINEMENT
SENSITIVITY TO DROPLET ASPERSION

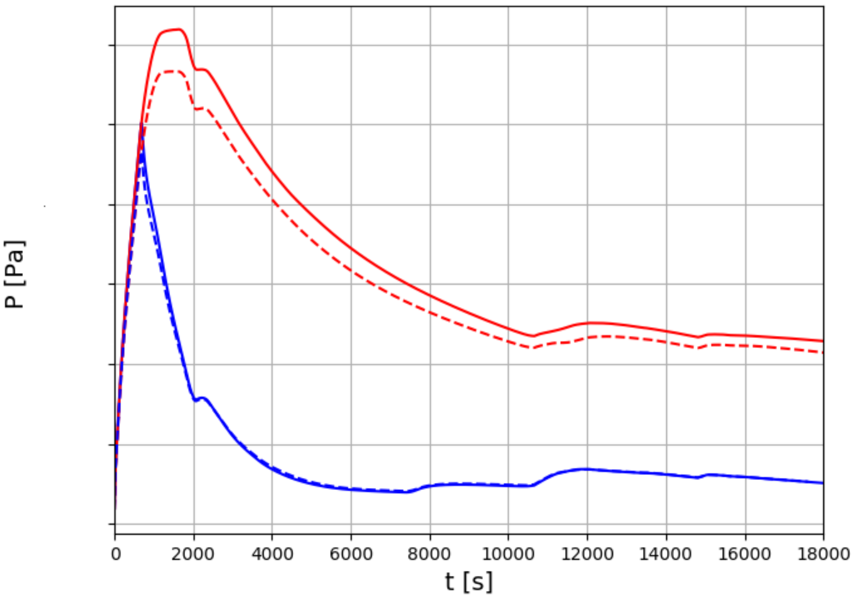

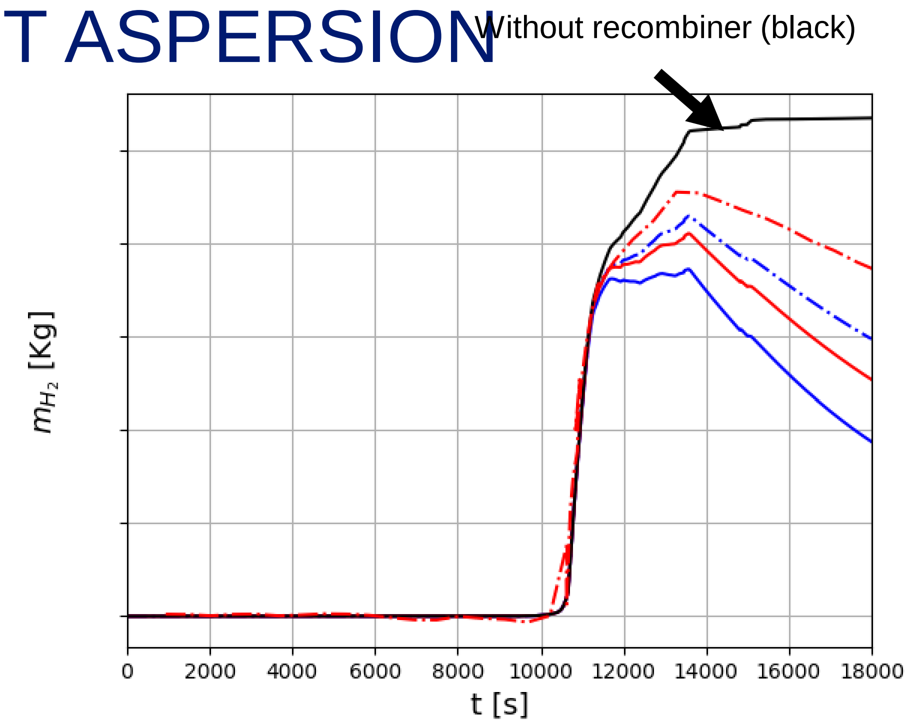

Comparison between coarse and reference meshes on the simulation of enclosure pressure.
referent mesh with eas (blue), without eas (red) and in coarse mesh with eas (blue thick) and without eas (red thick).

→ eas inhances homogenization of the hydrogen in the containment which increases H2 consumption by the recombiners

CONCLUSION FOR SPRAY CASES

- A spray modelling is available in the NEPTUNE_CFD code.
- Validation cases : CARAIDAS, TOSQAN, PANDA, CALIST, MISTRA, COTHYD (see oral presention of Tian CHEN in CFD4NRS)

- Spray model extended to wall Condensation at the wall (+ H2 recombiner): COPAIN, TOSQAN ISP47, PANDA 25, H2PAR, THAI HR49, …

Simulation of Flow-Accelerated Corrosion (FAC) using Computational Fluid Dynamics (CFD)

Lasseur Théo[a,b], Shkirskiy Viacheslav[a], Kanoufi Frédéric[a], Mimouni Stéphane[b]

[a]Université Paris Cité, ITODYS, CNRS, 75013 Paris, France

[b]EDF R&D Lab, 78400 Chatou, France

Contents

Contents

Flow-Accelerated Corrosion *(FAC)* : chemical degradation accelerated by a flowing elec

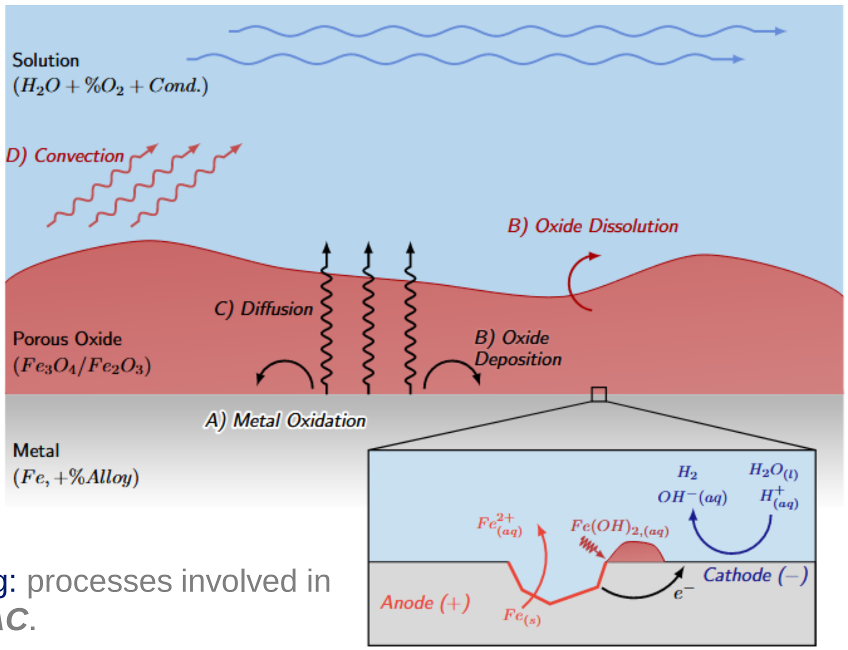

Fig: processes involved in ***FAC***.

Fig: failure of the piping integrity due to exacerbated wall thinning.

- **Local wall thinning prediction:** major security and availability issue (+ environmental and economical impacts)
- **Large application sectors impacted:** energy production and transport, chemical industry, etc.
- **Study environment:** Pressurized Water Reactor 2^{nd} circuit (non/low alloy steel, liquid-vapor flow, reducing+alkaline chemistry)

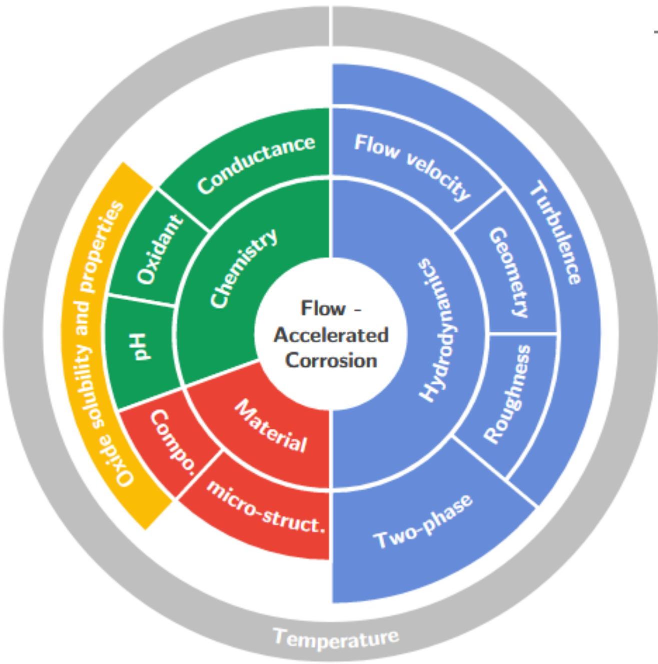

Fig: FAC influenced by a multitude of physical phenomena.

Fig: different family of predictive model with various advantages/inconvenients

code_saturne

- 1-phase liquid
- equations: mass, momentum, scalars
- case : stationary, turbulent, incomp., isotherm.

code_saturne

neptune_cfd

- 2-phase liquid-gas
- equations: mass*2, momentum*2, scalars
- case : turbulent, incomp., without phase change

→ Importance in predicting correct flow regime

Increase use of CFD with various level of modelization:

- *complex geometries, two-phase flows, local corrosion enhancement*
- *function of the understanding of the underlying mechanisms*

Uncoupled « Classical » approach / elementary

Flow simulation → Local FAC kinetics

Hypothesis: reactions limited by mass transport.
Estimation: $V_{FAC} \propto k_m(C_{O-S} - C_b) \approx k_m \cdot C_{eq}$

Coupled approach / mechanistic

Flow simulation → $C_{O-S} = f(k_m \dots)$ → Chemical species concentrations ↔ Local FAC kinetics

Hypothesis: No assumption on the rate-limiting step.
Estimation: From laws of the theory of electrochemistry.

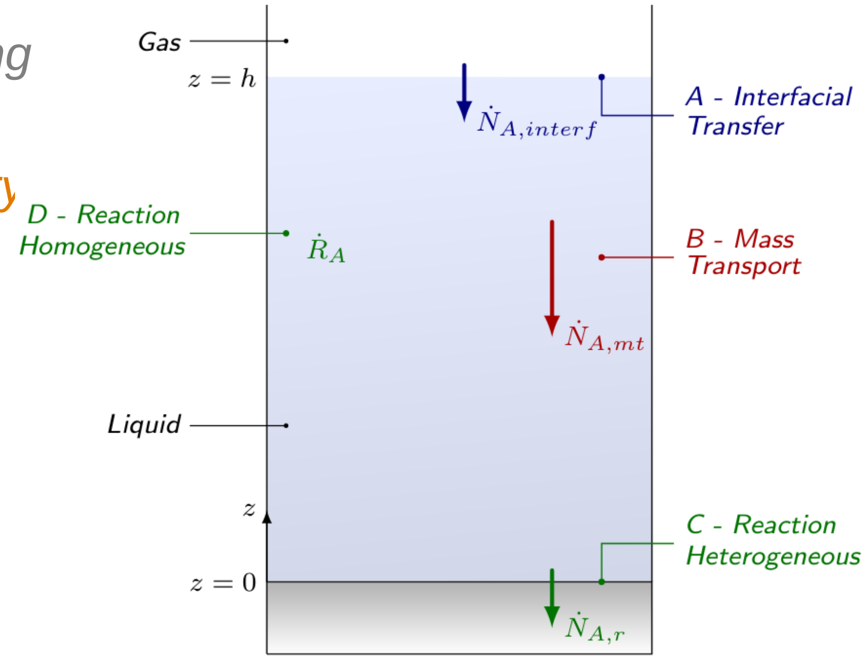

Fig: In the coupled approach: mass transport of a passive scalar *A* : $H^+, Fe^{2+}, \dots$ with different fluxes and reactions.

Turbulence modeling of Wall Mass Transfer

Comparison and proposition of suitable High/Low-Re approaches

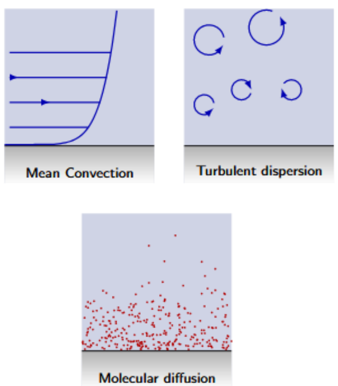

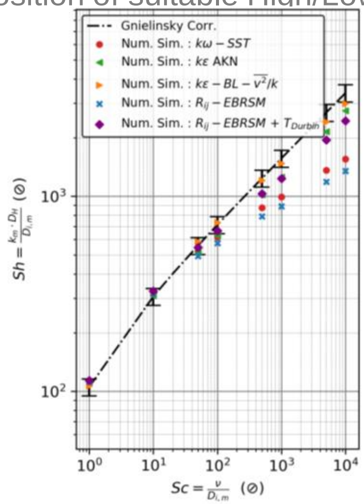

Accounting for roughness effect

via modified wall functions for scalar transport

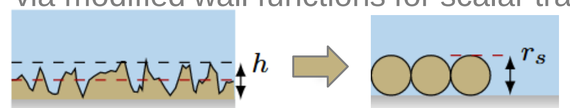

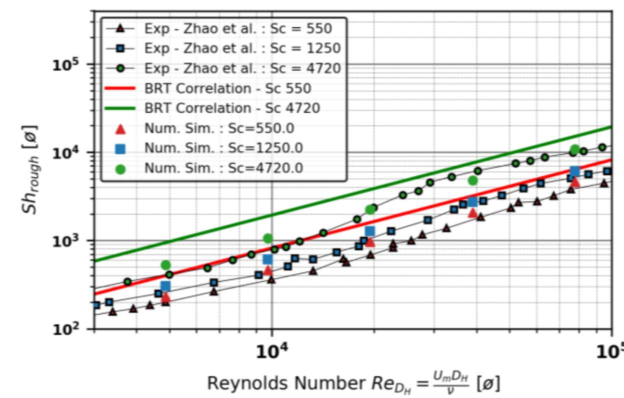

Integration of (electro)-chemical reactions

Wall reactions, bulk reactions, interphase mass transfer

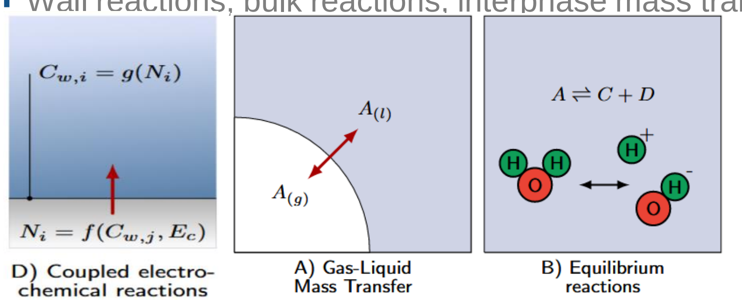

Modification in 2-Phase flow

Adapt the methodology

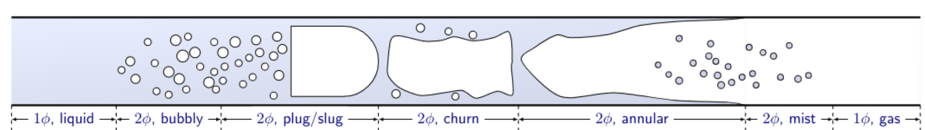

Contents

1. Context, Phenomenology, & State of the Art

2. Numerical Methodology Step-by-Step

3. Conclusion & Perspectives

Study case

- Regardless of the corrosion model: Wall Mass Transfer = key process → must be adequately captured.
- What are the turbulence RANS approaches/models valid to simulate this phenomenon ?

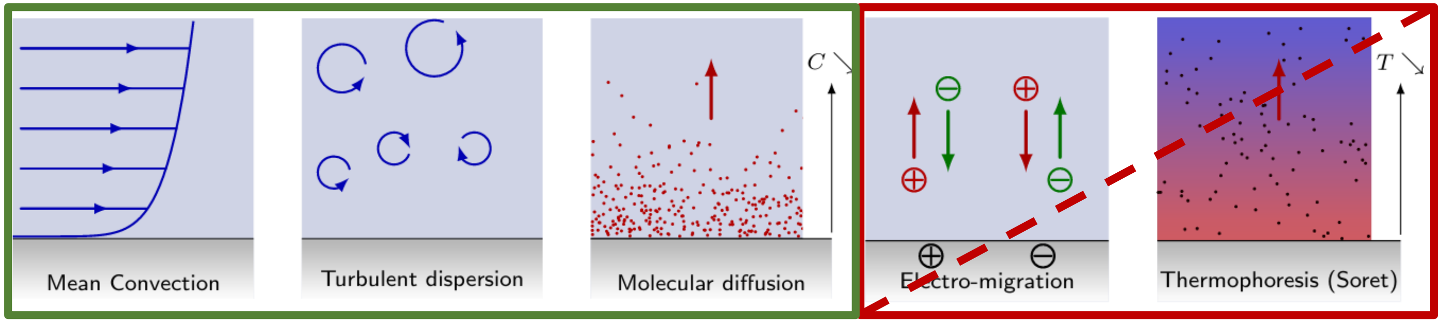

Fig: major modes of mass transport
in simplified corrosion system.

Mass transport equation & dimensionle

$$\partial_t \overline{C} + \nabla \cdot (\overline{u}\overline{C}) = \nabla((D + D_t)\nabla\overline{C})$$

Schmidt	Mass Transfer Coeff.	Sherwood
$Sc = \frac{\nu}{D}$	$k_m = \frac{N}{C_w - C_b}$	$Sh = \frac{k_m D_H}{D}$

$\underbrace{\qquad\qquad\qquad}_{\text{Compared to empirical correlations}}$

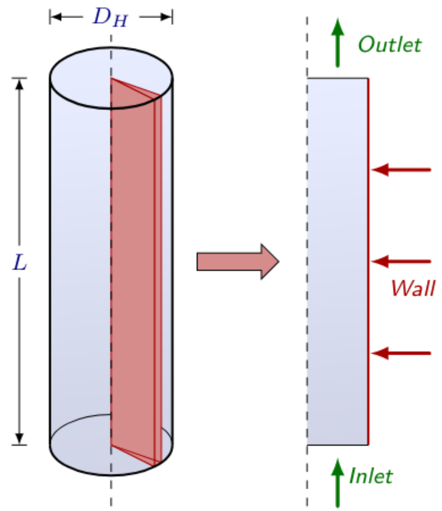

C_w : wall concentration - *imposed* BC

C_b : bulk concentration - *computed*

$$C_b = \frac{\int_S \rho\, u_i C\, dS}{\int_S \rho u_i\, dS}$$

N : molecular flux - *computed*

$$N = -D \left.\frac{\partial C}{\partial n}\right|_{wall}$$

Fig: schematic representation of the geometry.

2 – Wall Mass Transfer of low and high Sc in smooth pipes

2 approaches to deal with walls

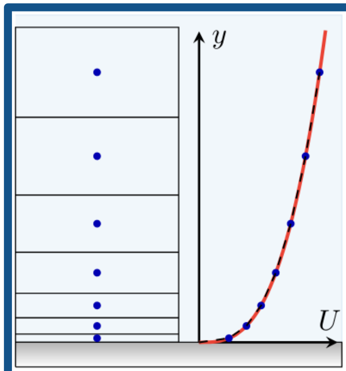

Low-Re = Resolved

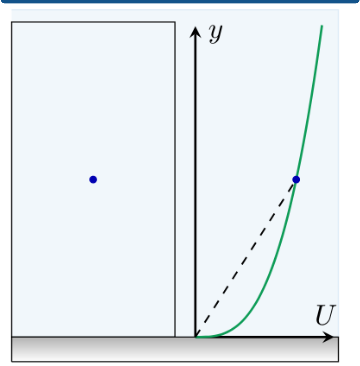

High-Re = Modeled (WF)

Solve transport eq.

$$\partial_t \overline{C} + \nabla \cdot \left(\overline{u}\overline{C} \right) = \nabla \left(\left(\frac{\nu}{Sc} + \frac{\nu_t}{Sc_t} \right) \nabla \overline{C} \right)$$

➔ 2 limit cases

1) Turbulent diff. ≪ Molecular diff.

2) Turbulent diff. ≫ Molecular diff.

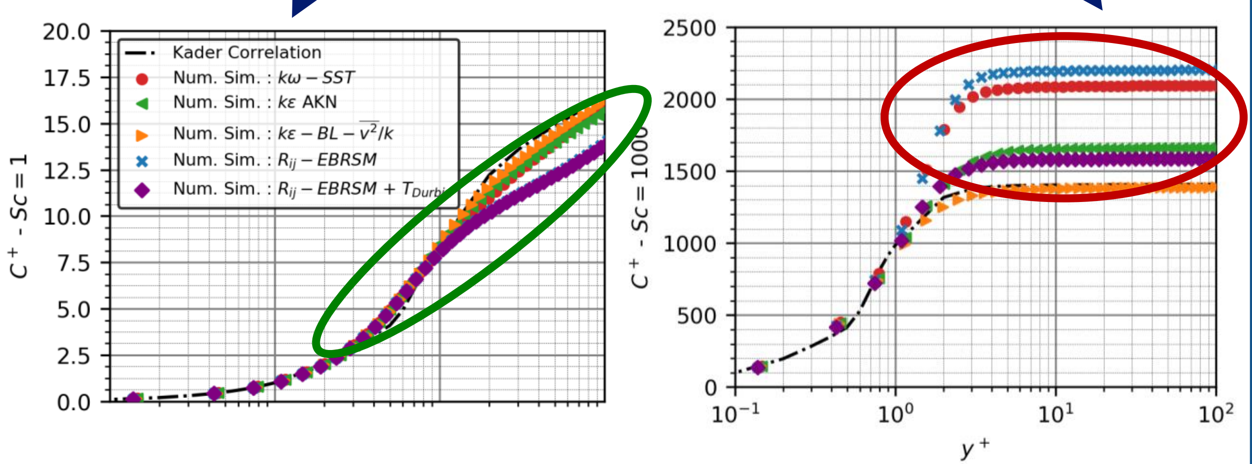

Fig: dimensionless concentration profile C^+ as function of dimensionless wall distance y^+ for $Sc = 1$ (thick BL) and $Sc = 1000$ (thin BL).

Conclusion

Low-Re approach: wrong turbulent viscosity profile at wall vicinity = wrong concentration profile for $Sc \gg 1$ (thin conc. BL).

Method : High-Re approach (roughness not resolved but modeled) → modified wall functions via "sand-grain roughness"

Unique Roughness scale:

$$R^+ = r_s u^*/\nu$$

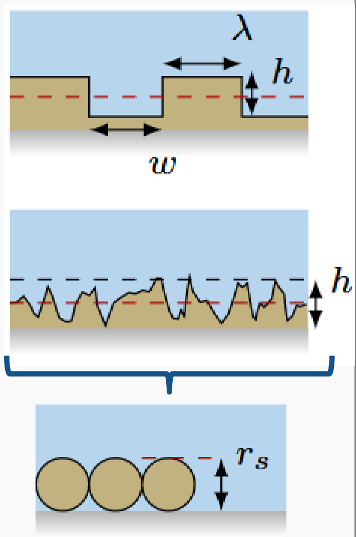

Fig: roughness patterns simplified to sand-grain.

Proposed wall functions of the type:

$$C^+ = C^+_{lisse} - \Delta C^+_{rough}(Sc, R^+)$$

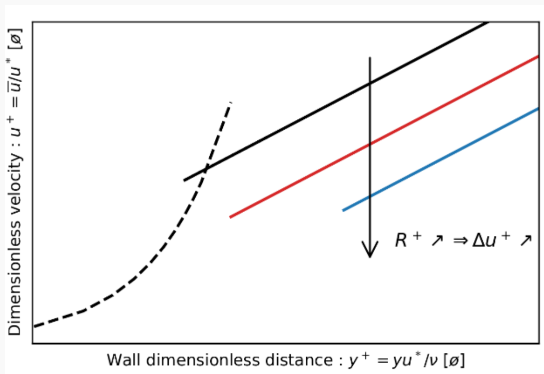

Fig: effect of rough wall functions on velocity U^+ (velocity at wall vicinity ↗, sharper gradients)

Investigations in pipes and bends:

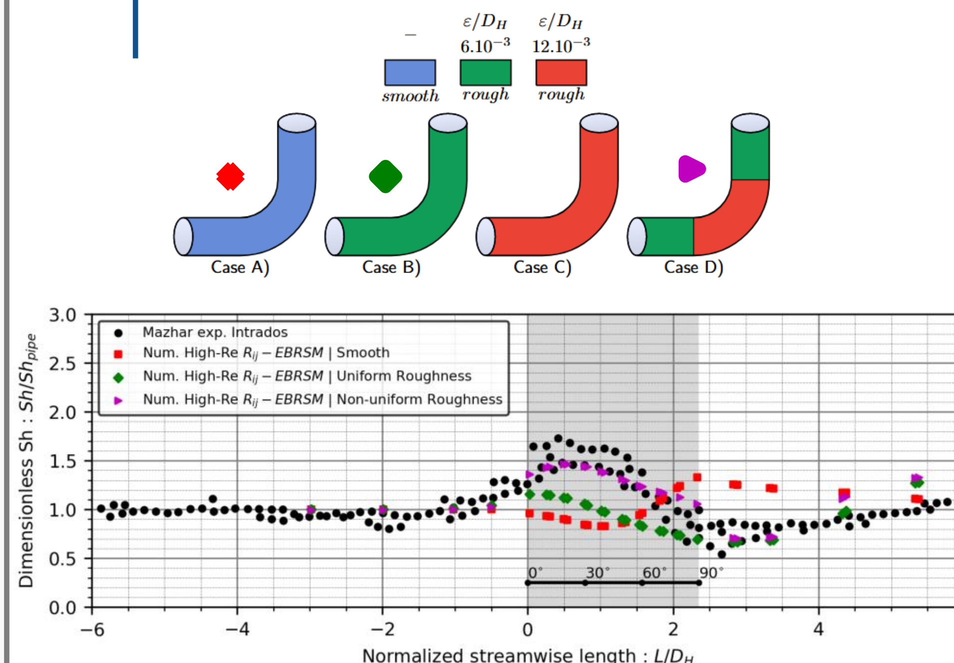

Fig: resulting simulation results with different case of numerical roughness distribution. Expe from Mazhar et al., **2013**

Conclusion

Clear improvements in the prediction for low and high Sc in all types of rough regimes: smooth/transitional/full-rough.

2 – Mass Transfer: Extension to two phase (2-P) flow

GOAL Validate Wall Mass Transfer in different two-phase flow regimes (methodology adaptation)

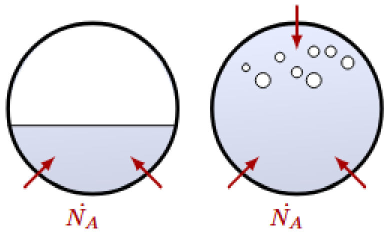

Fig: Boundary conditions for mass transfer

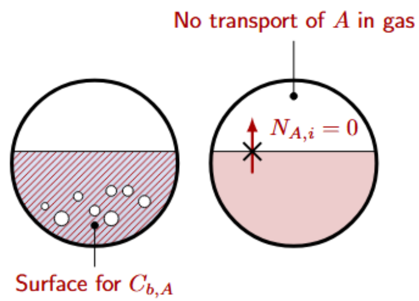

Fig: Mass transport and carrying phase

Autor	*Regime*	Sc
Wang et al. (2002)	Liquid, slug	1620
Langsholt et al. (1997)	Stratified, slug	473
Pecherkin et al. (2007)	Liquid, bubbly	1500
Zheng et al. (2006)	Slug	1140
Mazhar et al. (2013)	Liquid, annular	1280

Tab: Experience list for validation of Wall Mass Transfer in 2-P flow.

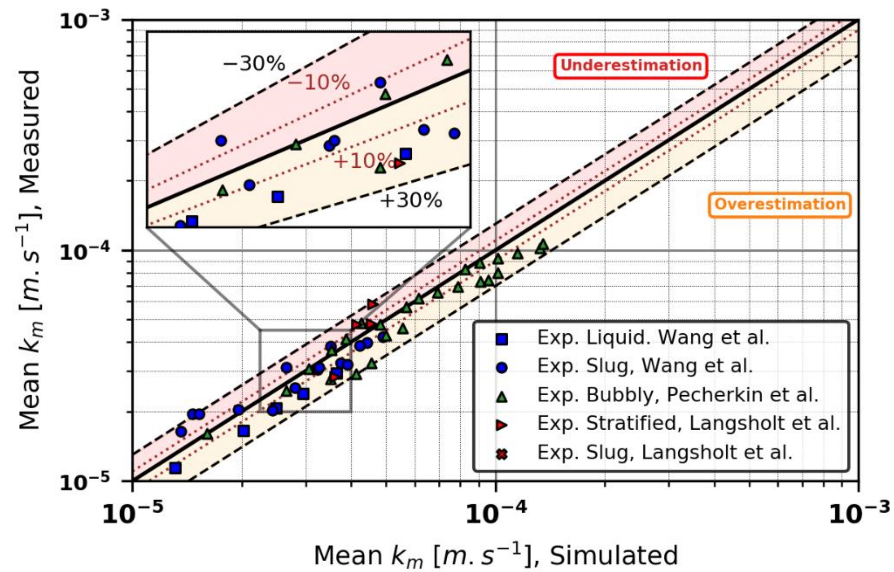

Fig: Final results - complete a prediction map for any 2-P flow regimes.

Study Case – *Bubbly Flow* : Pecherkin et al. *(2007)*

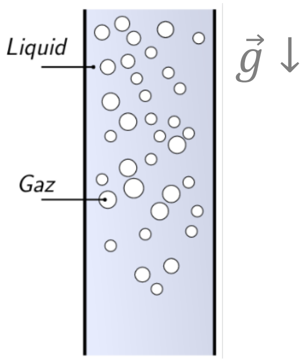

Characteristics
- Upward
- Steady
- Wall-packing of bubbles

Study Case - *Slug Flow* : H. Wang et al. *(2002)*

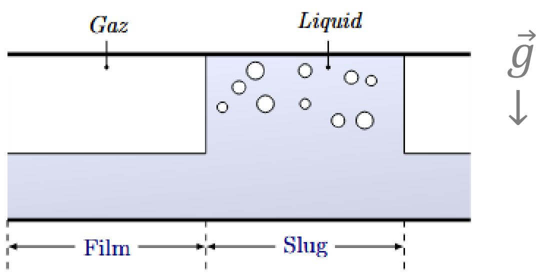

Characteristics
- Horizontal
- Intermittent

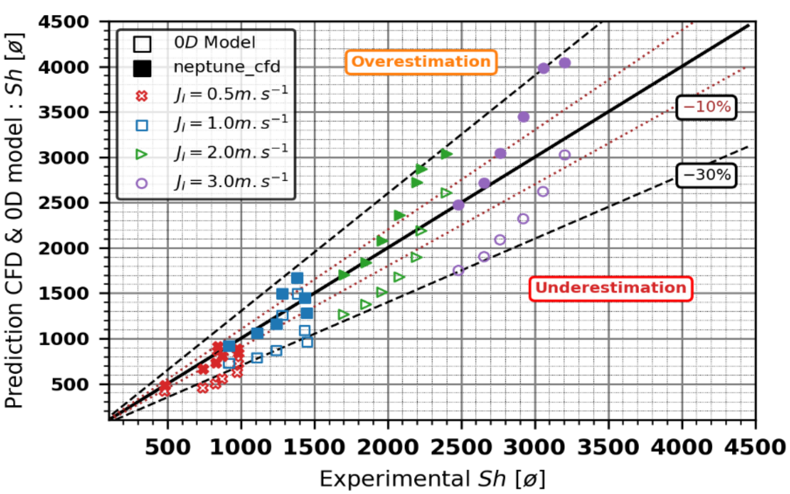

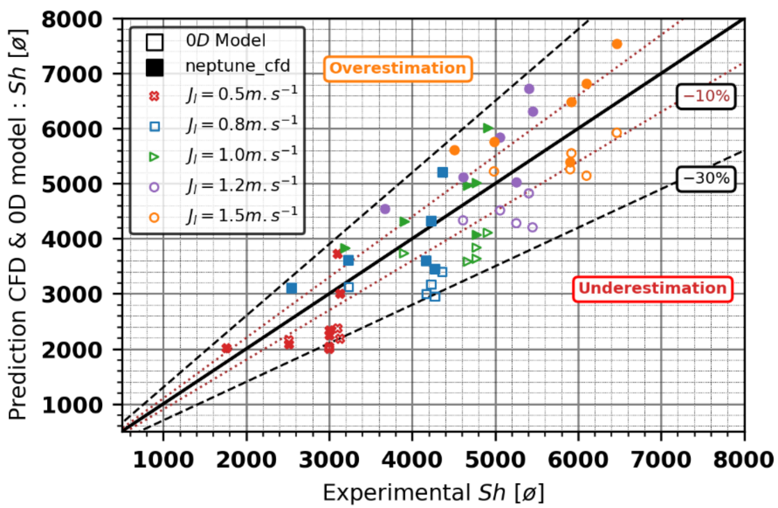

Fig: Comparison: experiments / 0D-model / numerical simulations for different liquid (J_l) and gas (J_g) superficial velocities (mean values).

M. Bouchacourt, *IWG-RRPC-88-1, 1988*

Study Case – *FAC* of straight pipe

Classical elementary model

- assume mass transfer limited kinetics and steady-state

$$V_{FAC}[mm.y^{-1}] \propto k_m \cdot C_{eq}$$

Uncoupled influence of : ***Hydraulics*** + ***Chemistry***

- Scalar transport, no reactions in bulk solution + simple 1^{st} order dissolution reaction (Uniform Dirichlet)

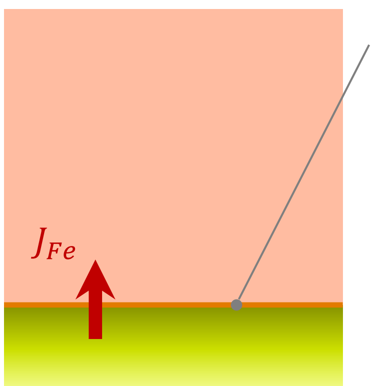

Imposed Boundary Condition

$$C_w = C_{eq} = \sum_{j=0} f_j(T, pH)$$

Compute Mass Flux

$$\boxed{V_{FAC} \propto J_{Fe} \propto \left.\frac{\partial C}{\partial n}\right|_{wall}}$$

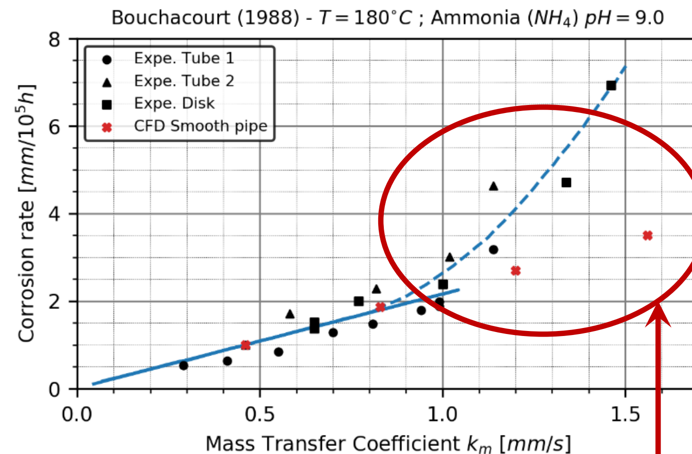

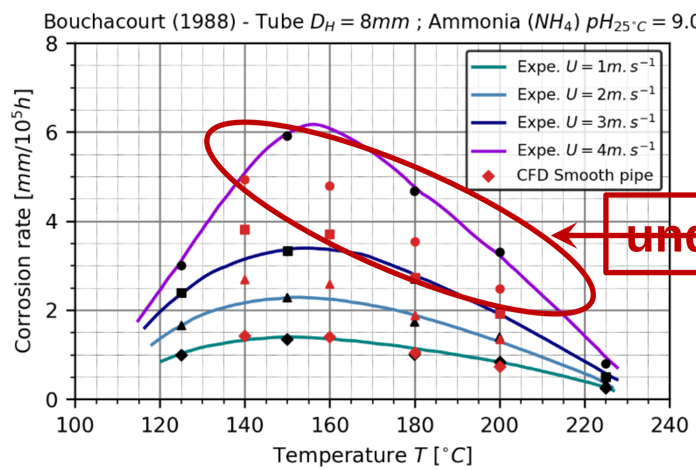

underestimation

Source of errors from the use of simple classical model ? → Roughness ? Lack of electrochemistry… ? Wrong rate limiting step ?

2 – Comprehensive mechanistic model from CO_2-corrosion to 2^{nd} coolant systems

Mass-Transport (Electrochemical) coupled for CO_2 corrosion

- System extensively studied with empirical & mechanistic approaches.
- Validated quantitatively & qualitatively against experiments for ≠ pH, velocity, geometry…

(1)	$CO_{2(g)} \rightleftharpoons CO_{2(aq)}$
(2)	$CO_{2(aq)} + H_2O_{(l)} \rightleftharpoons H_2CO_{3(aq)}$
(3)	$H_2CO_{3(aq)} \rightleftharpoons HCO^-_{3(aq)} + H^+_{(aq)}$
(4)	$HCO^-_{3(aq)} \rightleftharpoons CO^{2-}_{3(aq)} + H^+_{(aq)}$
(5)	$H_2O_{(l)} \rightleftharpoons OH^-_{(aq)} + H^+_{(aq)}$

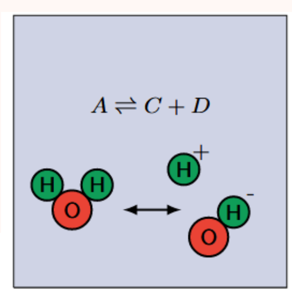

B) Equilibrium reactions

(1)	$2H^+ + 2e^- \rightleftharpoons H_2$
(2)	$2H_2CO_3 + 2e^- \rightleftharpoons 2HCO3^- + H_2$
(3)	$2HCO_3^- + 2e^- \rightleftharpoons 2CO_3^{2-} + H_2$
(4)	$2H_2O + 2e^- \rightleftharpoons 2OH^- + H_2$
(5)	$Fe_{(s)} \rightleftharpoons Fe^{2+}_{(aq)} + 2e^-$

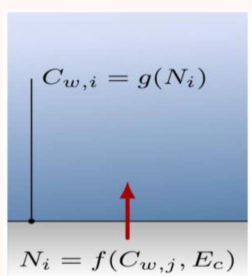

D) Coupled electro-chemical reactions

Mass-Transport (Electrochemical) coupled for H_2O corrosion

- Same framework
- Simplified reaction system

(1)	$H_2O_{(l)} \rightleftharpoons OH^-_{(aq)} + H^+_{(aq)}$

Tab: Bulk Reactions

(1)	$2H^+ + 2e^- \rightleftharpoons H_2$
(2)	$2H_2O + 2e^- \rightleftharpoons 2OH^- + H_2$
(3)	$Fe_{(s)} \rightleftharpoons Fe^{2+}_{(aq)} + 2e^-$

Tab: Wall Reactions

Formation of magnetite film (Fe_3O_4) disturb corrosion by reducing:

- available reactive surface
- mass transport through oxide pores

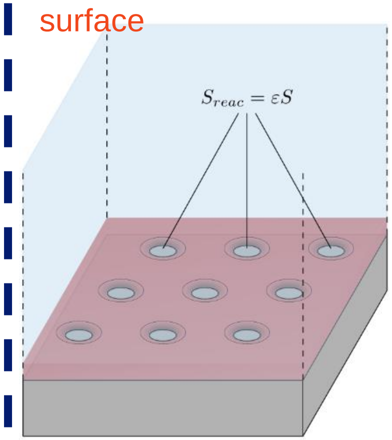

ε : porosity
τ : tortuosity

$$D_{eff} = \frac{\varepsilon}{\tau} D_m$$

$\tau = L_2/L_1$ $\varepsilon = V_{void}/V_{ox}$

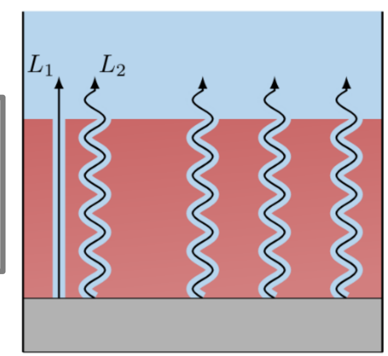

Adapt chemistry (reactions, chemical species, rates constant…), then propose solution for new unknowns :

oxide properties (porosity ε, thickness δ)

1 **Empirical functions ?**

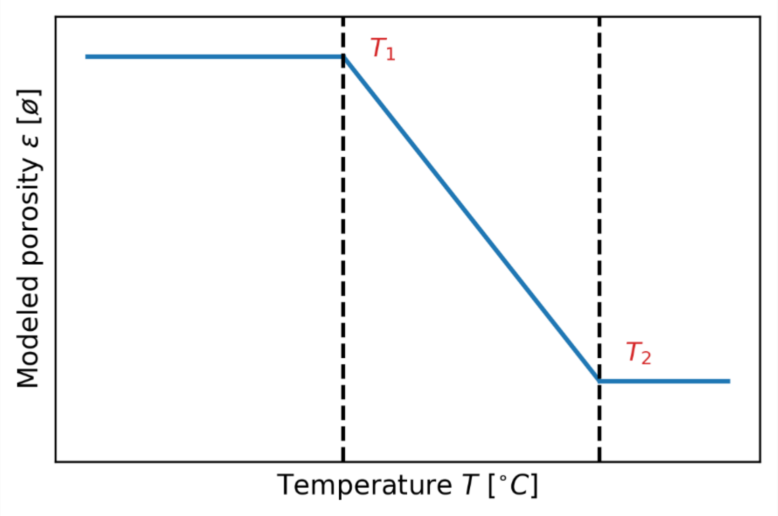

Fig: Porosity function of temperature (Sanchez-Caldera type).

2 **Solve equation set based on reactive mechanisms**

First qualitative results…

… still improvements

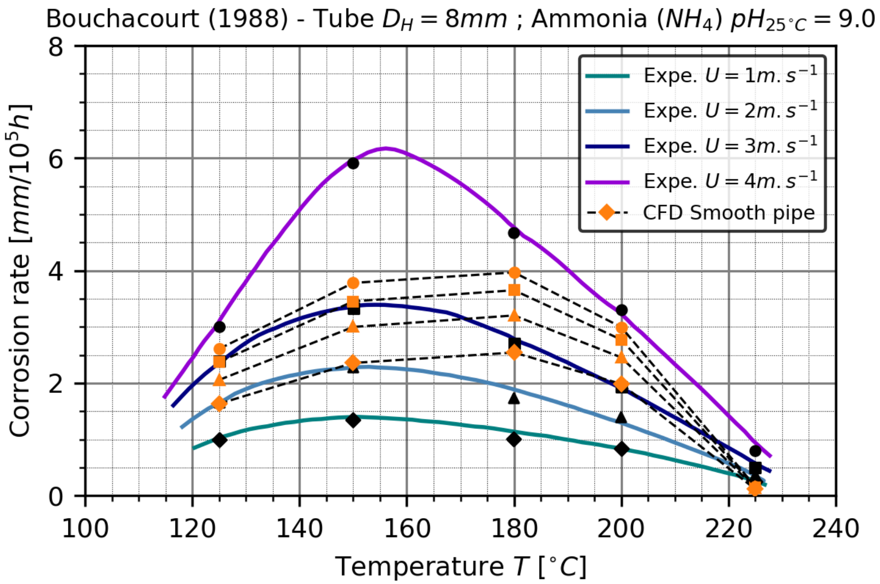

Fig: Comparison of experimental data and electrochemical model of H_2O corrosion with oxide effect.

Contents

Main objective: develop a numerical methodology for FAC predictions valid in single and two-phase flow.

Proposed solution: mechanistic approach with coupled models of mass-transport/electrochemistry integrated into CFD tools.

General conclusions

Pure Mass Transfer - No reactions

1 – Comparisons of RANS turbulence modeling of Wall Mass Transfer: passive scalar at low/high Sc.

2 – Account for roughness effect which derives from surface degradation (with High-Re/Wall Functions).

3 – Extend validation in two-phase flow conditions.

With reactions

4 – Integration of a coupled mechanistic approach to predict corrosion in complex CO_2 chemical system.

5 – Preliminary results of *FAC* predictions extended to PWR secondary coolant conditions.

"Close term" perspectives

- Finalize: wall mass transfer in several roughness pattern, map of two-phase flow mass transfer.
- Improve mechanistic model for "*secondary-water*" environment (High-pH, large temperature range…).
- Exhaustive comparison: "*mass-transfer controlled*" and "*all–coupled*" models for FAC predictions.

CONCLUSION

Industrial needs: **DNB, hydrogen risk, steam generator tube vibration, two-phase flows in cracks, sodium fast reactors, …**

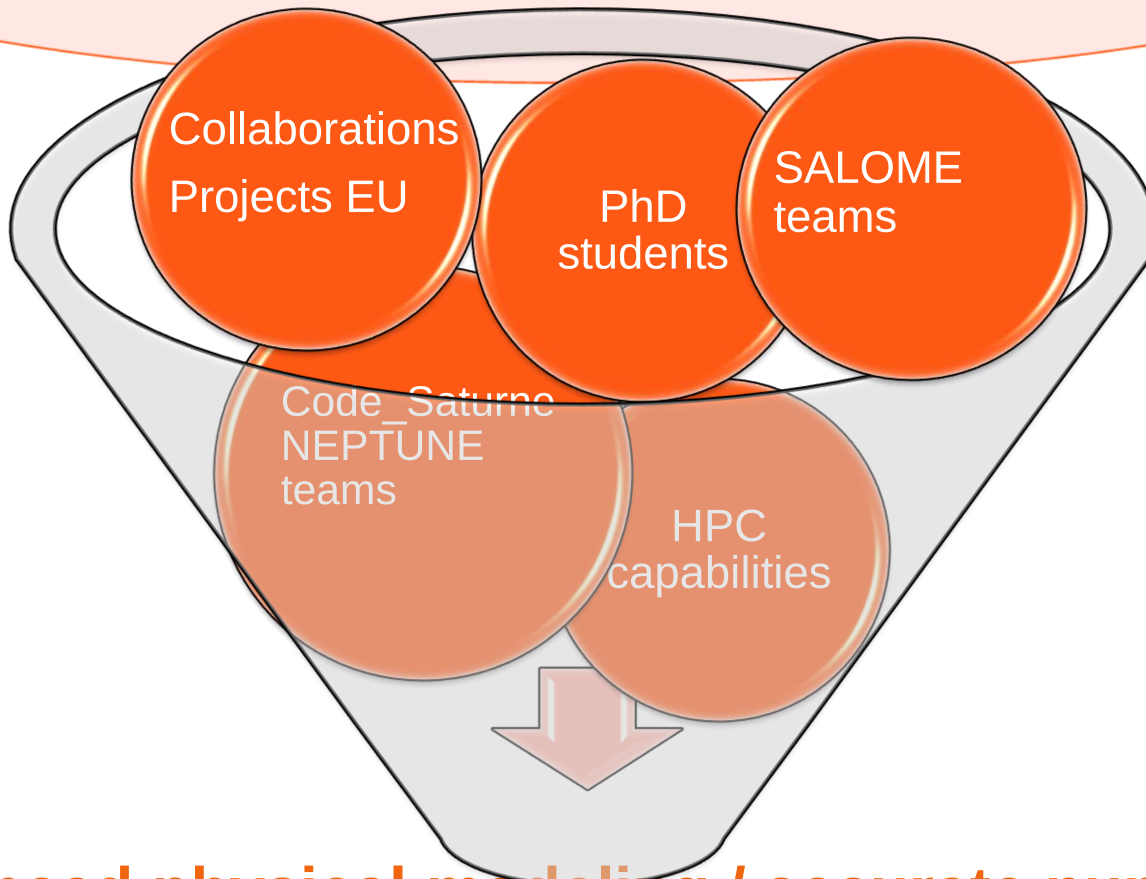

Advanced physical modeling / accurate numerical simulations

Thank you for your attention

To my father (1939-2020)

SHORT BIOGRAPHY

1. engineering degree (M.Sc.) in aerospace in 1991 from ISAE. In 1996, Ph.D. in fluids mechanics from the Ecole Polytechnique ("fractal analysis of interfaces for the rayleigh-taylor instabilities"; Accreditation to supervise research (2018) Eiffel University.

2. over 100 publications in refereed journals and international congresses

3. European projects : NURESIM, NURISP, NURESAFE, SARNET, SARNET2, SETH2 and HYMERES. He is currently implied in the european projects ESFR-SMART, SAMHYCO-NET, SAMOSAFER.

4. He has been the industrial/academic supervisor of 20 Ph.D.

5. He has been also the industrial supervisor of 35 M.Sc. Students.

6. Stephane Mimouni gave lectures in university Descartes (m.Sc.), INSTN (national institute of science and nuclear technology), Eiffel university, FJOH summer school, Mines Saint Etienne,…

EFFECT OF NON-UNIFORM AXIAL HEAT FLUX

At PWR conditions, DNB will not occur at the tube exit with a cosinusoidal or skewed cosinusoidal flux distribution.

In this case, the DNB is

- in the high flux region

- governed by local conditions.

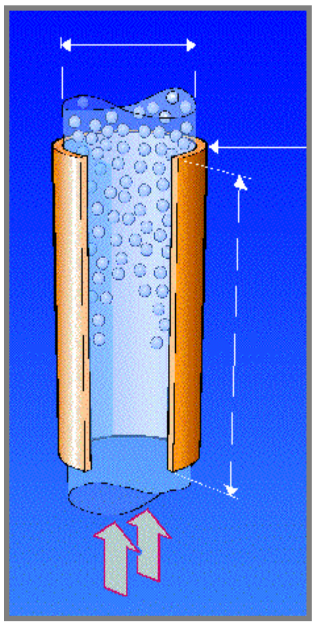

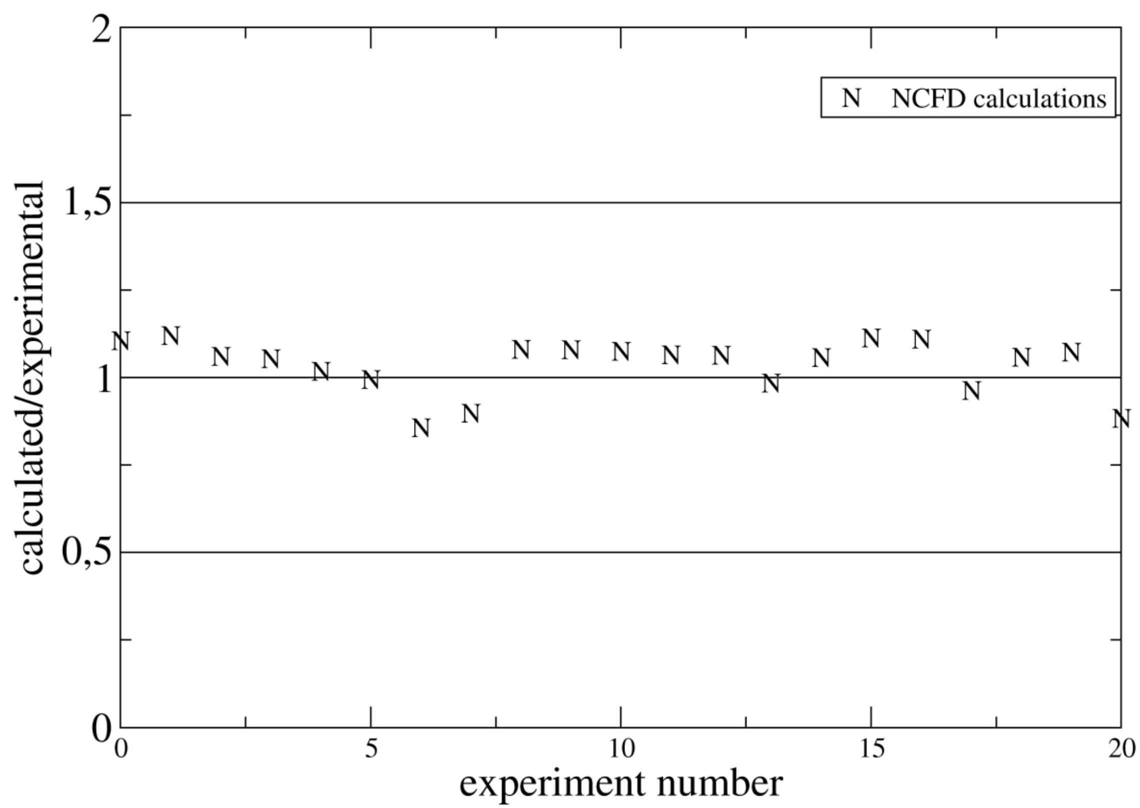

EFFECT OF VOLUME FRACTION CRITICAL VALUE

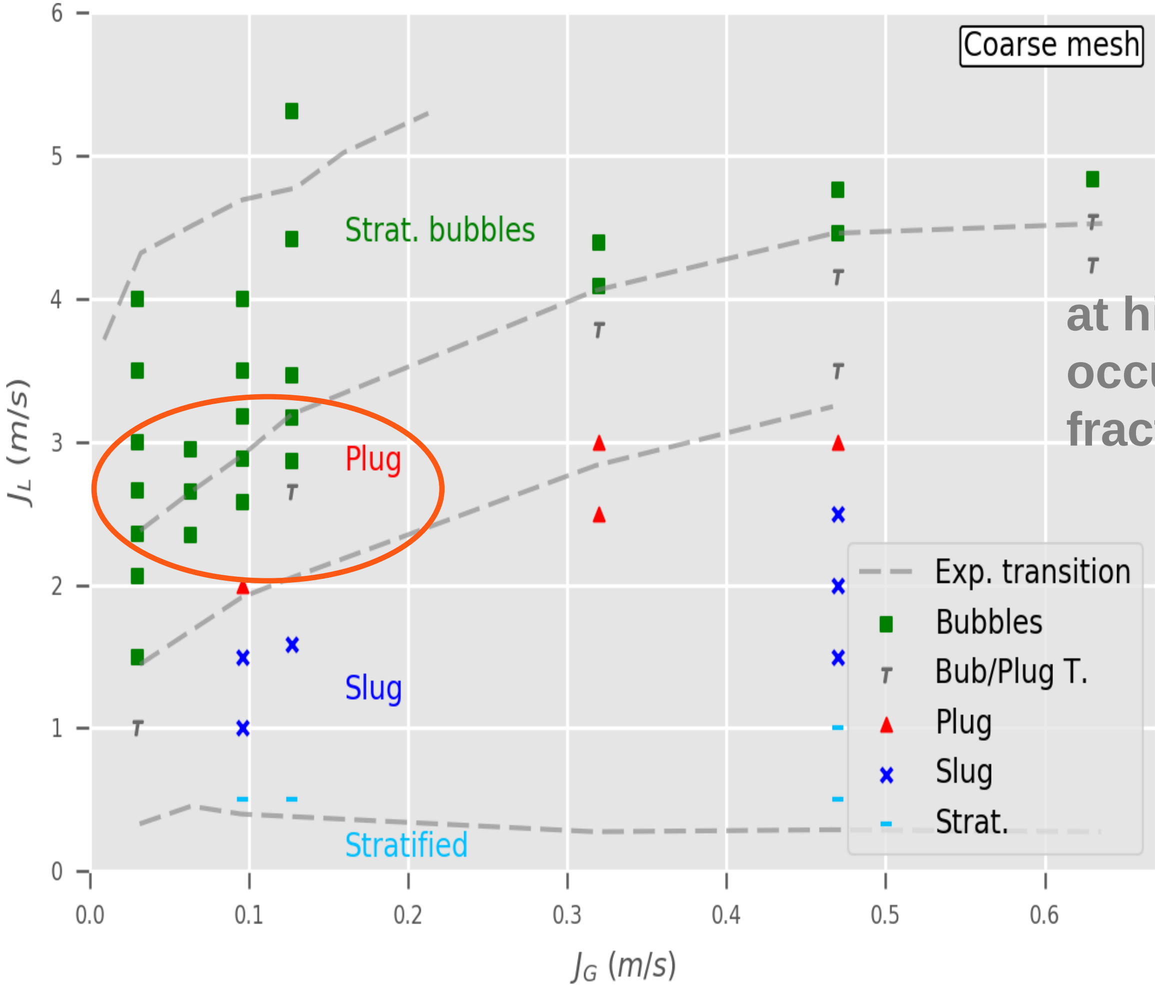

at high pressure → bubbly flows occur at higher values of gas fraction (>60%)

α critical = 30% → α critical = 45%

critical value should depend on physical properties of the fluid

Stephane.Mimouni@edf.fr